USGS
science for a changing world

Prepared in cooperation with the Illinois Center for Transportation, the Illinois Department of Transportation, and the Federal Highway Administration

Estimation of Peak Discharge Quantiles for Selected Annual Exceedance Probabilities in Northeastern Illinois

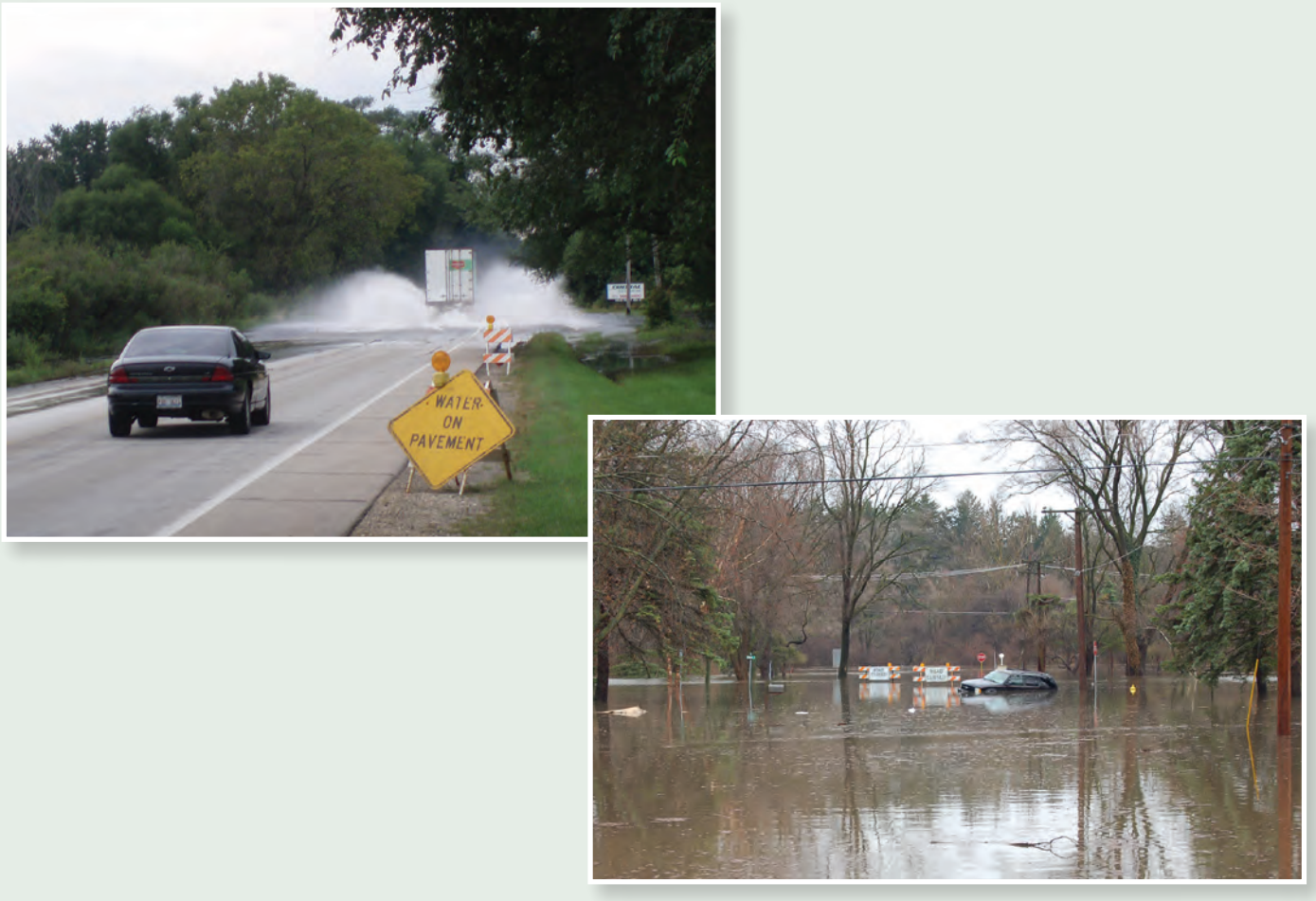

Scientific Investigations Report 2016–5050
Version 3.0, June 2021

U.S. Department of the Interior
U.S. Geological Survey

Cover. Photograph showing Illinois 176 where it crosses the South Branch of the Kishwaukee River in McHenry County, Illinois, by E. Perry Masouridis of the Illinois Department of Transportation on August 27, 2007 (left). Photograph showing flooding of Osage Drive at Illinois 53 along the East Branch of the DuPage River in DuPage County, Illinois, by Scott D. Czaplicki of the Illinois Department of Transportation on April 18, 2013 (right).

Estimation of Peak Discharge Quantiles for Selected Annual Exceedance Probabilities in Northeastern Illinois

By Thomas M. Over, Riki J. Saito, Andrea G. Veilleux, Padraic S. O'Shea, Jennifer B. Sharpe, David T. Soong, and Audrey L. Ishii

Prepared in cooperation with the Illinois Center for Transportation, the Illinois Department of Transportation, and the Federal Highway Administration

Scientific Investigations Report 2016–5050
Version 3.0, June 2021

U.S. Department of the Interior
U.S. Geological Survey

U.S. Geological Survey, Reston, Virginia
First release: June 2016
Revised: April 2021 (ver. 3.0)

For more information on the USGS—the Federal source for science about the Earth, its natural and living resources, natural hazards, and the environment—visit https://www.usgs.gov or call 1–888–ASK–USGS.

For an overview of USGS information products, including maps, imagery, and publications, visit https://store.usgs.gov/.

Suggested citation:
Over, T.M., Saito, R.J., Veilleux, A.G., O'Shea, P.S., Sharpe, J.B., Soong, D.T., and Ishii, A.L., 2021, Estimation of peak discharge quantiles for selected annual exceedance probabilities in northeastern Illinois (ver. 3.0, June 2021): U.S. Geological Survey Scientific Investigations Report 2016–5050, 50 p. with appendix, https://doi.org/10.3133/sir20165050.

Also published as:
Over, T.M., Saito, R.J., Veilleux, A.G., O'Shea, P.S., Sharpe, J.B., Soong, D.T., and Ishii, A.L., 2021, Estimation of peak discharge quantiles for selected annual exceedance probabilities in northeastern Illinois: Illinois Center for Transportation Report, FHWA-ICT-16-013, 317 p. with appendix, https://doi.org/10.36501/0197-9191/16-014.

ISSN 2328-0328 (online)

Acknowledgments

The guidance of the Technical Review Panel for this project, chaired by Matt O'Connor of the Illinois Department of Transportation (IDOT) and including as members Steve Ferguson (IDOT), Dan Ghere (Federal Highway Administration), Rick Gosch (IIIinois Department of Natural Resources), Perry Masouridis (IDOT), Tzuoh-Ying Su (U.S. Army Corps of Engineers), Neil VanBebber (IDOT), and Rick Wojcik (IDOT) was critical to the success of this project.

Marvin Harris and John Latour of the U.S. Geological Survey (USGS) IIIinois Water Science Center, John Walker and Robert Waschbusch of the USGS Wisconsin Water Science Center, and Donald Arvin of the USGS Indiana Water Science Center provided key input on the quality of streamgage records used in this study.

Allan Curtis (Midwestern Regional Climate Center) assisted with downloading and understanding the National Weather Service cooperative daily precipitation data used in this study.

This publication is based on the results of ICT-R27-144, Development and Implementation of Updated Urban Regional Flood Frequency Equations for Illinois. ICT-R27-144 was conducted in cooperation with the Illinois Center for Transportation; the Illinois Department of Transportation, Division of Highways; and the U.S. Department of Transportation, Federal Highway Administration.

Contents

Figures

Tables

Conversion Factors

[U.S. customary units to International System of Units]

Multiply	By	To obtain
	Length	
inch (in.)	2.54	centimeter (cm)
inch (in.)	25.4	millimeter (mm)
foot (ft)	0.3048	meter (m)
mile (mi)	1.609	kilometer (km)
	Area	
acre	4,047	square meter (m^2)
acre	0.4047	hectare (ha)
acre	0.4047	square hectometer (hm^2)
acre	0.004047	square kilometer (km^2)
square mile (mi^2)	259.0	hectare (ha)
square mile (mi^2)	2.590	square kilometer (km^2)
	Volume	
cubic foot (ft^3)	28.32	cubic decimeter (dm^3)
cubic foot (ft^3)	0.02832	cubic meter (m^3)
acre-foot (acre-ft)	1,233	cubic meter (m^3)
acre-foot (acre-ft)	0.001233	cubic hectometer (hm^3)
	Flow rate	
cubic foot per second (ft^3/s)	0.02832	cubic meter per second (m^3/s)

Temperature in degrees Celsius (°C) may be converted to degrees Fahrenheit (°F) as follows:

$$°F = (1.8 \times °C) + 32.$$

Temperature in degrees Fahrenheit (°F) may be converted to degrees Celsius (°C) as follows:

$$°C = (°F - 32) / 1.8.$$

Datum

Vertical coordinate information is referenced to the North American Vertical Datum of 1988 (NAVD 88).

Horizontal coordinate information is referenced to the North American Datum of 1927 (NAD 27) except as otherwise noted.

Elevation, as used in this report, refers to distance above the vertical datum.

Abbreviations

AEP	annual exceedance probability
AFPD	annual flood-probability discharge
AMS	annual maximum series
B–GLS	Bayesian generalized least squares
B–WLS	Bayesian weighted least squares
BDF	basin development factor
CCPN	Cook County Precipitation Network
COOP	cooperative network
CSG	crest-stage gage
DEM	digital elevation model
EMA	Expected Moments Algorithm
Esri	Environmental Systems Research Institute, Inc.
GIS	geographic information system
GLS	generalized least squares
HDB	hand-drawn boundary
ICT	Illinois Center for Transportation
IDOT	Illinois Department of Transportation
MACS	MRCC Applied Climate System
MRCC	Midwestern Regional Climate Center
MSE	mean squared error
MWRDGC	Metropolitan Water Reclamation District of Greater Chicago
NED	National Elevation Dataset
NHD	National Hydrography Dataset
NID	National Inventory of Dams
NLCD	National Land Cover Dataset
NWI	National Wetlands Inventory
NWIS	National Water Information System
NWS	National Weather Service
OLS	ordinary least squares
OVB	omitted variable bias
PDS	partial duration series
PeakFQ	Peak flow FreQuency program
PILF	potentially influential low flood

PRISM	Parameter-elevation Relationships on Independent Slopes Model
SE	standard error
SSURGO	State Soil Survey Geographic database
USGS	U.S. Geological Survey
VIF	variance inflation factor
WLS	weighted least squares
WREG	Weighted-Multiple-Linear Regression program
WY	water year; a water year is the 12-month period October 1 through September 30 designated by the calendar year in which it ends.

Estimation of Peak Discharge Quantiles for Selected Annual Exceedance Probabilities in Northeastern Illinois

By Thomas M. Over, Riki J. Saito, Andrea G. Veilleux, Padraic S. O'Shea, Jennifer B. Sharpe, David T. Soong, and Audrey L. Ishii

Abstract

This report provides two sets of equations for estimating peak discharge quantiles at annual exceedance probabilities (AEPs) of 0.50, 0.20, 0.10, 0.04, 0.02, 0.01, 0.005, and 0.002 (recurrence intervals of 2, 5, 10, 25, 50, 100, 200, and 500 years, respectively) for watersheds in Illinois based on annual maximum peak discharge data from 117 watersheds in and near northeastern Illinois. One set of equations was developed through a temporal analysis with a two-step least squares-quantile regression technique that measures the average effect of changes in the urbanization of the watersheds used in the study. The resulting equations can be used to adjust rural peak discharge quantiles for the effect of urbanization, and in this study the equations also were used to adjust the annual maximum peak discharges from the study watersheds to 2010 urbanization conditions.

The other set of equations was developed by a spatial analysis. This analysis used generalized least-squares regression to fit the peak discharge quantiles computed from the urbanization-adjusted annual maximum peak discharges from the study watersheds to drainage-basin characteristics. The peak discharge quantiles were computed by using the Expected Moments Algorithm following the removal of potentially influential low floods defined by a multiple Grubbs-Beck test. To improve the quantile estimates, regional skew coefficients were obtained from a newly developed regional skew model in which the skew increases with the urbanized land use fraction. The skew coefficient values for each streamgage were then computed as the variance-weighted average of at-site and regional skew coefficients. The drainage-basin characteristics used as explanatory variables in the spatial analysis include drainage area, the fraction of developed land, the fraction of land with poorly drained soils or likely water, and the basin slope estimated as the ratio of the basin relief to basin perimeter.

This report also provides the following: (1) examples to illustrate the use of the spatial and urbanization-adjustment equations for estimating peak discharge quantiles at ungaged sites and to improve flood-quantile estimates at and near a gaged site; (2) the urbanization-adjusted annual maximum peak discharges and peak discharge quantile estimates at streamgages from 181 watersheds including the 117 study watersheds and 64 additional watersheds in the study region that were originally considered for use in the study but later deemed to be redundant.

The urbanization-adjustment equations, spatial regression equations, and peak discharge quantile estimates developed in this study will be made available in the web application StreamStats, which provides automated regression-equation solutions for user-selected stream locations. Figures and tables comparing the observed and urbanization-adjusted annual maximum peak discharge records by streamgage are provided at https://doi.org/10.3133/sir20165050 for download.

Introduction

Estimates of the magnitude and frequency of floods, particularly in urban areas where there is an increased density of lives and property at risk, is a critical ingredient to floodplain management, emergency response planning, and infrastructure design tasks such as sizing of bridges and culverts. At the same time, urbanization, particularly the construction of impervious surfaces, changes the response of watersheds to precipitation by reducing infiltration and increasing flow velocities, which increases flood volumes and magnitudes of peaks (Konrad, 2003).

Predictions of the effects of urbanization in ungaged basins or in basins where future urbanization is expected or planned are usually obtained by following one of two general approaches: (1) simulation with rainfall-runoff models driven by historical precipitation (either as design storms or by continuous simulation of long-term records), usually calibrated to observed streamflow data; and (2) regressions of peak discharge quantiles obtained from observed streamflow data at a collection of streamgages in and near the region of interest on relevant basin characteristics such as drainage area and fraction of urbanized area. The two approaches have different advantages and disadvantages (Rosbjerg and others, 2013); generally the simulation model approach is preferred for predicting the response of a basin to changes in the basin properties or climate characteristics, whereas for ungaged basins over a historical period, the regional regression approach may be more accurate (Hodgkins and others, 2007).

Indeed, the regional regression equation approach is a well-developed form of regional calibration of a watershed model, whereas significant challenges remain for regional calibration of simulation models (Vogel, 2006).

Regional regression equations for urbanization-affected areas of northeast Illinois were first published by Allen and Bejcek (1979) who used data beginning around 1960 and ending in 1976. Since 1976 there have been many years of additional streamflow data, extensive growth of the urbanized area of northeast Illinois, and several historic floods (Juhl, 2005). As a result, the U.S. Geological Survey (USGS) Illinois Water Science Center in cooperation with the Illinois Department of Transportation (IDOT) and the Federal Highway Administration (FHWA), through the Illinois Center for Transportation (ICT), developed a project to update the spatial regression equations of Allen and Bejcek (1979) for urbanization-affected streams in northeastern Illinois and for adjusting rural peak discharge quantile estimates for the effect of urbanization.

Purpose and Scope

This report presents the methods and results of a study that applied a regional spatial regression approach to develop equations for estimating peak discharge quantiles with annual exceedance probabilities (AEPs) of 0.5, 0.2, 0.1, 0.04, 0.02, 0.01, 0.005, and 0.002 (often referred to as the 2-, 5-, 10-, 25-, 50-, 100-, 200-, and 500-year floods, respectively) for Illinois flood-frequency region 2 (previously defined by Soong and others, 2004). Flood-frequency region 2 consists of northeastern and parts of north-central Illinois and includes the greater Chicago region. This report updates the existing spatial regression equations (Soong and others, 2004; Allen and Bejcek, 1979) for northeastern Illinois in the following ways: (1) it uses streamflow data through water year (WY) 2009, compared to through 1999 for Soong and others (2004) and through 1976 for Allen and Bejcek (1979); (2) it tests and implements wetland-open water and slope variables replacing those of Soong and others (2004); and (3) it uses the updated flood-frequency estimation methods and software, particularly in the estimation of at-site peak discharge quantiles by using multiple Grubbs-Beck potentially influential low flood (PILF) detection, the Expected Moments Algorithm (EMA) for handling censored and historical floods, and regional skew estimation by Bayesian generalized least squares.

The study described in this report also implements the temporal regression approach of Over and others (2016) to the analysis and adjustment of annual maximum peak discharge records for the exceedance probability-dependent effect of urbanization. By this approach the observed peak discharge records are adjusted to current (2010) urbanization conditions before they are used in the spatial regression analysis; and a set of "temporal" urbanization coefficients are obtained that are applicable wherever hydrologic effects of urbanization are similar to those in northeastern Illinois. Because the historical urbanization data used in the temporal regression approach are available beginning 1940, the earliest streamflow data used in this study are from WY 1940.

There are three primary products from the study described in this report: (1) this report, published in ICT and USGS versions, having the same content, and presenting the methods and results, including the two sets of regression equations for estimating peak discharge quantiles; (2) an implementation of the spatial and temporal regression equations in StreamStats (https://streamstats.usgs.gov/); and (3) a collection of figures and tables comparing the observed and urbanization-adjusted peak discharges at https://doi.org/10.3133/sir20165050.

Description of Study Area

The study area covers northeastern Illinois and parts of north-central Illinois, northwest Indiana, and southeast Wisconsin (fig. 1). The physiography of the region is determined by recent glacial episodes. The last glacial episode was the Wisconsinan, which ended about 12,000 years ago and during which all except the western lobe of the study area in the valley of the Green River was covered in ice (Hansel and McKay, 2010). The entire study region was covered with ice during the previous glacial episode, the Illinoian, which ended about 125,000 years ago. The glaciers of the Wisconsinan episode left behind various glacial features, the most prevalent of which are a series of moraines (Arnold and others, 1999). The physiographic regions of northeastern Illinois follow these glacial features, with the Chicago Lake Plain and the Wheaton Morainal Country making up the Great Lakes Section, and then, to the west and south, the Till Plains Section (Leighton and others, 1948), with corresponding regions in Indiana (Schneider, 1966). As a result, the surficial geology in the study region consists of unconsolidated glacial drift of varying thickness up to 400 feet (Piskin and Bergstrom, 1975). The character of the drift ranges from end moraines and till plains to outwash fans and lacustrine deposits (Hansel and McKay, 2010).

Subsequent warmer and drier periods added loess to the surface, thinner toward Lake Michigan, so that soil parent materials combine the loess and the underlying drift (Fehrenbacher and others, 1984). Soil orders of the region vary with the original vegetation type. Alfisols, which form under forests, dominate nearer to Lake Michigan, whereas mollisols, which form under grasslands, cover most the rest of the region (Fehrenbacher and others, 1984). The permeability of the soils varies with the parent material from very low on clayey deposits to high on sandy outwash (Arnold and others, 1999).

The climate of the study region is classified as "Dfa" in the Köppen-Geiger system, which means humid continental with warm summers (Peel and others, 2007; Belda and others, 2014). This classification means winters are cold, summers are warm, and precipitation is common during the whole year. Based on 1971–2000 data, the average temperature at Chicago

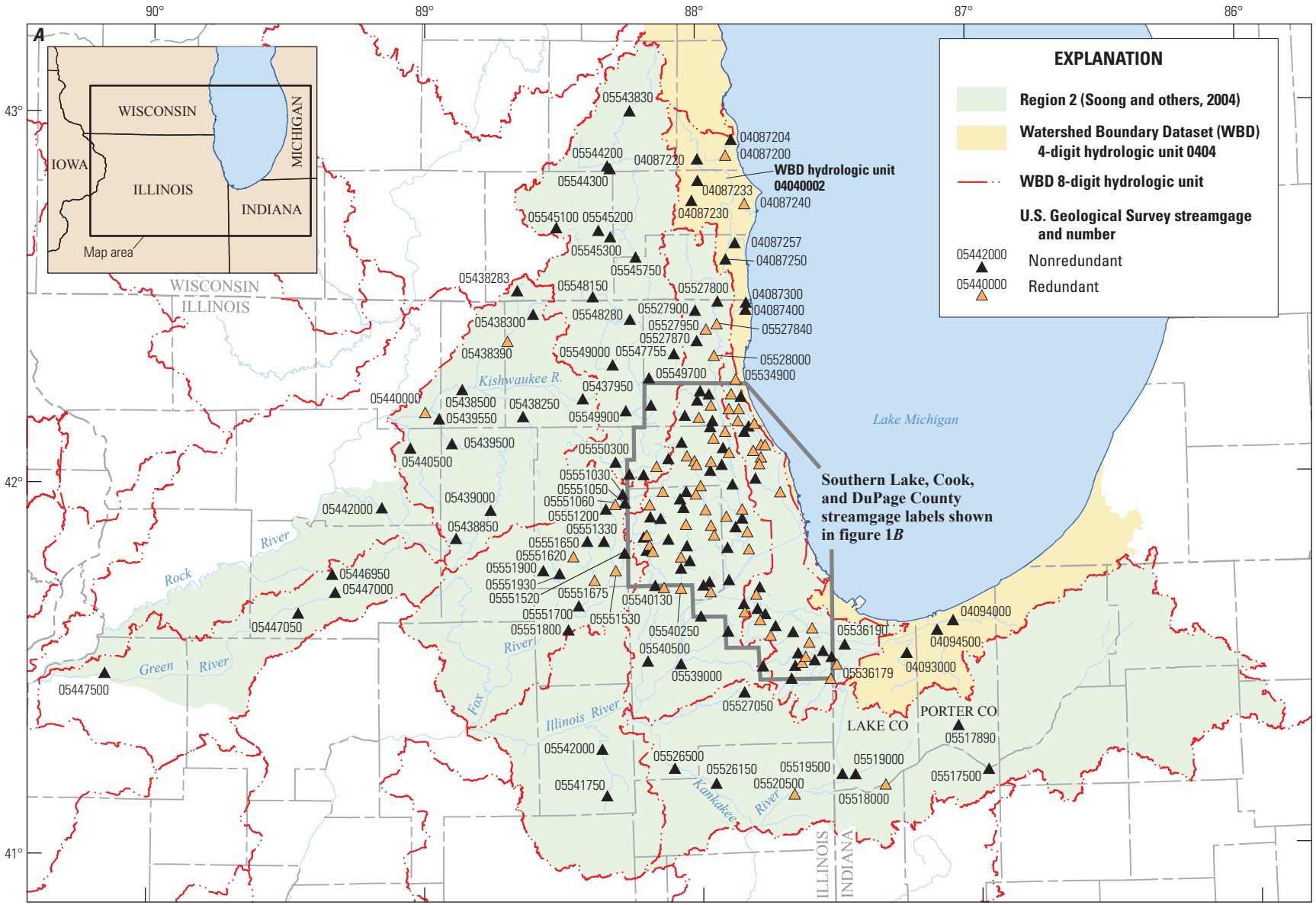

Base from U.S. Geological Survey digital data, 2000, 2012, 1:100,000
Albers Equal-Area Conic projection, Standard parallels 45° and 33°,
central meridian -89°. Watershed Boundary Dataset from Natural
Resources Conservation Service, 2012

Figure 1. Study area and streamgages used in this study: *A*, entire area; *B*, detail showing southern Lake, Cook, and DuPage counties in detail.

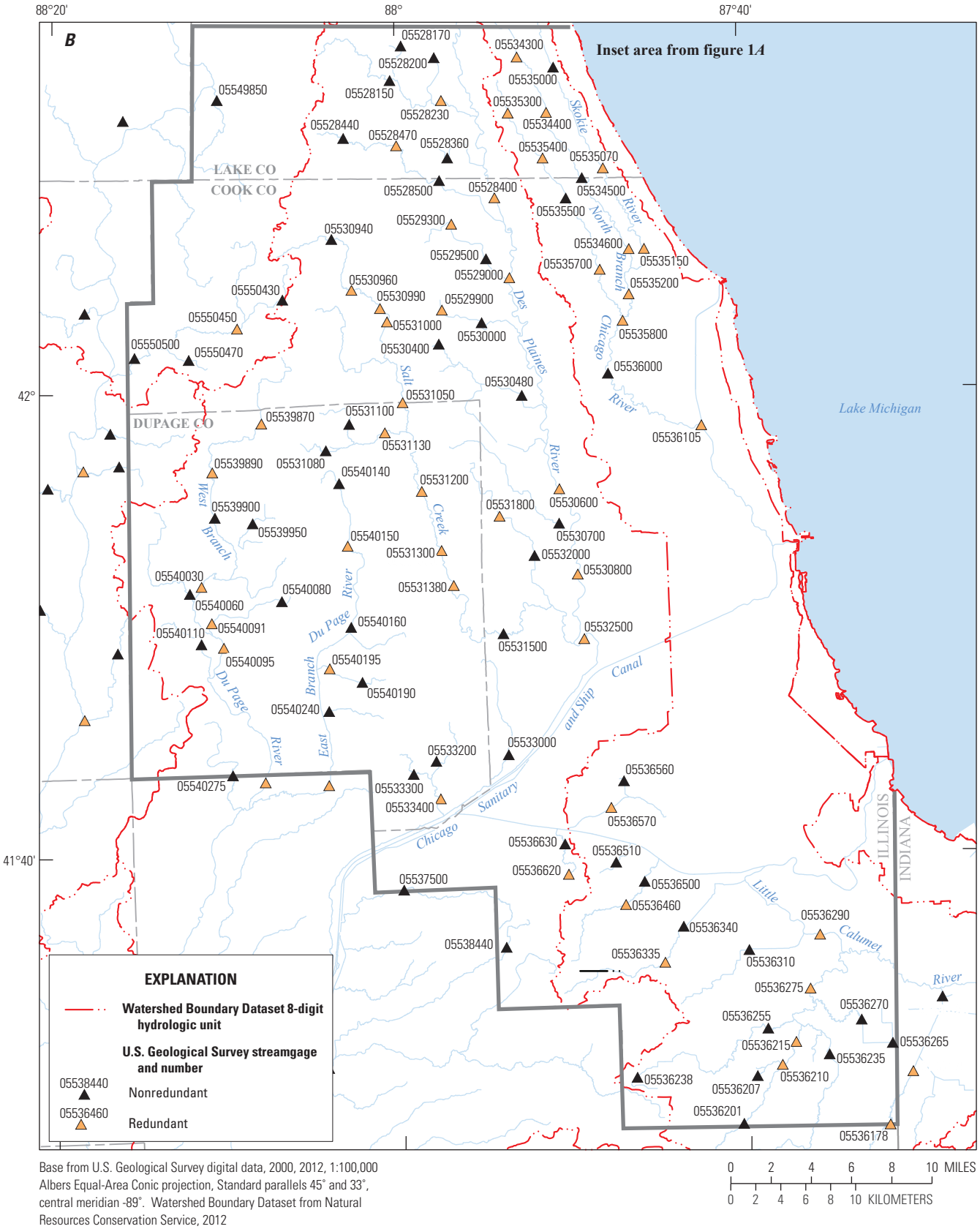

Base from U.S. Geological Survey digital data, 2000, 2012, 1:100,000
Albers Equal-Area Conic projection, Standard parallels 45° and 33°,
central meridian -89°. Watershed Boundary Dataset from Natural
Resources Conservation Service, 2012

Figure 1. Study area and streamgages used in this study: *A*, entire area; *B*, detail showing southern Lake, Cook, and DuPage counties in detail.—Continued

is about 50 °Fahrenheit (F), with average winter (December–February) daily highs of about 33 °F and lows of 17 °F and average summer (June-August) daily highs of about 82 °F and lows of 62 °F (Changnon and others, 2004). Based on 1981–2010 Parameter-elevation Relationships on Independent Slopes Model (PRISM) data (http://www.prism.oregonstate.edu/normals/, accessed April 15, 2014), precipitation for Chicago is about 35 inches per year, with a minimum monthly amount of about 2 inches in both January and February, increasing to about 4 inches per month during May–August before decreasing through the fall toward the winter minimum. About half the total precipitation is the result of thunderstorms and 3 to 3.5 inches falls as snow, based on 1941–1995 data (Changnon and others, 2004).

In the flood climate classification of Hayden (1988), the study area lies at the border of the "TsuCpSs**" region to the north and the "TsuCpSe*" region to the south, where "Tsu" indicates barotropic (nonfrontal or convective) and unorganized (that is, without tropical cyclones) in the summer, "Cp" indicates that frontal storms are possible throughout the year, and "Ss**" indicates that winter snow cover is seasonal and exceeds 50 centimeters (cm), so that there may be substantial spring snowmelt flooding, whereas "Se*" indicates seasonal, ephemeral snow cover for 10–50 days per year that may contribute to flooding during winter when rain falls on existing snow. The seasonality of precipitation in the study region and its flood classification explain the wide distribution of the timing of the annual maximum peak discharges used in this study (see "Streamgage Selection" section), with the largest monthly fractions in March, April, and June, but also substantial fractions in February and May, with smaller fractions during July to September.

Nonurbanized land cover in the study area includes a substantial fraction of row crop agriculture and also more forest, grassland, and open water and wetlands than the surrounding regions, which are primarily agricultural (Illinois Department of Natural Resources, 1996). Urbanized land use in the study area has been driven by population growth in metropolitan Chicago, which was dominated by that of the City of Chicago until 1940, when its population leveled off and population growth shifted to the suburbs (fig. 2). This suburban population growth was accompanied by even larger growth in developed land use; for example, from 1970 to 1990, the population grew by 4 percent, but developed land use grew by 40 percent, during which time more than 400 square miles (mi^2) of farmland that had been previously drained for agricultural use (Juhl, 2005) were developed (Mariner, 2005). This growth in developed land use is shown geographically in figure 3.

The hydrologic effects of this expansion of developed land in northeastern Illinois can be inferred from the series of historic floods that began in the 1950s and have extended to the present (2015) (Juhl, 2005; Changnon, 1999; Changnon and Westcott, 2002a, b; Angel and Changnon, 2008; Changnon, 2010; Changnon, 2011; Fazio and Sharpe, 2012; Villarini and others, 2013), though increases in precipitation

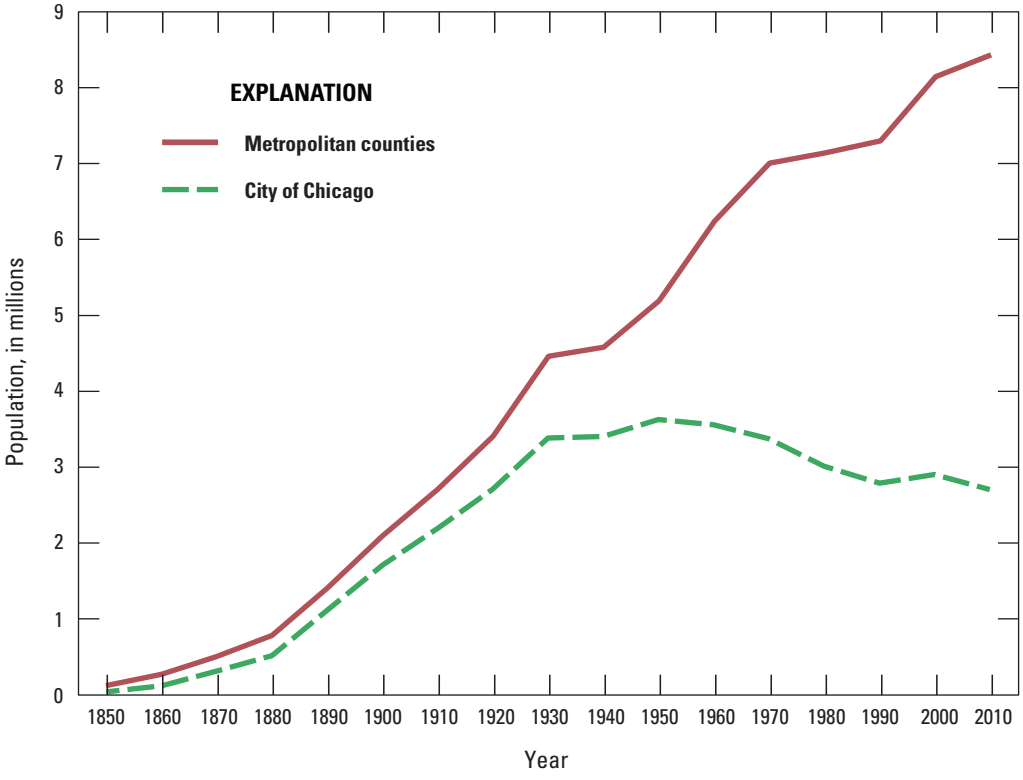

Figure 2. Population growth in northeastern Illinois, 1850–2010 (from Karstensen and others, 2013).

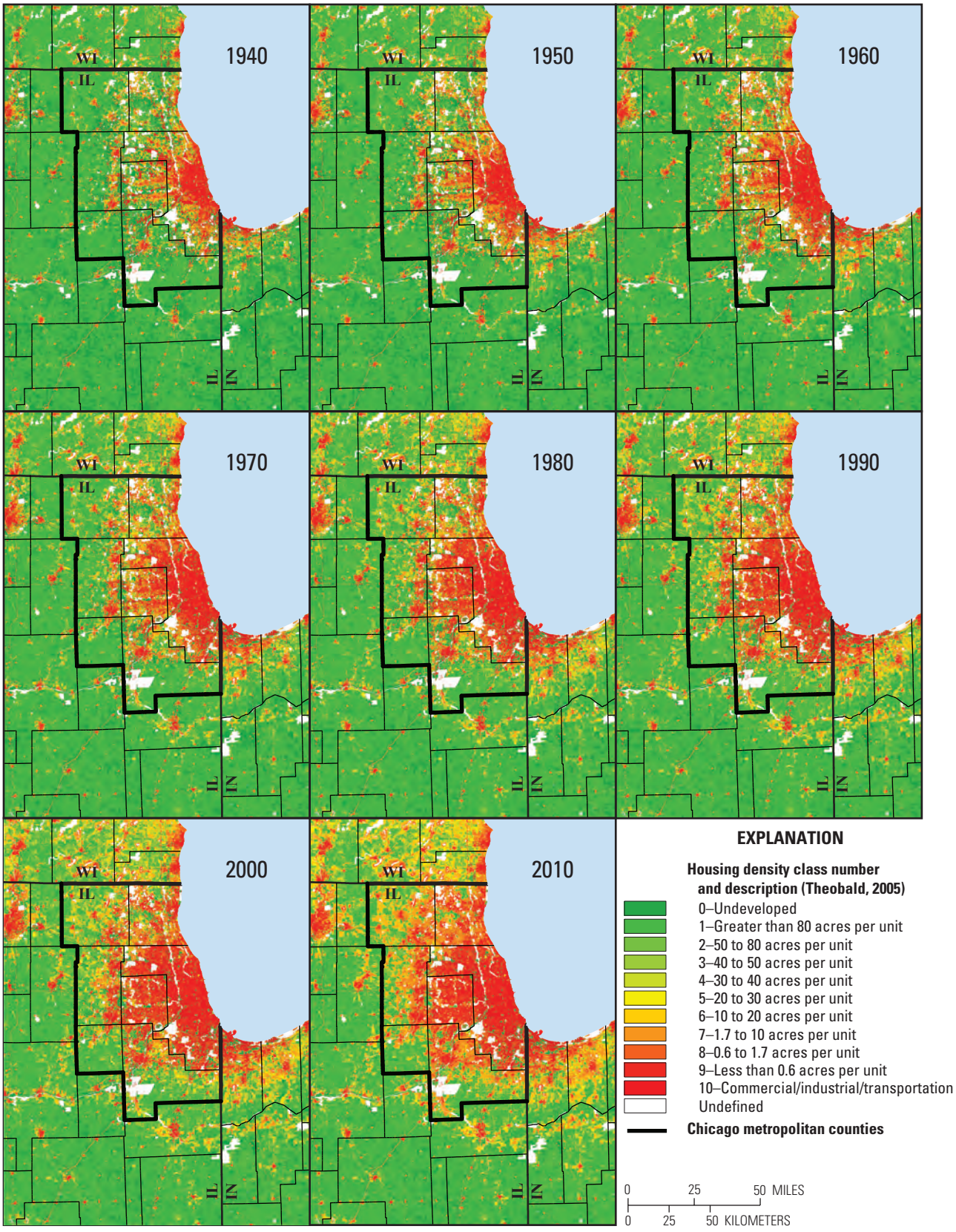

Figure 3. Housing density by decade in northeastern Illinois (modified from Karstensen and others, 2013).

have also been identified (Rougé and Cai, 2014; Winters and others, 2015). These floods led to several policy and engineering responses (Juhl, 2005). One such policy response was the introduction of ordinances requiring stormwater detention on new development, the first of which was promulgated in 1972 by the Metropolitan Water Reclamation District of Greater Chicago (MWRDGC). Another policy response was the passage of legislation by the State of Illinois allowing five suburban counties to plan and fund countywide stormwater management programs (Resource Coordination Policy Committee, 1998). A third policy response was the planning and construction of channel improvements and flood-control reservoirs (Resource Coordination Policy Committee, 1998).

Previous Studies

Allen and Bejcek (1979) developed regional spatial regression equations for peak discharge quantiles for the urbanized area of northeastern Illinois using data through WY 1976 as a function of impervious percentage, drainage area, and slope (all log-transformed). They used 103 streamgage records, including 70 crest-stage gages (CSGs), for many of which they developed stage-discharge ratings as part of the study. Drainage areas of the basins ranged from 0.07 to 630 mi^2 and impervious fractions from 1 to 38.7 percent. A decreasing effect of urbanization (measured as an estimated fraction of impervious area) was determined with increasing flood magnitude (decreasing AEP), as is generally expected (Konrad, 2003). The authors also suggest that the urbanization effect factor from their equations would be appropriate to use outside their study area elsewhere in Illinois and surrounding regions to adjust existing rural equations for use in urban areas, but that their results would not be appropriate for basins "completely served by underground drainage systems" or where "flood detention or retention reservoirs substantially affect the flood peaks" (Allen and Bejcek, 1979, p. 8).

Sauer and others (1983) completed a nationwide spatial regression study of the effect of urbanization on flood frequency that used the results of Allen and Bejcek (1979). Sauer and others used 199 streamgage records including 18 from Illinois, excluding streamgages with substantial manmade detention effects and excluding those for which the developed fraction had increased by more than 50 percent during the period of record. They developed three sets of spatial regression equations. Two sets include seven explanatory variables and the remaining set has three. The two seven-variable equation sets have the same variables except one uses basin lag time (estimated from observed rainfall-runoff data, where available) in place of a measure of channel efficiency determined following the methods of Espey and Winslow (1974). All three sets of equations include as explanatory variables drainage area, the rural peak discharge quantile, and the basin development factor (BDF), which is a numerical index of the presence of channel improvements, curbs and gutters, and storm sewers, and is not easily computable from standard GIS databases. These three common explanatory variables constitute the variables of the three-variable equation set. Impervious area fraction is included in the two seven-variable sets of equations, but it is not as significant as BDF. The coefficients of their equations also indicate a decreasing effect of urbanization for larger floods.

More recently, Moglen and Shivers (2006) developed an iterative method of adjusting rural flood frequency equations for the effects of time-varying urbanization, measured by one of two GIS-computable quantities, estimated impervious fraction and population density. Among their 78 study streamgages are 22 from Illinois, of which just one (Boneyard Creek at Urbana, USGS streamgage 03337000) is outside northeastern Illinois. One of the conclusions of the study listed as "Model Weaknesses" is that the apparent effects of urbanization are "relatively mild." In the use of GIS-computable quantities as the urbanization variable and directly incorporating time-varying urbanization, Moglen and Shivers' study is similar to this study. Their method does not, however, produce an adjusted time series of annual maximum peak discharges for each streamgage; rather, it produces just a set of urbanization-adjusted peak discharge quantiles.

Other studies that have characterized the effect of urbanization on flooding in northeastern Illinois include Changnon and Demissie (1996), Changnon and others (1996), Hejazi and Markus (2009), Villarini and others (2013), and Rougé and Cai (2014).

Soong and others (2004) divided the State of Illinois into seven hydrologic regions and developed regional regression equations for both annual maximum series (AMS) and partial duration series (PDS) peak discharges for rural basins in each region, using data through WY 1999. The basin characteristics used in the regression equations are drainage area, main channel slope, basin length, soil permeability, and percent open water and herbaceous wetland. For region 2, which is the focus area of this study, they used drainage area, main channel slope, and percent open water and herbaceous wetland. The AMS regression equations from the study were later implemented in StreamStats (Ishii and others, 2010).

Data Development

Data development for this study consisted of the computation of two sets of data values: (1) observed peak discharge quantiles, that is, the statistical relation between flood magnitudes and frequencies based on observed floods at selected streamgages and (2) basin characteristics, that is, quantitative descriptors of characteristics of the basins draining to the locations of the streamgages. Regression equations for estimating the peak discharge quantiles at ungaged locations were then developed using the basin characteristics.

Peak Discharge Quantiles at Streamgages

To develop equations for estimating peak discharge quantiles for ungaged stream locations, such quantiles were first computed at selected streamgages with at least 10 years of annual maximum peak discharges. This computation included four steps: (1) streamgage selection; (2) removal of redundant streamgages, where one streamgage of streamgage pairs whose basins are nested with substantial overlap are removed from the set of streamgages on which the regression analyses are done; (3) regional skew analysis, where a regional regression of at-streamgage skewness values is done to provide a regional estimate that is weighted with the at-streamgage skewness values in the frequency analysis; and (4) frequency analysis, where peak discharge quantiles at the selected AEPs are computed for each selected streamgage by fitting to the log-Pearson type III by a generalized method-of-moments method.

Streamgage Selection

The streamgages were chosen from the urbanized area of northeastern Illinois and nearby urbanized areas in northwestern Indiana and southeastern Wisconsin within hydrologic unit 0404, along with region 2 of Soong and others (2004) (figs. 1 and 3). In Indiana, the nearby urbanized area was selected as Lake and Porter Counties, and in Wisconsin, as consisting of the 8-digit hydrologic unit 04040002 (Pike-Root) (fig. 1). The decision to update only region 2 of Soong and others (2004) as part of this study was in part made on the assumption that only this region includes substantial numbers of streamgages identified as rural drainage basins that contain substantial fractions of urbanized land use. This assumption is verified in figure 4, which shows for example that 40 percent of gaged basins in region 2 used by Soong and others (2004) had urbanized fractions greater than 20 percent as of the last year of record used by Soong and others (2004), whereas only about 2 percent of gaged basins outside region 2 used by Soong and others (2004) had such an urbanized fraction.

A minimum record-length criterion of 10 years of record between WYs 1940 and 2009 was applied when selecting stations. Water year 1940 was chosen as the starting point of the study period because that is the earliest year available in the housing density data of Theobald (2005) that is used to estimate historical urbanization in this study. Water year 2009 was chosen as the ending point of the study period for consistency with the analysis of Over and others (2016).

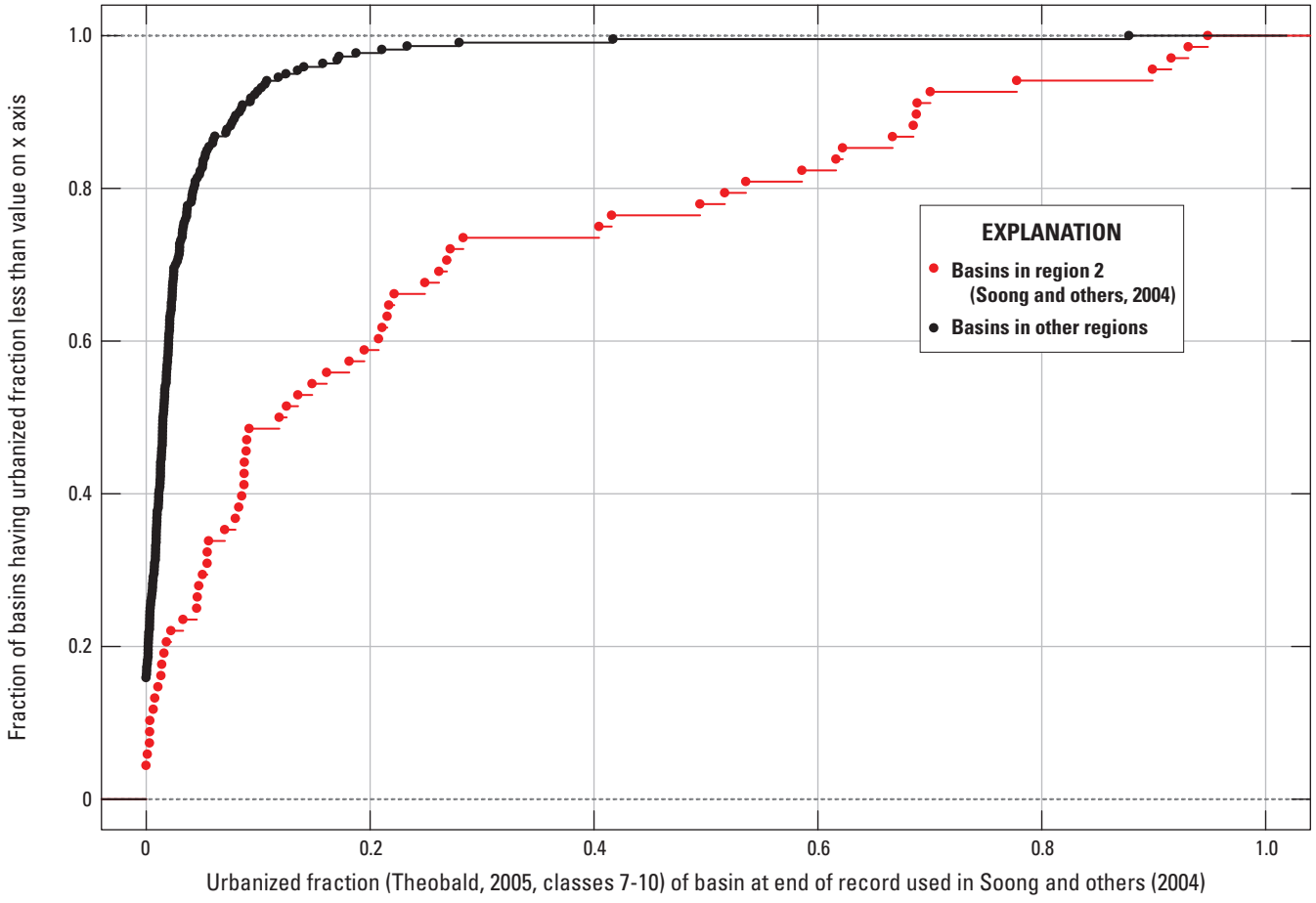

Figure 4. Empirical distribution functions of urbanized fraction of gaged basins in Illinois flood-frequency regions of Soong and others (2004).

The list of streamgages with at least 10 years of record in the study area was screened to eliminate those with potential measurement accuracy issues using several criteria. One was to refer to the list of streamgages used in the most recent published rural flood-frequency studies (Soong and others [2004] in Illinois, Rao [2006] in Indiana, and Walker and Krug [2003] in Wisconsin). John Walker (USGS, written commun., 2013) also provided a list of streamgages being used in an on-going flood-frequency study in Wisconsin. If a streamgage had been used in one of those studies, it was retained for this study unless specific problems were identified by data section staff at the Illinois, Indiana, or Wisconsin USGS Water Science Centers.

The 181 selected streamgages and some properties of their records and drainage basins are listed in table 1 (available at https://doi.org/10.3133/sir20165050). Histograms of the annual maximum peak discharge record properties at the selected streamgages are shown in figure 5. These histograms show a maximum in streamgage records beginning around 1960 and ending around 1980, which were primarily CSGs on small (less than about 10 mi²) drainage basins (table 1). Histograms of the urban fractions of the streamgage drainage basins in figure 6 show substantial urban fraction increases throughout the streamgage periods of record and further urban fraction increases between the ends of the streamgage records and 2010. These increases in urbanization underscore the nonstationary nature of the land use in the study basins and the need for adjustment to current (2010) conditions. Overall, drainage areas range from less than 0.01 mi² to more than 1,000 mi², but the most are between 1 and 300 mi² (fig. 6).

Annual maximum peak discharge data for the selected stations were retrieved from the National Water Information System (NWIS) (U.S. Geological Survey, 2013).

Redundancy Analysis

The generalized least-squares analysis that is used to fit the regression models for the peak discharge quantiles that form the basis of the final results of this study allows for cross-correlation among the observed quantiles that is induced by temporal factors such as the same storm hitting two nearby basins and causing the annual maximum peak discharge for both. Generalized least-squares regression, however, does not account for correlation in the model error that arises when two nested basins have an appreciable overlap in drainage area (Veilleux, 2009). When the overlap is large enough, one of the basins is considered redundant for purposes of regional regression modeling (Veilleux, 2009). To address this issue, a redundancy analysis was carried out to determine an optimal nonredundant subset of the original 181 stations.

Because any one gaged basin may be nested within multiple other gaged basins or have multiple other gaged basins nested within it, a way to decide in what order basins should be removed was needed. For this study, the decision was made by assigning a score to each gaged basin based on its record length and drainage-basin properties and its amount of overlap with other gaged basins, removing the basin with the worst (highest) score, followed by re-computation of the scores, removing the remaining basin with the worst recomputed score, and proceeding in this way until no basin remained with an overlap fraction larger than 0.205, where the overlap fraction DAR_{ij} for two nested basins i and j is defined as

$$DAR_{ij} = \min\left[\frac{DA_i}{DA_j}, \frac{DA_j}{DA_i}\right], \quad (1)$$

where

DA_i and DA_j are the drainage areas of basins i and j, respectively.

Originally a maximum overlap fraction of 0.2 as suggested by Veilleux (2009) was chosen, but it was determined that a few basins could be retained by increasing the value slightly to 0.205. A script was written in R (R Core Team, 2014) to implement this algorithm.

The details of computation of the score are as follows: The score $S_i(t)$ for basin i at iteration step t is computed as the sum, $\sum_j s_{ij}(t)$, over all remaining basins j having basins overlap with basin i, where $s_{ij}(t)$, the subscore of basin i with overlapping basin j at step t, is computed as

$$s_{ij}(t) = DAR_{ij}\left[2 - RL_i/\max(RL)\right]\left[d_i(t)+1\right], \quad (2)$$

where

DAR_{ij} is the overlap fraction between basins i and j (eq. 1),

RL_i is the record length of the streamgage at basin i, in years,

$\max(RL)$ is the maximum record length in the dataset (70 years), and

$d_i(t)$ is the probability density value of the drainage area of station i at step t scaled to lie between 0 and 1.

Based on their definitions, DAR_{ij} lies between 0 to 1, $2 - RL_i/\max(RL)$ between 1 and 2, and $d_i + 1$ between 1 and 2. The effect of each of the factors making up the subscore s_{ij} on its value is as follows: (a) with more overlap of basin areas, DAR_{ij} is larger, and so is s_{ij}; (b) with shorter record length RL_i, $2 - RL_i/\max(RL)$ is larger and so is s_{ij}; and (c) when the drainage area of basin i is at a larger density value (where there are many basins of similar drainage areas), d_i is larger and so is s_{ij}; consequently, larger basin overlaps, shorter records, and larger drainage area overlaps raise the subscore and therefore the score, making the associated streamgage more likely to be removed.

The result of applying this algorithm was to remove 64 of the original 181 to leave 117 nonredundant streamgages, of which 57 were CSGs throughout their peak discharge record, 13 were CSGs during part of their peak discharge record, and 47 had continuous record throughout their peak discharge records. These 117 streamgages were used for all subsequent analyses. Streamgages that were used and streamgages that

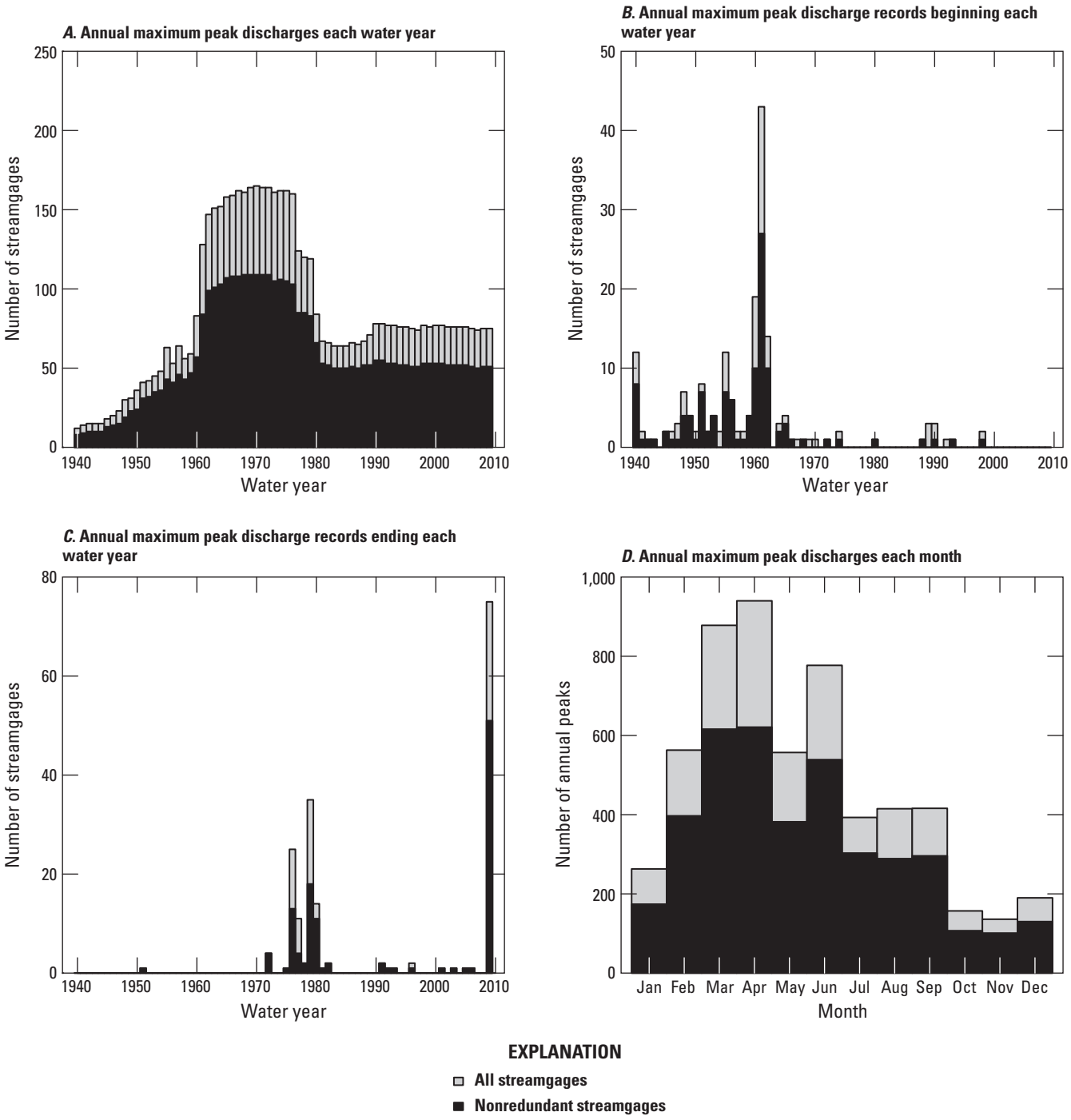

Figure 5. Properties of U.S. Geological Survey streamgage records used in this study in northeastern Illinois. *A*, number of streamgages with annual maximum peak discharges each water year; *B*, number of streamgages with annual maximum peak discharge records beginning each water year; *C*, number of streamgages with peak discharge records ending each water year; *D*, number of annual maximum peak discharges in each month of the year.

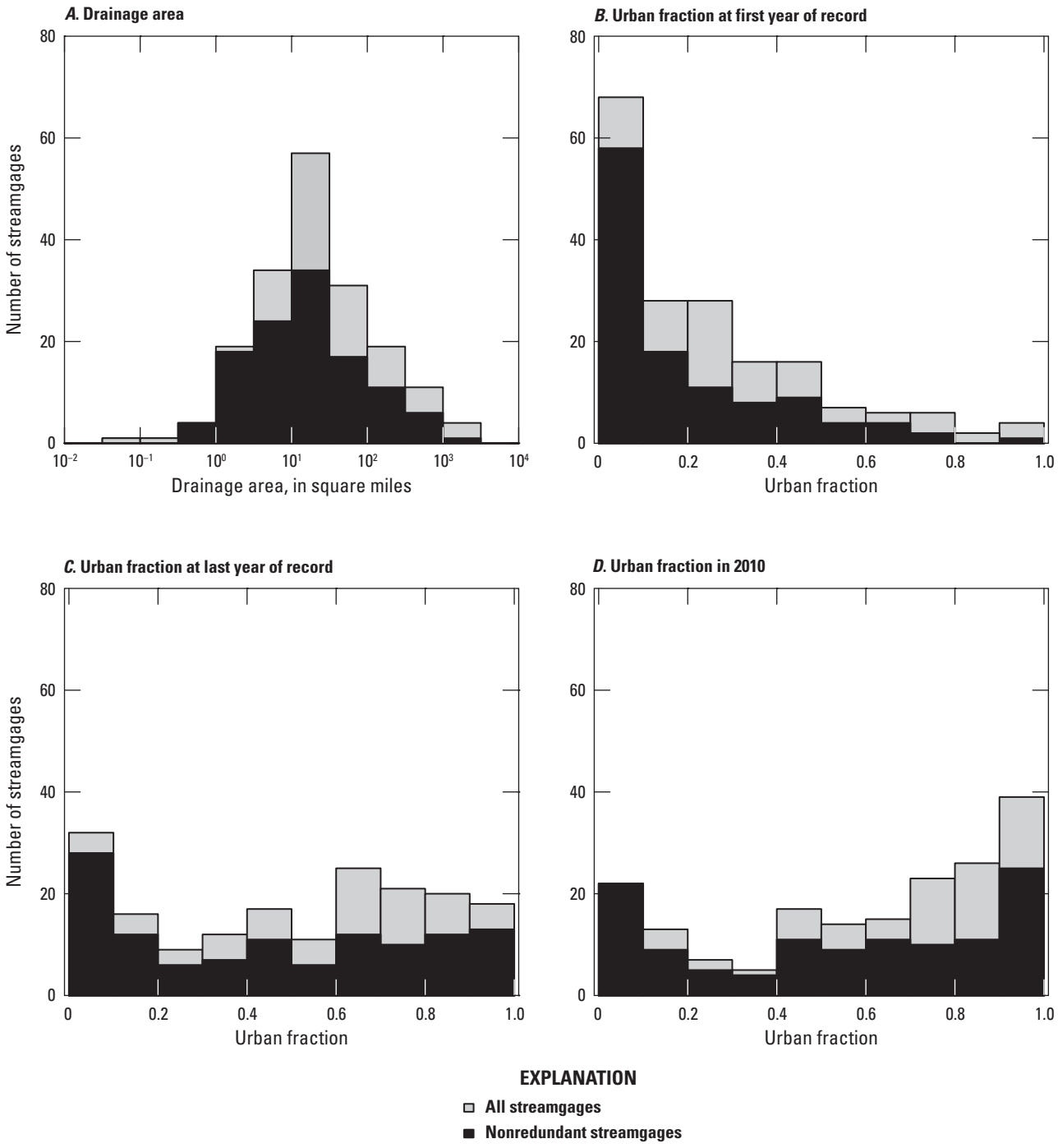

Figure 6. Properties of basins of U.S. Geological Survey streamgages used in this study in northeastern Illinois. *A*, basin drainage areas, *B*, urbanized basin fractions at first year of streamgage records, *C*, urbanized basin fractions at last year of streamgage record, and *D*, urbanized basin fractions in 2010, where urbanized is defined as Theobald (2005) housing density fewer than 10 acres per house plus commercial/industrial/transportation land use.

were considered redundant are indicated in the study area maps (fig. 1), the histograms describing the basic properties of the streamgage records and their basins (figs. 5 and 6), and in the table listing the basic properties of the streamgage records and their basins (table 1).

Regional Skew Analysis

Although the Expected Moments Algorithm (EMA) (Cohn and others, 1997 and 2001) used in this study to obtain estimates of the peak discharge quantiles generalizes the method-of-moments method of Bulletin 17B (U.S. Interagency Advisory Committee on Water Data, 1982), it still relies on estimates of the mean, variance, and skewness of the logarithms of the annual maximum peak discharge data at each streamgage. Of these moments, the skewness, because it involves raising the data values to the third power, is very sensitive to extreme values and thus has a large uncertainty when estimated from the data at a single site. Therefore, weighting at-site and regional skew estimates in inverse proportions to their uncertainties to obtain a weighted skew estimate was recommended in Bulletin 17B and continues to be recommended. Because the map in Bulletin 17B showing a grid of regional skew values has become outdated, newer and more refined maps have been created, such as the one in Soong and others (2004) for Illinois. These maps, however, do not address the effects of urbanization. Furthermore, a new approach to the estimation of regional skew through Bayesian generalized least-squares (GLS) analysis has been developed (Reis and others, 2005; Gruber and others, 2007; Gruber and Stedinger, 2008; Veilleux, 2011) that has shown the ability to reduce the uncertainty in regional skew estimates and allows the regional skew estimate to take into account basin characteristics where applicable.

Details of the new approach and its application in this study are given in appendix 1. The data analyzed were the annual maximum peak discharges at the nonredundant streamgages adjusted to 2010 urbanization conditions. The selected regional skew model is dependent on the urban fraction as measured by the *NLCD_22_23_24* variable, that is, the sum of fractions of National Land Cover Database (NLCD) 2011 classes 22 (developed, low intensity), 23 (developed, medium intensity), and 24 (developed, high intensity), according to the linear relation:

$$\hat{\gamma}_R = -0.39 + 0.97 NLCD\_22\_23\_24^{1/2}, \quad (3)$$

where

$\hat{\gamma}_R$ is the regional skewness.

Skewness increases substantially with urbanization from a value of -0.39 for a basin with no urbanization ($NLCD\_22\_23\_24 = 0$) to $-0.39 + 0.97 = 0.58$ for a basin where the *NLCD_22_23_24* fraction is 100 percent. The regional skewness estimate from equation 3 was combined with the at-site skewness according to their associated uncertainties to obtain a weighted skew estimate for use in computing the at-site peak discharge quantile estimates as described in the "Frequency Analysis" section.

Frequency Analysis

The peak discharge quantiles with AEPs of 0.50, 0.20, 0.10, 0.04, 0.02, 0.01, 0.005, and 0.002 for redundant and nonredundant streamgages (table 2, available at https://doi.org/10.3133/sir20165050) were computed by applying the EMA approach (Cohn and others, 1997 and 2001), along with the Multiple Grubbs-Beck test (Cohn and others, 2013) to detect and censor PILFs, to the annual maximum peak discharges adjusted to 2010 urbanization conditions as described in the "Regional Temporal Regression Analysis and Adjustment" section below. The EMA methodology generally follows guidelines provided in Bulletin 17B of the U.S. Interagency Advisory Committee on Water Data (1982) by using the log-Pearson Type III distribution fitted by the method-of-moments for estimating discharge frequency; however, the EMA methodology provides updated procedures for incorporating historical and censored peak discharges. Use of the EMA approach and the Multiple Grubbs-Beck test are as recommended by the Hydrologic Frequency Analysis Work Group (https://acwi.gov/hydrology/Frequency/HFAWG-B71B-Recommended-Rev-SOH-12June2013-revised-final.pdf). Software developed by the USGS to analyze peak discharge data (PeakFQ version 7.3, https://water.usgs.gov/software/PeakFQ/) was used for these computations (Veilleux and others, 2013).

As part of the frequency analysis, the skewness values for each streamgage were computed as a weighted average $\hat{\gamma}_W$ of the station and regional skew values following the method suggested in Bulletin 17B (U.S. Interagency Advisory Committee on Water Data, 1982):

$$\hat{\gamma}_W = \frac{AVP_{new} * \hat{\gamma}_S + MSE[\hat{\gamma}_S] * \hat{\gamma}_R}{AVP_{new} + MSE[\hat{\gamma}_S]}, \quad (4)$$

where

$\hat{\gamma}_W$ is the weighted skewness,

$\hat{\gamma}_R$ is the regional skewness computed as described in the "Regional Skew Analysis" section and in appendix 1,

$\hat{\gamma}_S$ is the station skewness computed by using the EMA approach as implemented in PeakFQ for each streamgage,

$AVP_{new} = 0.19$ is the average variance of prediction at a new site computed as described in appendix 1, and

$MSE[\hat{\gamma}_S]$ is the mean square error of the at-site skewness, which also is computed by using the EMA approach as implemented in PeakFQ.

Basin Characteristics

The starting point in defining basin characteristics for regional statistical analyses is to delineate the basin boundaries. Following delineation, basin characteristics for this study were computed following two main approaches. The first was the traditional approach in projects of this type, using spatially averaged or basin-wide properties such as drainage area, fractions of various land uses and soil types, average soil properties, and physiographic properties such as basin slope. The second approach was to develop and analyze spatially distributed basin characteristics based on properties of estimated instantaneous unit hydrographs (for example, Grimaldi and others, 2010). The spatially distributed approach was proposed as a way to see if the effects of basin shape and the location, not just the amount, of different types of hydrologically relevant characteristics such as urbanized areas and open water and wetland on flood-frequency characteristics were significant and could improve flood- frequency prediction. Preliminary results with the spatially distributed approach were not promising and as a result it was dropped from further consideration. As this approach was not used in the final results, it is not discussed further in this report.

Basin Delineation

Most basins were delineated by using the online Illinois StreamStats application (https://streamstats.usgs.gov/), which is based on Environmental Systems Research Institute's (Esri's) Arc Hydro Tools software (Maidment, 2002). Illinois StreamStats uses the 1:100,000-scale National Hydrography Dataset (NHD) for hydrography and the 30-meter National Elevation Dataset (NED) resampled to a 10-meter resolution for elevation information for Illinois, Wisconsin, and Indiana. Seven Indiana basins were delineated using the Indiana StreamStats application, a similar application to Illinois StreamStats, because the results were slightly better in delineating the Kankakee River than the Illinois StreamStats results. Eight Wisconsin basins in the hydrologic unit 0404 (Lake Michigan) were provided by the USGS Wisconsin Water Science Center because the Illinois StreamStats does not cover that area and Wisconsin StreamStats did not exist at the time of the analysis. Resulting drainage areas from the Illinois StreamStats application were compared to the drainage areas of hand-drawn boundary (HDB) basin delineations, which are considered to be the most accurate delineation type. For those basins with discrepancies larger than about 10 percent, it was decided that the HDB delineations were preferable. These basins are usually small urban basins with records that ended around 1980, where it is difficult to determine basin boundaries because of urban development and the related potential for later modifications to the hydrography and topography.

Spatially Averaged Basin Characteristics

A common challenge in projects of this type is to select among the many basin characteristics that are available in GIS databases. As this project is in part an update of the regional regression equations for region 2 from the rural flood-frequency study by Soong and others (2004), which used spatially averaged basin characteristics, it was decided to simplify the process of the selection of basin characteristics by considering only the categories of characteristics used by Soong and others (2004) in that region, which were drainage area, slope, and wetland-open water fraction, plus measures of urbanized area (table 3, available at https://doi.org/10.3133/sir20165050).

The slope variable used in Soong and others (2004) is main channel slope. The determination of the main channel requires sometimes lengthy computations in StreamStats and is in any case ambiguous, so alternative slope variables were considered for this study. These alternatives included the basin average of digital elevation model (DEM) slopes, the basin average of the State Soil Survey Geographic Database (SSURGO) soil slopes, and basin slope computed as maximum–minimum basin elevations divided by basin perimeter (table 3).

The wetland-open water variable used in Soong and others (2004) was percent water and herbaceous wetland from the 2001 NLCD (Soong and others, 2004, p. 16). Additional open water and wetland variables derived from the 2011 NLCD, National Wetlands Inventory (NWI), and SSURGO were considered in this study (table 3).

The urbanized area variable used for temporal analysis and adjustment of the annual maximum peak discharge records (Over and others, 2016) was derived from a year 2000 U.S. Census housing density database developed by David Theobald (Theobald, 2005). For the spatial modeling of the peak discharge quantiles, it was preferred that the urbanization variable be something that is regularly updated; therefore developed area fractions and impervious percentage from the 2011 NLCD were chosen, with the Theobald housing density urbanization estimates retained for comparison (table 3).

Regional Temporal Regression Analysis and Adjustment

The purpose of the temporal analysis of the annual maximum peak discharges is to provide a means of adjusting the peak discharge records from the streamgages used in the study to their levels of urbanization at a common year (2010). This adjustment is needed to provide approximately stationary and contemporary streamgage records. The method of the analysis is to use regression to determine values of coefficients

that characterize the regional average effect of urbanization on peak discharge quantiles as a function of exceedance probability in Illinois flood-frequency region 2. The coefficients also are used to develop factors for adjusting estimates of peak discharge quantiles in other regions of Illinois for the effect of urbanization. The adjusted annual maximum discharges and associated peak discharge quantiles also are made available herein for general use (see table 2 for quantiles and the "Adjustment of Annual Maximum Peak Discharges to Current (2010) Urban Fractions" section for discharges).

The effects of changes in urbanization in a streamgage record are potentially problematic in a regression analysis of peak discharge quantiles on basin characteristics for at least two reasons. One is that peak discharge records on basins with substantial changes in the fraction of urbanization over the streamgage period-of-record are difficult to use because no single value of urbanization fraction characterizes the entire record. The second is that historical urbanization information is needed to characterize the urban fraction of records that ended some time ago and urbanization of their basins continued after the records ended. Because both of these situations are fairly common in the study region (fig. 6), a method for adjustment of peak discharge records to their levels of urbanization at a common year was needed if such stations were going to be included in the study.

The methods used here for temporal analysis and adjustment were described by Over and others (2016); a summary of the application of their method in this study follows. Over and others use a two-step regression method applied to annual maximum peak discharge records as a function of contemporaneous urbanization and precipitation. In the first step, after breaking the peak discharge records into segments at the time of major abrupt changes in the basins, if any, ordinary least-squares (OLS) regression is used to estimate an intercept for each segment. In the second step, after subtracting the segment intercepts to homogenize the data across all the segments, the homogenized data are analyzed with quantile regression, which provides regional urbanization and precipitation coefficients for a sequence of AEPs and a means of assigning AEPs to each flood-discharge observation. The urbanization coefficient for the AEP assigned to each peak discharge observation is then used to adjust the observation to the estimated 2010 urbanization level in the basin where it was observed. Adjustment for changes in precipitation was not implemented, because, unlike changes in urbanization, changes in precipitation are highly uncertain and may reverse themselves in the future.

Data Used in This Analysis

In addition to the annual maximum peak discharge data from the nonredundant streamgages, three types of data were used for the temporal analysis and adjustment method applied in this study: (1) historical urbanization, (2) precipitation associated with each peak discharge, and (3) information on reservoirs and other structural flood-control measures such as channelization.

The historical urbanization data used, as in Over and others (2016), were those of Theobald (2005), which are 1940–2010 decadal housing density data based on the 2000 U.S. Census for 10 categories of housing density (including undeveloped) plus nonhousing urbanization (commercial, industrial, and transportation) (fig. 3). Theobald's nonhousing urbanization estimates, which are constant year 2000 values, were adjusted in proportion to changes in housing density for each basin according to a technique presented in Over and others to obtain 1940–2010 decadal estimates. Following Over and others, the decadal values of housing density classes 7–10 (fig. 3), which encompass areas with housing densities of no more than 10 acres per unit plus adjusted nonhousing urbanization, were linearly interpolated to annual values and used as the urbanization measure for the temporal analysis and adjustment in this study.

To account for effects of trends in precipitation alongside the effects of urbanization on peak discharges, precipitation values were estimated for each observed peak discharge used in this study. Because the density of daily precipitation gages is much higher than that of hourly gages, daily data were used. Three sets of daily precipitation data were used for the estimates: (1) National Weather Service (NWS) cooperative network (COOP) stations in the study area; (2) the Cook County Precipitation Network (CCPN) (Westcott, 2015); and (3) precipitation data collected by the Argonne National Laboratory (http://www.atmos.anl.gov/ANLMET/, accessed March 10, 2011). Data from COOP were downloaded from the Midwestern Regional Climate Center (MRCC) Applied Climate System (MACS) at https://mrcc.illinois.edu/CLIMATE/. Missing data during the study period (WYs 1940–2009) were filled by using a weighted average of values at neighboring gages, where weights were determined by an inverse-distance weighting technique (Over and others, 2016). Precipitation data were distributed spatially by using Thiessen polygons (Thiessen, 1911) (fig. 7), and daily values for the basin upstream from each streamgage in the study were computed as area-weighted average of the values in each Thiessen polygon overlying the basin. An estimate of the precipitation associated with each annual maximum peak discharge was obtained by selecting the maximum daily precipitation during the period from 3 days before to 1 day after the date of the peak discharge. Precipitation data dated after the peak discharge were used because NWS cooperative precipitation measurements typically are made during the early morning of the date assigned to the data, and therefore include precipitation from the previous day.

Information on reservoirs and other structural flood-control measures were obtained by accessing the 2013 National Inventory of Dams (NID; U.S. Army Corps of Engineers, 2013), reviewing relevant reports, inquiring of various Federal, State, county, and local agencies involved in flood control in northeastern Illinois, and searching historical imagery on Google Earth. By reviewing this information, reservoirs and

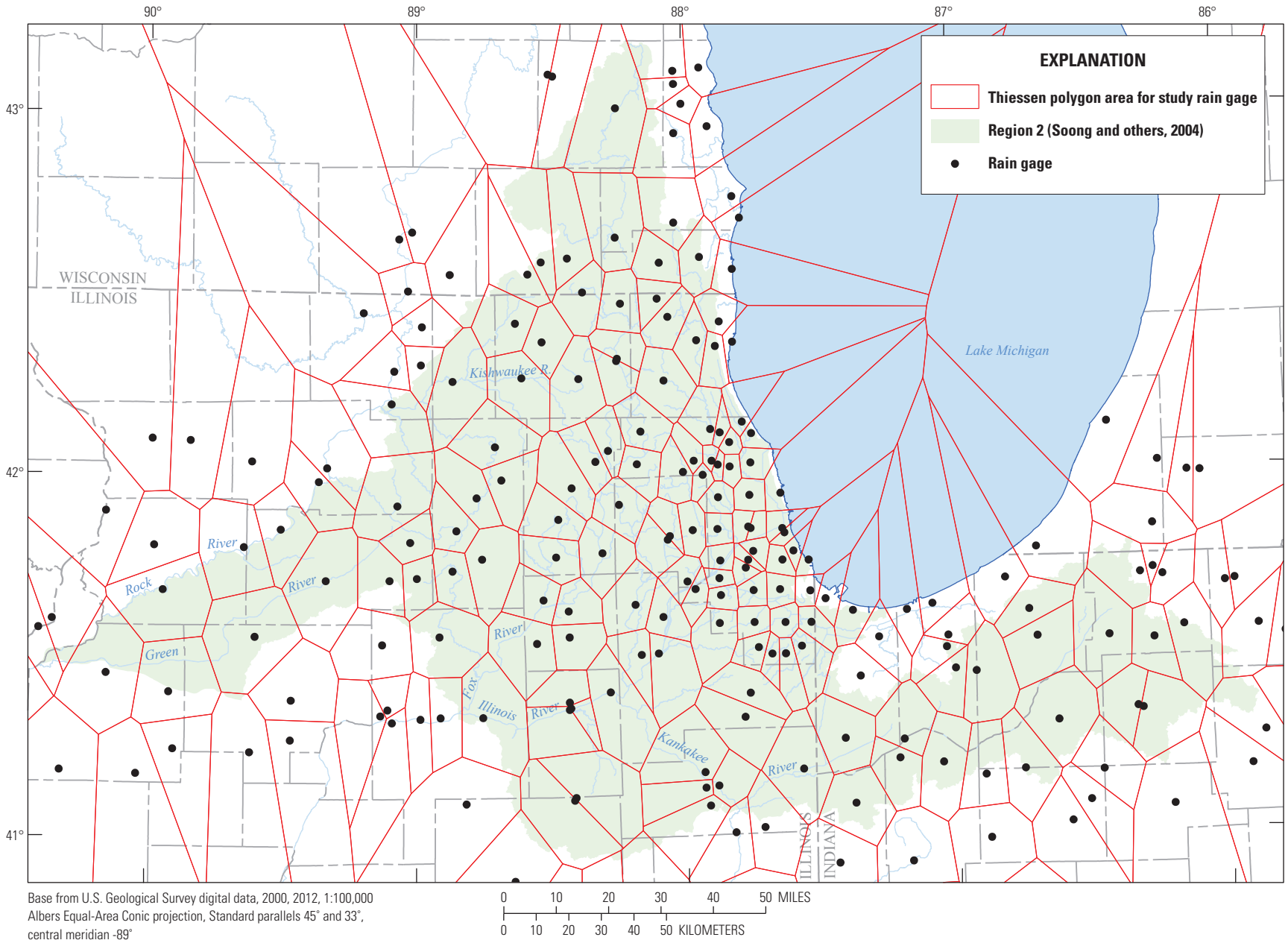

Figure 7. Locations of precipitation stations used in this study and their Thiessen polygons.

other structural flood-control measures (for example, channelization) within the basins of the streamgages used in this study were determined. For the identified reservoirs, three particular quantities were obtained: (1) the year of construction, (2) the volumetric capacity, and (3) the basin area upstream from the reservoir or other flood-control measure.

The volumetric capacity and upstream area were used to estimate the magnitude of the hydrologic effect of the reservoir. When a reservoir controlling at least 10 percent of the streamgage drainage area and with a volumetric storage capacity divided by the streamgage drainage area of 0.40 inches or other substantial change in the effect of a basin's structural flood-control measures was deemed to have changed during the period-of-record of a streamgage used in the study, the year of the change was dropped from the temporal analysis and the remaining record was broken into segments at that year. After the segment y-intercept values were obtained by a preliminary run of the first, OLS, step of the temporal analysis procedure, if the intrastreamgage y-intercept values were anomalous (for example, showing a significant increase following the construction of a flood-control reservoir), further research was completed on the basin history. If no reason to explain the anomaly was found, the segment break where the anomaly occurred was dissolved and the record was reconnected. The final set of segments used is presented in table 4 (available at https://doi.org/10.3133/sir20165050). According to table 5, all but 18 of the 117 nonredundant streamgages have only 1 segment, and only 3 streamgage records were split into more than 2 segments. Peak discharges associated with segments shorter than 5 years, historic peak discharges, censored peak discharges, and peak discharges for which the date is not known also were dropped from the temporal analysis.

Temporal Analysis of Urbanization Effect

The annual maximum peak discharges at the nonredundant streamgages during the study period, separated into segments as necessary based on the construction of structural flood-control measures with certain years of data dropped as described in the "Data Used in This Analysis" section, along with associated precipitation and urban fraction values, constituted the database for the temporal analysis of the effect of urbanization (table 6, available at https://doi.org/10.3133/sir20165050). The results of this analysis were used to adjust the annual maximum peak discharges to their urban factions at a common year (2010) based on an analysis to determine the regional effect of changes in urban fraction on peak discharge magnitude.

In addition to the peak discharge values dropped from the temporal analysis because of segment breaks, certain coded peak discharge values were also dropped. Peak codes as they appear in the peak discharge data downloaded from NWIS are given in table 6, column titled "NWIS peak codes," and whether or not a particular peak discharge value was used in the temporal regression analysis to perform the urbanization adjustment is indicated in table 6, column titled "Discharge value used in adjustment regression." As documented by those two columns of table 6, peak discharge values with codes of 1, 4, 7, 8, or B were dropped from the temporal regression analysis. These codes indicate that the published values are subject to censoring (codes 1, 4, 8), are historic peaks (code 7), or the date of the peak discharge event is not known (code B). These peak discharge values were nevertheless adjusted, and the adjusted values appear in table 6. These values also were used in the spatial regression analysis, because the spatial analysis does not require knowing the date of the event and the EMA methodology is designed to handle censored and historic values, as discussed in the "Frequency Analysis" section.

The temporal analysis was carried out by the method described in Over and others (2016), which follows a two-step linear regression technique suggested by Canay (2011), where the first step uses OLS regression to estimate intercepts for each segment of peak discharge data, and the second step applies quantile regression (Koenker, 2005) to the peak discharge data with the segment intercept values subtracted. The segment intercepts are subtracted from the peak discharge observations to obtain segment-independent observations that are approximately homogeneous (that is, segment-independent), to which quantile regression can be applied. Quantile regression is used in the second step because it provides an estimate of the coefficients of the regression model for different quantiles (exceedance probabilities). Because of this property, the disparate effect of urbanization at different exceedance probabilities (Espey and Winslow, 1974, and references therein; Allen and Bejcek, 1979; Konrad, 2003, and references therein; Over and others, 2016, and references therein) can be estimated, and the adjustment of the peak discharges to their urban fractions at a common year (2010) can take this disparate effect into account.

The independent variables in the two-step regression analysis are urban fraction and precipitation. Precipitation

Table 5. Number of segments per streamgage record used in regression analysis of peak discharge for 117 streamgages, northeastern Illinois and adjacent states.

[>, greater than]

Number of segments per streamgage record	>0	>1	>2	>3	>4
Number of records	117	18	3	2	0

is used in the regression analysis not so that the peak discharges can be adjusted to a present (2010) precipitation regime, as it was beyond the scope of this study to establish one, but so that by including precipitation, trends that happened to exist in the precipitation causing the observed peak discharges would not be falsely interpreted as the effect of changes in the urban fraction.

The following linear regression model was used for the least-squares regression analysis and was the first step of the method:

$$y_i(t) = \hat{y}_i(t) + \varepsilon_i(t) = a_i + b_1 P_i(t) + b_2 U_i(t) + \varepsilon_i(t), i = 1, 2, \ldots, N, \quad (5)$$

where

$y_i(t) = \log_{10} Q_i(t)$ is the base-10 logarithm of the annual maximum peak discharge at the *i*th segment during year *t*,

$\hat{y}_i(t)$ is the fitted value of $y_i(t)$ according to the regression relation,

a_i is the intercept of the *i*th segment,

$P_i(t)$ and $U_i(t)$ are the precipitation and urban fraction, respectively, for the *i*th segment during year *t*,

b_1 and b_2 are the regression coefficients for precipitation and urban fraction, respectively, and

$\varepsilon_i(t) = y_i(t) - \hat{y}_i(t)$ is the regression error for the *i*th segment during year *t*.

Notice there is one intercept for each segment, whereas there is only one value of each of the coefficients; therefore they are estimated from the effect of precipitation and urbanization on all the segments combined, and are equivalent in value to an uncertainty-weighted mean of the coefficients of segment-by-segment least-squares regression analysis (Frees, 2004, p. 32). Therefore, the segment intercepts contain all the information that distinguishes one segment from another; the effects of urbanization and precipitation, captured in their coefficients in equation 5, are assumed to be the same for all segments. The computation of the regression model was done in R (R Core Team, 2014) using the plm function from the plm package (Croissant and Millo, 2008).

The coefficients obtained by fitting the regression relation (eq. 5) are given in table 7, and the values of the intercepts for each segment are given with the other segment information in table 4 and are plotted in figure 8. As can be seen from the linear relation with limited scatter in figure 8, the segment intercept values are mostly but not completely explained by drainage area. According to the coefficients in table 7, there is a small, positive effect of precipitation, which is highly significant because the magnitude of the coefficient is much larger than its standard error (SE). The urban fraction coefficient is also positive but larger and also highly significant. Because the regression relation is of the form $\log_{10} Q = a + b_2 U$, the ratio of peak discharge for two different values of urban fraction U_1 and U_2 at the same site is given by $Q_2 / Q_1 = 10^{b_2 (U_2 - U_1)}$; the value of the urban fraction coefficient b_2 indicates that for a 10-percent increase in urban fraction, the ratio of peak discharges is $Q_2 / Q_1 = 10^{b_2 (0.10)} = 10^{0.5079 * 0.10} = 1.124$, or about a 12-percent increase. Although the urbanization coefficient from this step of the analysis method is not used for adjustment of the peak discharges, the median value from the results of the next step is quite similar, so this coefficient gives an approximation of the average result.

In the second, quantile regression-based, step of the method, the distinction between the segments is removed by subtracting the applicable segment intercept value from the dependent variable values for each segment, that is,

$$y'_k = y_i(t) + \bar{a} - a_i, \quad (6)$$

where

$\bar{a} = \sum_i T_i a_i \Big/ \sum_i T_i$, where T_i is the number of observations in the *i*th segment, is the weighted mean of the segment intercepts obtained from the least-squares regression.

Table 7. Results of ordinary least-squares linear regression of 117 streamgages in northeastern Illinois and adjacent states to diagnose the temporal effects of urbanization and precipitation on annual maximum peak discharges.

[SE, standard error]

Precipitation coefficient b_1	Precipitation coefficient SE	Urban fraction coefficient b_2	Urban fraction coefficient SE	Weighted mean segment intercept (log units)
0.110	0.005	0.508	0.042	2.388a

[a]See equation 6 for the computation of the weighted mean segment intercept value.

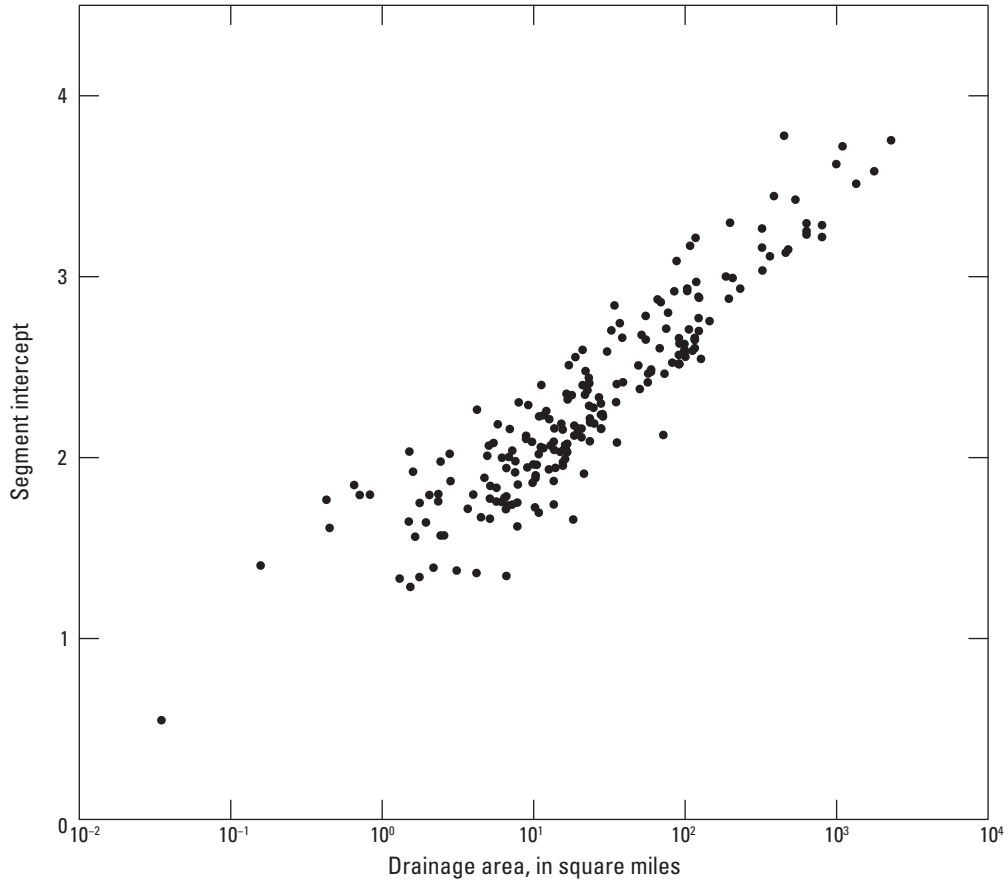

Figure 8. Segment intercepts as a function of drainage area for 181 streamgages used in this study in northeastern Illinois.

The independent variables are again the urban fractions and precipitation values associated with each peak discharge.

The quantile regression model is as follows:

$$y'_k = \hat{y}'_k(p) + \varepsilon'_k(p) = a'(p) + b'_1(p)P_k + b'_2(p)U_k + \varepsilon'_k(p), \quad (7)$$

where

p is an element of a sequence of AEPs (table 8),

$\hat{y}'_k(p)$ is the fitted value of the quantile with $AEP = p$ of the kth log-transformed peak discharge value y'_k,

$a'(p)$ is the intercept of the fitted linear relation between $\hat{y}'_k(p)$ and the independent variables,

P_k and U_k are the precipitation and urban fraction, respectively, of y'_k,

$b'_1(p)$ and $b'_2(p)$ are the quantile regression coefficients as a function of p (AEP) for precipitation and urban fraction, respectively, and

$\varepsilon'_k(p) = y'_k - \hat{y}'_k(p)$ is the regression error for the kth observation at $AEP = p$.

This model was solved with the rq function of the quantreg package (Koenker, 2013) of the R language.

Two post-processing steps were applied to obtain the final quantile regression coefficients and their SEs. First, a bootstrap resampling approach suggested by Canay (2011) was applied to obtain SEs and unbiased mean coefficient values. Second, a continuous and monotonic version of the bootstrap mean urban fraction coefficients as a function of exceedance probability was obtained by fitting a seventh-order polynomial. The original and bootstrap mean and SE values for all the quantile regression coefficients, along with the fitted urban fraction coefficients, are given in table 8 (available at https://doi.org/10.3133/sir20165050), and the three sets of urban fraction coefficients are plotted in figure 9. A subset of the urbanization coefficients at the AEPs of the standard flood-frequency quantiles are given in table 9.

The results in tables 7 through 9 indicate that the median urban fraction and precipitation coefficients are quite similar to the values computed by the OLS regression carried out in the first step of the analysis, with values of about 0.5 and 0.1. Results in these tables indicate that the precipitation coefficient varies only slightly with exceedance probability, whereas the urban fraction coefficient has a strong, mostly monotonic trend with exceedance probability, from a maximum value of 0.929 at an exceedance probability of 0.99 down to 0.294 at an exceedance probability of 0.002 (table 8). The dependence of the urban fraction coefficient on exceedance probability gives direct empirical evidence that urbanization in the study area

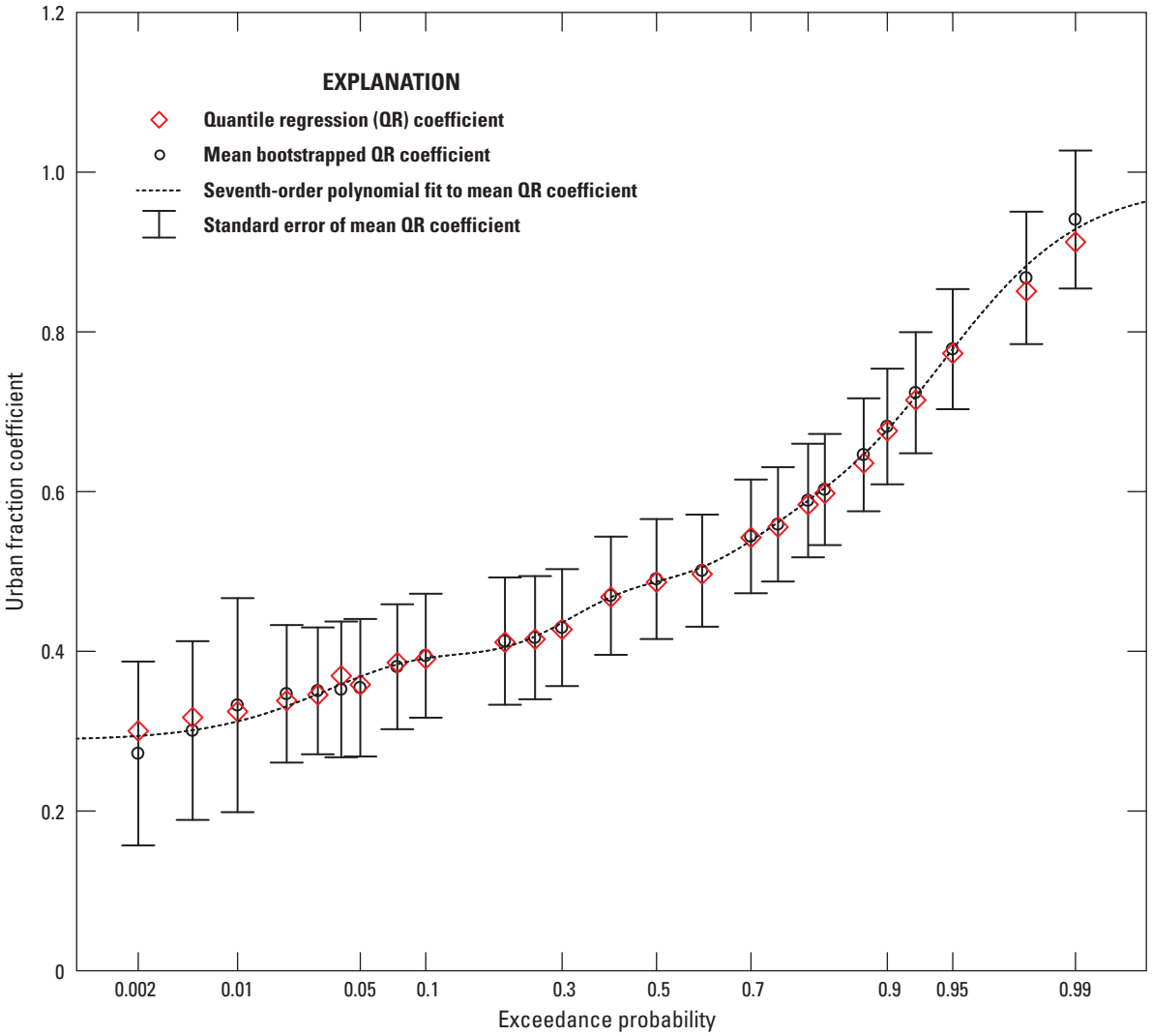

Figure 9. Urban fraction coefficients from temporal regression analysis of 117 streamgages in northeastern Illinois and adjacent states, as a function of exceedance probability.

Table 9. Quantile regression coefficients of urban fraction from temporal analysis of 117 streamgages in northeastern Illinois and adjacent states, at selected annual exceedance probabilities.

[AEP, annual exceedance probability]

AEP	0.5	0.2	0.1	0.04	0.02	0.01	0.005	0.002
Coefficient	0.487	0.405	0.391	0.359	0.331	0.312	0.301	0.294
Standard error	0.075	0.080	0.078	0.085	0.086	0.134	0.112	0.115

affects the magnitudes of the more common, large exceedance probability peak discharges more than it does the rarer, small exceedance probability peak discharges.

Adjustment of Annual Maximum Peak Discharges to Current (2010) Urban Fractions

Following the application of the two-step method to obtain exceedance probability-dependent urbanization and precipitation coefficients, each peak discharge is assigned an exceedance probability by a procedure described in Over and others (2016). This procedure was developed to adjust only for urbanization and therefore reduces the three-dimensional $\log_{10} Q$, U, and P space in which the least-squares and quantile regressions were carried out to a two-dimensional $\log_{10} Q$ and U space in which the quantile regression results are a set of lines in that space (fig. 10), where the diminishing effect of urbanization on the larger, rare floods can be seen graphically.

Using the exceedance probability assigned to each peak discharge observation and the continuous urban fraction coefficient function $\bar{b}_2''(p)$, the annual maximum peak discharges were adjusted to the 2010 urban fraction obtained from the Theobald (2005) data by using the following equation applied to each streamgage record segment i:

$$y_i''(t) = a_i^* - a_i + y_i(t) + \bar{b}_2''(p)\left[U_i(t^*) - U_i(t)\right], \quad (8)$$

where

$y_i''(t)$ and $y_i(t)$ are the base-10 logarithm of the adjusted and unadjusted, respectively, peak discharge value for year t and segment i,

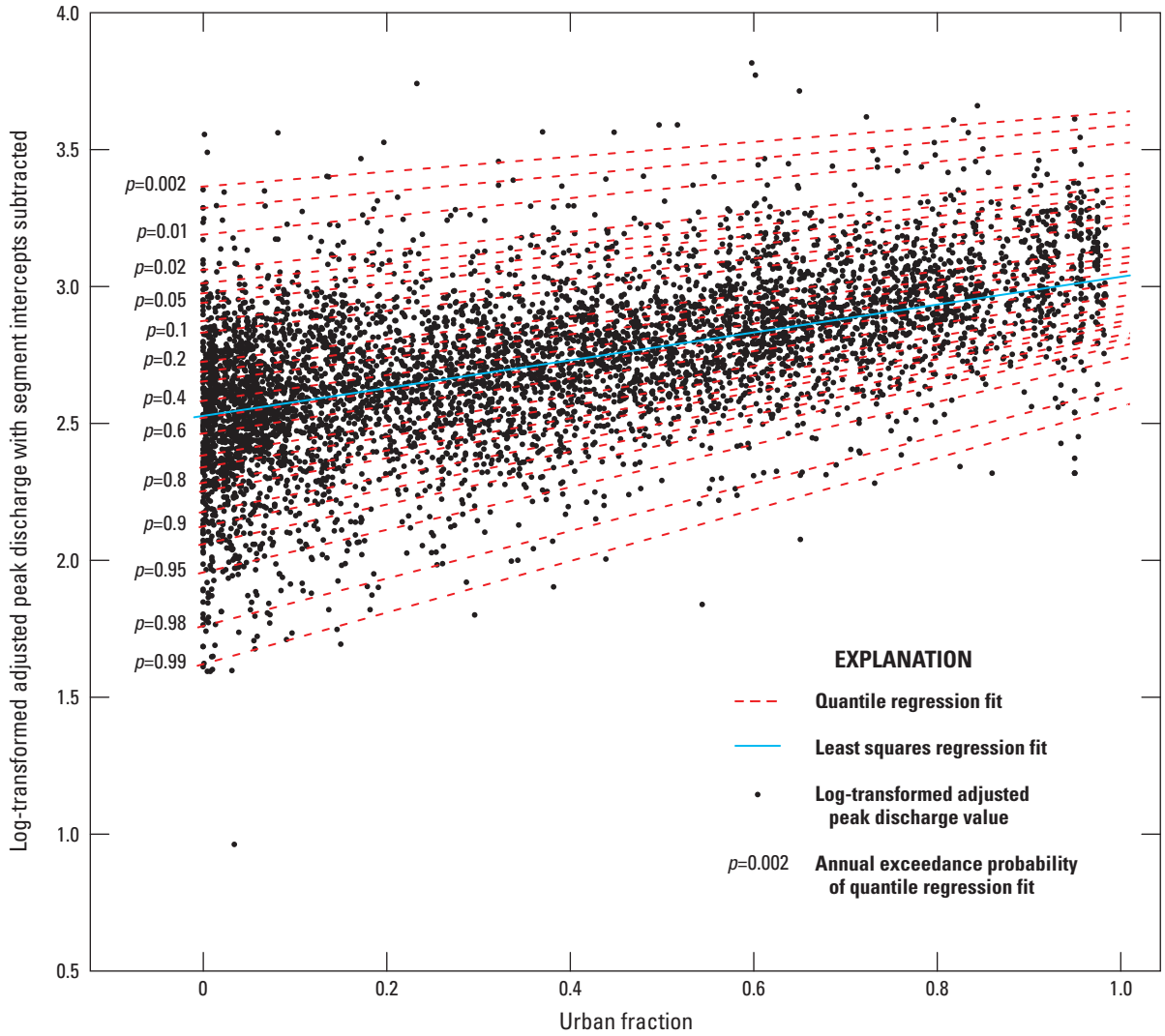

Figure 10. Segment intercept-subtracted log-transformed annual maximum peak discharge from 181 streamgages in northeastern Illinois and adjacent states as a function of urban fraction with quantile regression and least-squares regression line fits.

a_i^* and a_i are the segment intercept values for the most recent and current segments, respectively, of the streamgage record containing segment i,

$\bar{b}_2''(p)$ is the urban fraction coefficient value corresponding to the exceedance probability q assigned to the peak discharge value $y_i(t)$, and

$U_i(t^*)$ and $U_i(t)$ are the urban fraction values for the basin corresponding to segment i during the year t^* to which the peak discharges are being adjusted (here, 2010) and the year t of the observation of the peak discharge $y_i(t)$, respectively.

Notice that if a streamgage record has only one segment, then $a_i^* = a_i$ and the quantity $a_i^* - a_i$ drops out.

For the peak discharges and censoring levels that were dropped from the temporal analysis, where the correct segment could be determined, the adjustment method allows those values also to be adjusted so that these data can be used for at-site frequency analysis. For peak discharge values between two segments, the adjustment was interpolated. As a result, only peak discharge values associated with segments shorter than 5 years were not adjusted and thus were dropped from the at-site frequency analysis.

The set of adjusted values $Q_i''(t) = 10^{y_i''(t)}$ and the assigned exceedance probability values, p, on which the adjustment depends, are given in table 6. The effects of the adjustment on mean, standard deviation, and skewness of the log-transformed peak discharges at each streamgage in the study are shown in figure 11. The change in mean, which results from adjusting upward peaks with urban fractions less than the 2010 value, is almost always positive, and the change in standard deviation, which results from removal of urban fraction-induced trends in peak discharge in the observed data by the adjustment process and from the adjustment of smaller peak discharges more than larger ones, is almost always negative. The skewness increases more often than it decreases, also showing the effect of adjust-

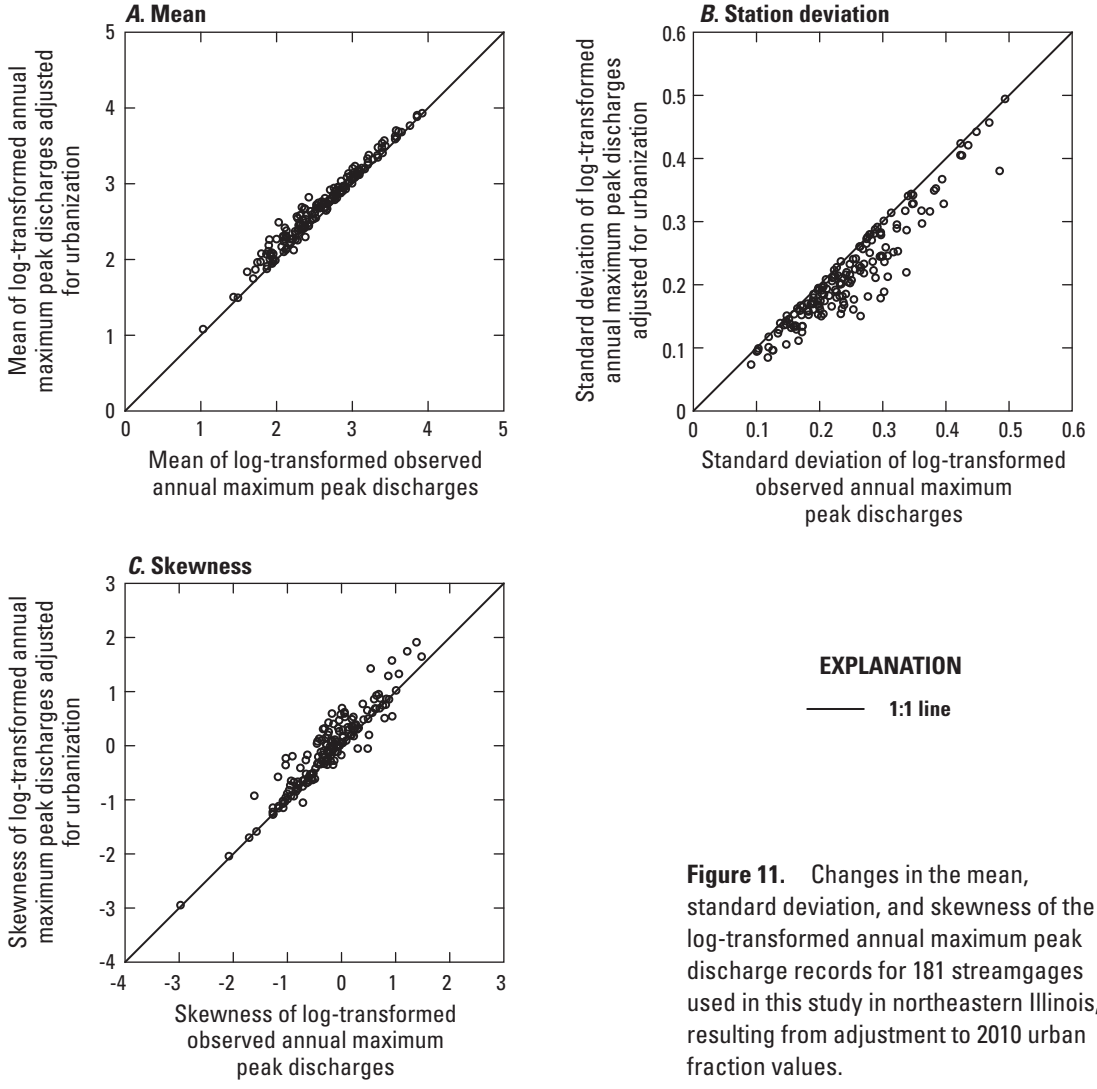

Figure 11. Changes in the mean, standard deviation, and skewness of the log-transformed annual maximum peak discharge records for 181 streamgages used in this study in northeastern Illinois, resulting from adjustment to 2010 urban fraction values.

ing the smaller peaks more than the larger ones. The overall increase in skewness as peaks are adjusted to more urbanized conditions is also consistent with the increase in skewness with urban fraction determined in the spatial analysis, as discussed in the "Regional Skew Analysis" section and appendix 1.

Regional Spatial Regression Analyses

After the annual maximum peak discharges were adjusted to their levels of urbanization at a common year (2010) as described in the "Regional Temporal Regression Analysis and Adjustment" section, peak discharge quantiles for the selected AEPs were computed as described in the "Frequency Analysis" section, including weighting with the regional skew model. The computed quantiles constitute the dependent variable for the spatial regression analyses; the spatially averaged basin characteristics developed as described in the "Spatially Averaged Basin Characteristics" section constitute the independent variables.

Selection of Basin Characteristics

The predictive capability of the basin characteristics in each category (table 3) were investigated by fitting weighted least-squares (WLS) linear regression models with regression weights in proportion to record length for each AEP for all possible combinations of basin characteristics where at most one variable is selected from each category with $\log_{10}$-transformed drainage area always included. For these exploratory regressions, a preliminary set of peak-flow quantiles developed using regional skew were used. An R script (R Core Team, 2014) was written to do the regression computations. The general form of the regression models fitted in this investigation was as follows in equation 9:

$$\log_{10} Q_p = (\beta_0)_p + (\beta_A)_p \log_{10} A + (\beta_U)_p (U + c_2)^{d_2} + (\beta_W)_p (W + c_3)^{d_3} + (\beta_S)_p (S + c_4)^{d_4},$$

$$p = 0.50, 0.20, 0.10, 0.05, 0.02, 0.01, 0.005, 0.002, \quad (9)$$

where

Q_p is the estimated peak discharge quantile with regional skew, in cubic feet per second, with annual exceedance probability p,

$(\beta_0)_p$, $(\beta_A)_p$, $(\beta_U)_p$, $(\beta_W)_p$, and $(\beta_S)_p$ are coefficients estimated by the WLS procedure,

A is the drainage area, in square miles,

U is an urbanization measure (a decimal fraction),

W is a basin water and wetness measure (a decimal fraction),

S is a basin slope measure, in feet per mile,

d_2, d_3, and d_4 are exponents used to transform the distribution of urbanization, water and wetness, and slope measures, respectively, to an approximately Gaussian shape ($d_i = 1, 1/2, 0$, where 1 implies no transformation, $1/2$ a square-root transformation, and 0 a $\log_{10}$-transformation were tested), and

c_2, c_3, and c_4 are constants added to the urbanization, water and wetness, and slope measures when a $\log_{10}$-transformation was used and the basin characteristic had zero values).

The selected transformations are listed in table 3.

Various plots of the regression results were made to facilitate examination of the results; the most useful plot was determined to be the adjusted coefficient of determination (R^2) (Helsel and Hirsch, 2002, p. 313) as a function of the t ratio of the coefficients of variables of the urbanization, slope, and wetness categories (fig. 12), where the t ratio is the coefficient value divided by its standard error (Helsel and Hirsch, 2002, p. 238). Such a plot shows which models provide the best fit (highest adjusted R^2) and the most significant coefficient values (largest magnitude t statistics), and, by retaining the sign of the coefficient values, such plots show if the sign of the coefficient is physically reasonable. The variables whose corresponding regression model fits have the largest magnitude t ratio values and highest adjusted R^2, along with the sign of the coefficient being physically reasonable, were selected as candidate variables for the development of the final spatial regression equations.

Plots of this type for each of the categories (urbanization, slope, and water and wetland) are shown in figure 12. The urbanization variable with the largest t ratio values and highest adjusted R^2 values is usually the square root of *NLCD*_22_23_24, except for AEPs 0.5 and 0.2 where Theobald_Urban is of similar quality, as shown in figure 12*A*. Both *NLCD*_22_23_24 and

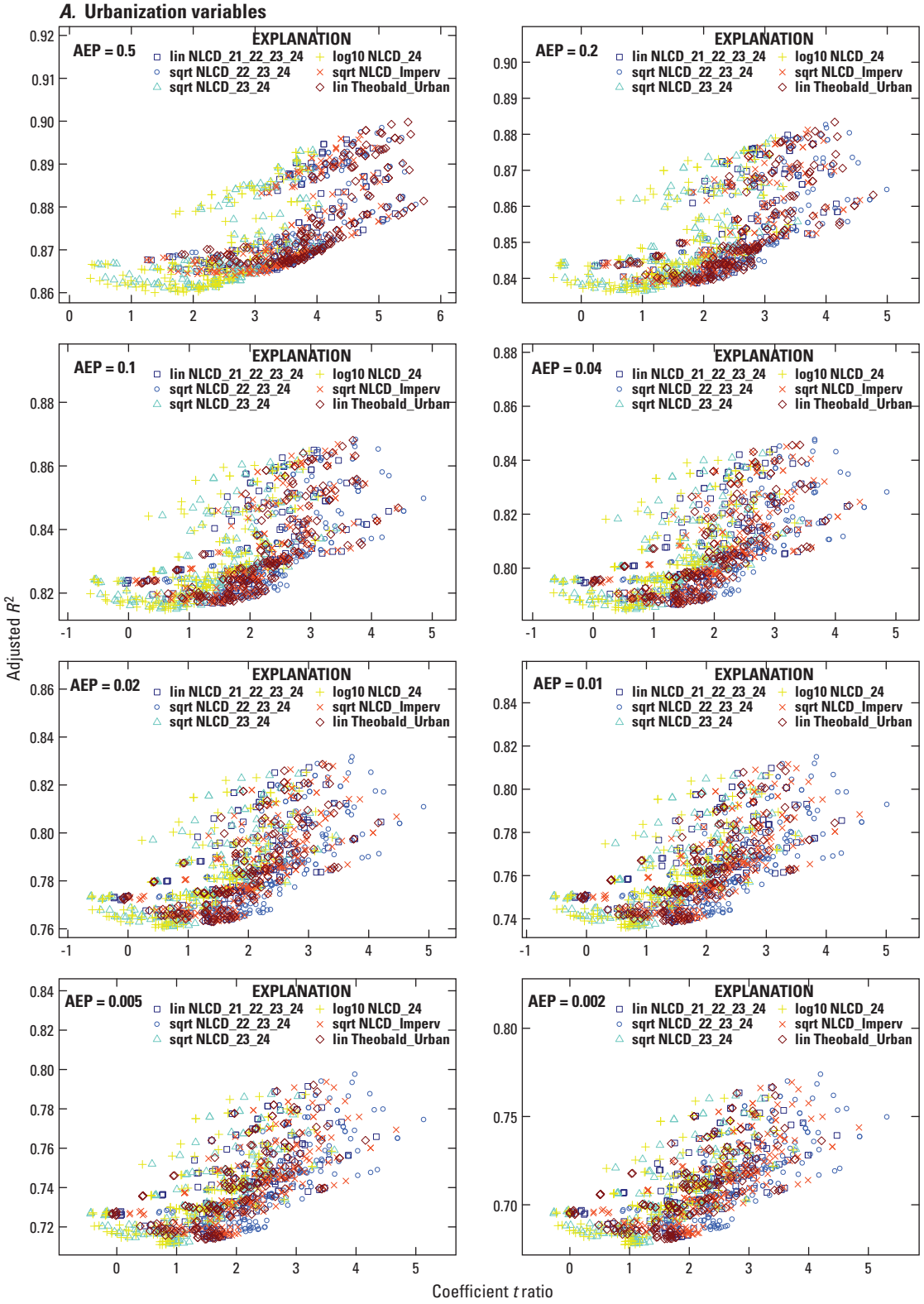

Figure 12. Annual exceedance probability (AEP) of adjusted coefficient of determination (R^2) as a function of the regression coefficient *t* ratio values for basin characteristic categories considered in this study in northeastern Illinois: *A*, urbanization variables; *B* and *C*, water and wetland variables; and *D*, slope variables. When the absolute value of the *t* ratio is greater than 2, then the coefficient is significantly different from zero at about the $\alpha = 0.05$ significance level (Helsel and Hirsch, 2002, p. 238). The variable names in the figure explanations are defined in table 3; the strings preceding the variable names in the figure explanations indicate the transformation applied to the variable, where "lin" means "linear" (that is, no transformation), "sqrt" means a square root transformation, and "log10" means a $\log_{10}$ transformation.

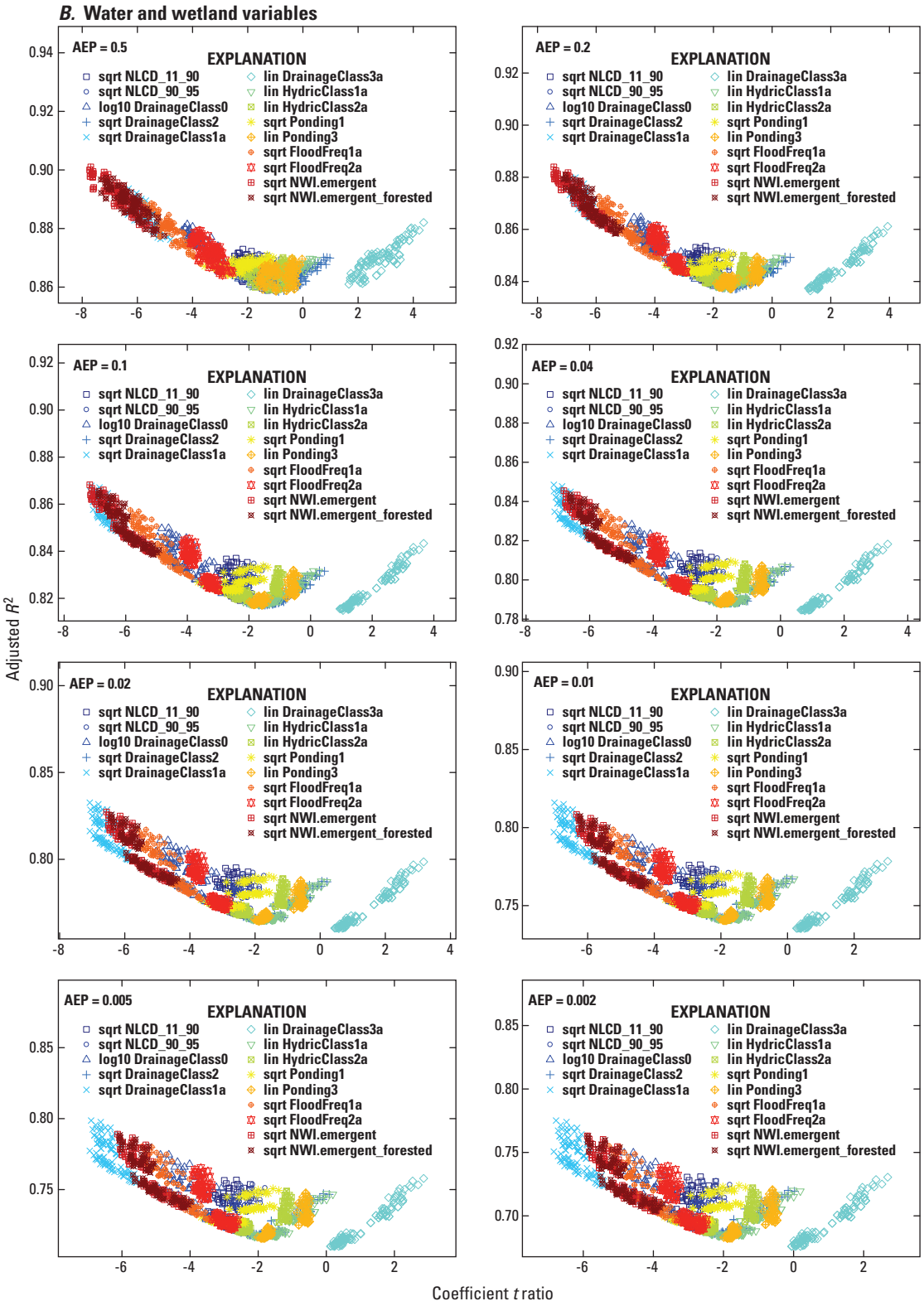

Figure 12. Annual exceedance probability (AEP) of adjusted coefficient of determination (R^2) as a function of the regression coefficient *t* ratio values for basin characteristic categories considered in this study in northeastern Illinois: *A*, urbanization variables; *B* and *C*, water and wetland variables; and *D*, slope variables. When the absolute value of the *t* ratio is greater than 2, then the coefficient is significantly different from zero at about the $\alpha = 0.05$ significance level (Helsel and Hirsch, 2002, p. 238). The variable names in the figure explanations are defined in table 3; the strings preceding the variable names in the figure explanations indicate the transformation applied to the variable, where "lin" means "linear" (that is, no transformation), "sqrt" means a square root transformation, and "log10" means a $\log_{10}$ transformation—Continued.

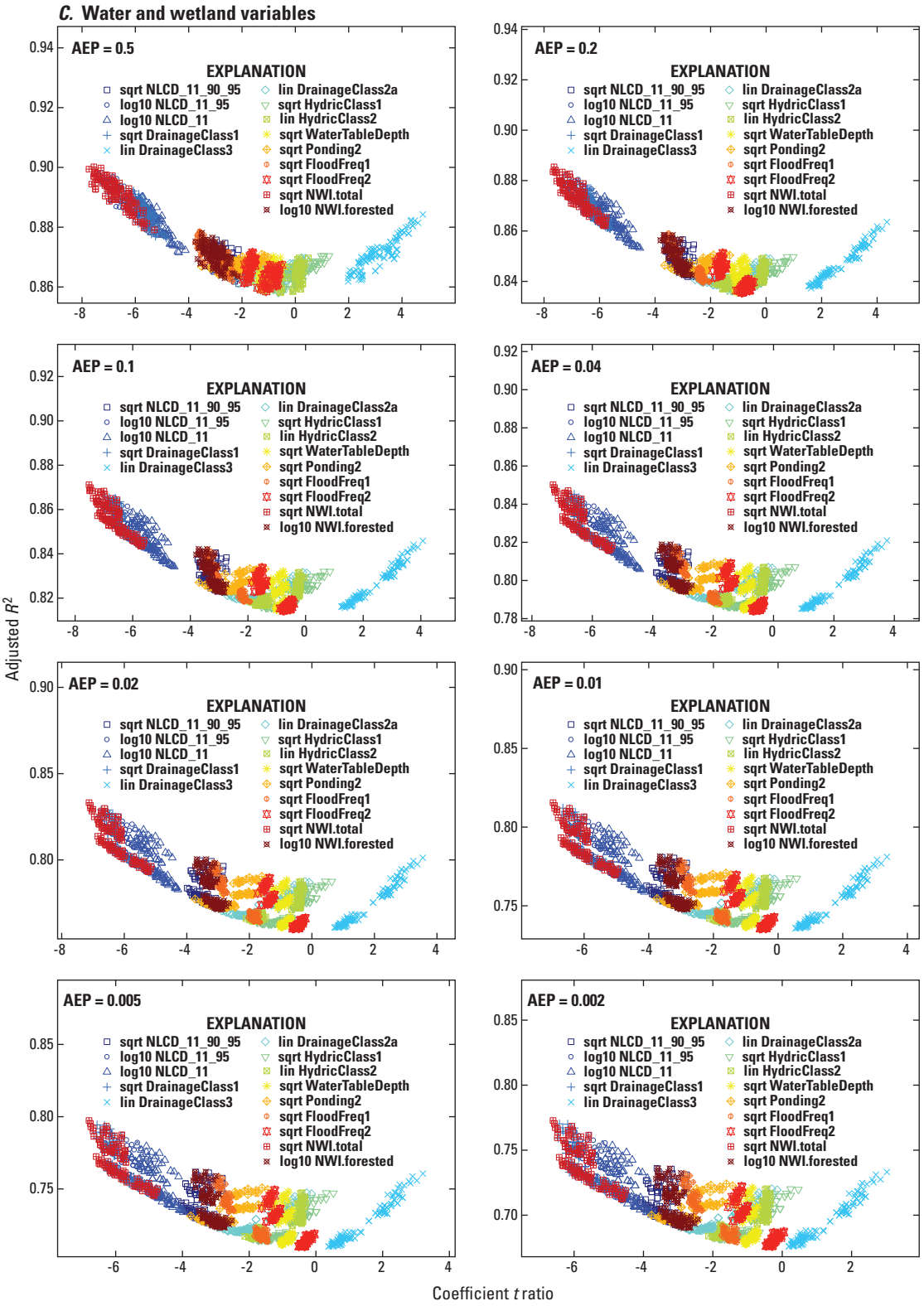

Figure 12. Annual exceedance probability (AEP) of adjusted coefficient of determination (R^2) as a function of the regression coefficient *t* ratio values for basin characteristic categories considered in this study in northeastern Illinois: *A*, urbanization variables; *B* and *C*, water and wetland variables; and *D*, slope variables. When the absolute value of the *t* ratio is greater than 2, then the coefficient is significantly different from zero at about the $\alpha = 0.05$ significance level (Helsel and Hirsch, 2002, p. 238). The variable names in the figure explanations are defined in table 3; the strings preceding the variable names in the figure explanations indicate the transformation applied to the variable, where "lin" means "linear" (that is, no transformation), "sqrt" means a square root transformation, and "log10" means a $\log_{10}$ transformation—Continued.

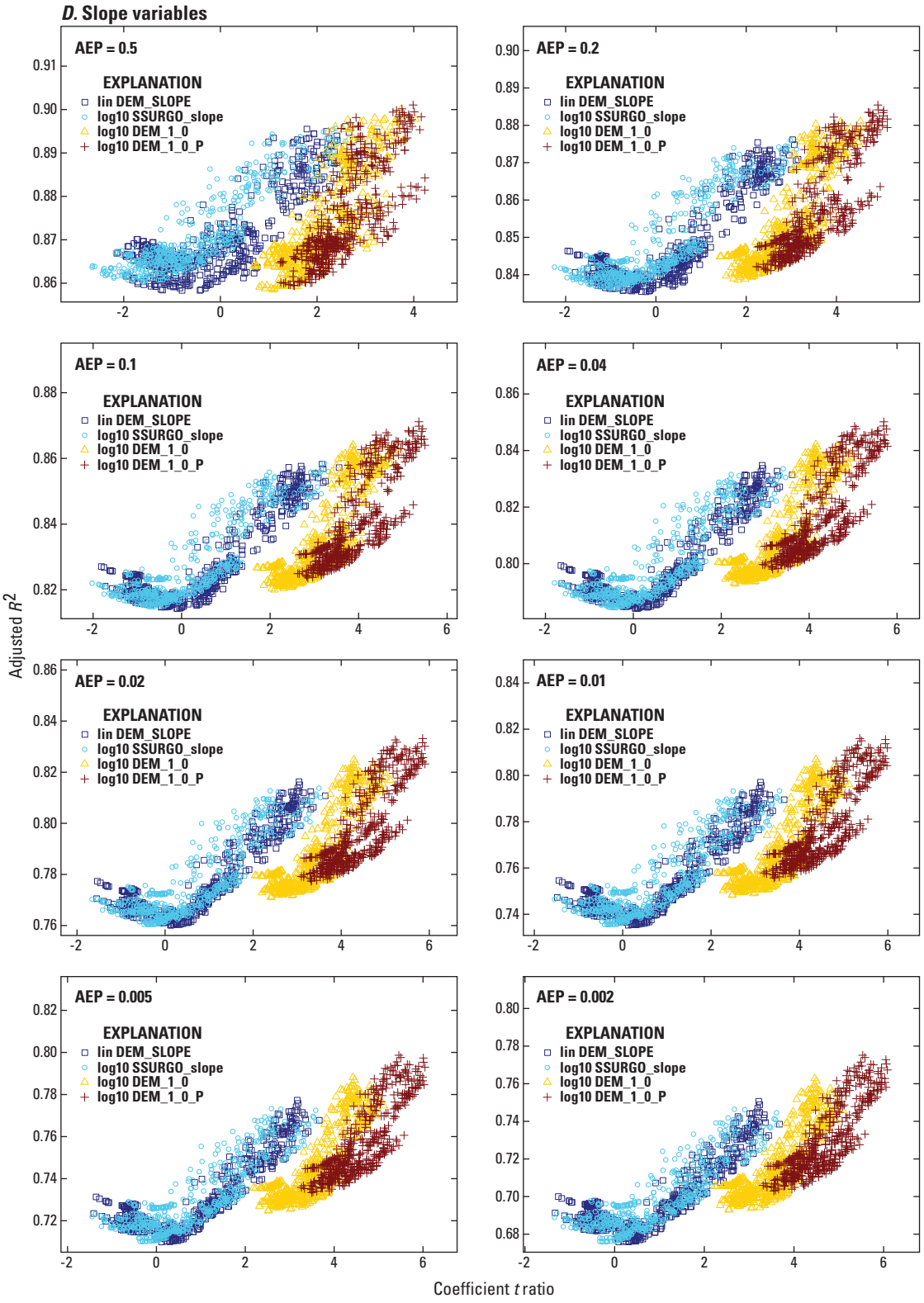

Figure 12. Annual exceedance probability (AEP) of adjusted coefficient of determination (R^2) as a function of the regression coefficient *t* ratio values for basin characteristic categories considered in this study in northeastern Illinois: *A*, urbanization variables; *B* and *C*, water and wetland variables; and *D*, slope variables. When the absolute value of the *t* ratio is greater than 2, then the coefficient is significantly different from zero at about the $\alpha = 0.05$ significance level (Helsel and Hirsch, 2002, p. 238). The variable names in the figure explanations are defined in table 3; the strings preceding the variable names in the figure explanations indicate the transformation applied to the variable, where "lin" means "linear" (that is, no transformation), "sqrt" means a square root transformation, and "log10" means a $\log_{10}$ transformation—Continued.

Theobald_Urban have positive coefficients, as is physically expected. Because only the NLCD-based urbanization variables are expected to be updated in the future, Theobald_Urban was eliminated from consideration for the spatial regression equations and *NLCD*_22_23_24$^{(1/2)}$ was chosen for all AEPs as the candidate urbanization variable for the final equations. Because there are too many water and wetland variables to distinguish on a single plot, the results for these are plotted on two sets of plots, figure 12*B* and 12*C*. The variable with the highest adjusted R^2 values and largest magnitude *t* ratio values varies from smaller to larger peak discharge quantiles, being NWI.emergent for the 0.5 annual exceedance probability (AEP) flood, NWI.total$^{(1/2)}$ for 0.2 to 0.04 AEP floods, and DrainageClass1a$^{(1/2)}$ for the larger floods (0.02 to 0.002 AEP), and all have physically expected negative coefficient values. Because NWI.total is almost as good as NWI.emergent for the 0.5 AEP flood, it was selected as the candidate variable for the smaller floods (AEPs of 0.5 to 0.04), and DrainageClass1a was selected for the larger floods (AEPs of 0.02 to 0.002). It can be seen in figure 12*D* that the slope variable with the highest adjusted R^2 values and largest magnitude *t* statistic values for all AEPs (and physically expected positive coefficients) is $\log_{10}$(*DEM*_1_0_*P*), so $\log_{10}$(*DEM*_1_0_*P*) was chosen for all AEPs as the candidate urbanization variable for the final equations.

Development of Final Spatial Regression Equations

Following the selection of the most promising basin characteristics in each category by the WLS regression investigation, the final equations were computed with generalized leastsquares (GLS) regression, which generalizes WLS regression by taking into account cross-correlations that arise among nearby streamgages with concurrent records. Stedinger and Tasker (1985) showed that GLS regression for regional spatial flood-frequency analysis provides more accurate coefficients and error estimates than OLS, with more modest improvement compared to WLS regression depending on the amount of cross-correlation among the streamgage records.

The GLS regression models were fitted with the function WREG.GLS from the package WREG (Farmer, 2017) in R version 3.6.3 (R Core Team, 2020). WREG.GLS implements a GLS approach to the estimation of peak discharge quantiles fit to a log-Pearson type III distribution using techniques described in Eng and others (2009) as developed by Stedinger and Tasker (1985), Tasker and Stedinger (1989), Griffis and Stedinger (2007), and Griffis and Stedinger (2009). The cross-correlations $\hat{\rho}_{ii}$ among streamgage records are estimated by selecting streamgage record pairs with a minimum number of concurrent years and fitting a function of the form

$$\hat{\rho}_{ij} = \theta^{d_{ij}/(\alpha d_{ij}+1)}, \tag{10}$$

where

d_{ij} is the distance between streamgages *i* and *j*, and

α and θ are dimensionless parameters fitted by a graphical method.

For this study the minimum number of concurrent years was taken as 45, and α and θ were taken as 0.005 and 0.975, respectively.

When the selected water and wetland variables were used in the GLS regression analysis, it was determined that use of DrainageClass1a gave a better fit than NWI.total from AEP 0.002 to AEP 0.20 and had only a very small difference at AEP 0.50, in the final equations, so DrainageClass1a is used for all AEPs in the final spatial regression equations. Values of the selected variables for each streamgage are given in table 1 and their cross-correlations and variance inflation factors (VIFs) in table 10.

Table 10. Correlation matrix and variance inflation factor (VIF) values of basin characteristics selected for use in spatial regression analysis of 117 streamgages in northeastern Illinois and adjacent states.

[*DA*, drainage area, in square miles; *NLCD*_22_23_24, sum of fractions of 2011 National Land Cover Database (NLCD) classes 22, 23, and 24; DrainageClass1a, sum of fractions of Soil Survey Geographic (SSURGO) fractions "very poorly drained" and "unknown (likely water)"; *DEM_1_0_P*, basin elevation range divided by basin perimeter, in feet per mile; --, redundant value]

	$\log_{10}$(*DA*)	*NLCD*_22_23_24$^{1/2}$	DrainageClass1a$^{1/2}$	$\log_{10}$(*DEM*_1_0_*P*)
$\log_{10}$(*DA*)	1	--	--	--
*NLCD*_22_23_24$^{1/2}$	-0.156	1	--	--
DrainageClass1a$^{1/2}$	0.288	0.221	1	--
$\log_{10}$(*DEM*_1_0_*P*)	-0.816	0.077	-0.215	1
Variance inflation factor	3.27	1.12	1.19	3.02

The general form of selected equations follows in equation 11:

$$\log_{10} Q_p = \left(b_0\right)_p + \left(b_A\right)_p \log_{10} A + \left(b_U\right)_p U^{1/2} + \left(b_W\right)_p W^{1/2} + \left(b_S\right)_p \log_{10} S,$$

$$p = 0.50, 0.20, 0.10, 0.05, 0.02, 0.01, 0.005, 0.002, \tag{11}$$

where

Q_p is the peak discharge quantile with weighted skew, in cubic feet per second, with annual exceedance probability p,
A is the drainage area, in square miles,
U is the selected urbanization measure for the spatial equations *NLCD*_22_23_24 (a decimal fraction),
W is the basin soil wetness measure DrainageClass1a (a decimal fraction),
S is the basin slope measure *DEM_1_0_P* (basin elevation range divided by basin perimeter), in feet per mile, and
$\left(b_0\right)_p$, $\left(b_A\right)_p$, $\left(b_U\right)_p$, $\left(b_W\right)_p$, and $\left(b_S\right)_p$ are coefficients estimated by using WREG (table 11).

After inverting the logarithmic transformation, the Q_p prediction equation 12 is the result:

$$Q_p = 10^{\left(b_0\right)_p} A^{\left(b_A\right)_p} 10^{\left(b_U\right)_p U^{1/2}} 10^{\left(b_W\right)_p W^{1/2}} S^{\left(b_S\right)_p},$$

$$p = 0.50, 0.20, 0.10, 0.05, 0.02, 0.01, 0.005, 0.002. \tag{12}$$

Table 11. Coefficients of the selected spatial regression equations in this study in northeastern Illinois.

[b_0, intercept; SE, standard error; b_A, coefficient of $\log_{10}$ of drainage area in square miles; b_U, coefficient of square root of urbanization measure *NLCD*_22_23_24 as a decimal fraction; b_W, coefficient of square root of basin wetness measure DrainageClass1a as a decimal fraction; b_S, coefficient of $\log_{10}$ of slope measure *DEM*_1_0_*P* in feet per mile]

Annual exceedance probability	b_0	SE(b_0)	b_A	SE(b_A)	b_U	SE(b_U)	b_W	SE(b_W)	b_S	SE(b_S)
0.5	1.496	0.133	0.784	0.043	0.268	0.070	-0.777	0.150	0.300	0.101
0.2	1.691	0.137	0.777	0.045	0.212	0.074	-0.878	0.156	0.371	0.105
0.1	1.783	0.144	0.774	0.047	0.198	0.079	-0.925	0.164	0.408	0.110
0.04	1.873	0.156	0.772	0.051	0.195	0.088	-0.972	0.178	0.447	0.119
0.02	1.925	0.166	0.771	0.054	0.200	0.096	-1.001	0.189	0.472	0.127
0.01	1.968	0.176	0.771	0.057	0.207	0.103	-1.025	0.201	0.494	0.135
0.005	2.005	0.187	0.771	0.060	0.216	0.110	-1.046	0.213	0.514	0.144
0.002	2.045	0.200	0.773	0.065	0.230	0.119	-1.071	0.227	0.539	0.155

Accuracy of Final Spatial Regression Equations

Several measures of the average accuracy of the final GLS spatial regression equations are presented in table 12, along with comparative values of the standard model error in percent from the corresponding WLS equations and the previous studies by Allen and Bejcek (1979) and Soong and others (2004). All these measures are averages for all the streamgages in the analysis. The pseudo R^2 measures the fraction of variability in the dependent variable that is explained by the regression model after removing the effect of the time-sampling error (Eng and others, 2009) and is analogous to the standard R^2. The average variance of prediction includes both the model error and time-sampling error components and indicates the expected accuracy of a prediction at an ungaged location with basin characteristics that are near the centroid of the basin characteristics used in the GLS analysis. The standard model error indicates the accuracy of the model fit without the component in the average variance of prediction that indicates the additional error of making a prediction at an ungaged location; as a result it is always somewhat smaller than the average variance of prediction. All the accuracy measures decrease as the AEP decreases, as expected, because of the fewer data available for less frequent events.

Techniques for computing accuracy estimates at individual locations (streamgages or ungaged locations) are also available, including the variance and standard error of prediction and confidence interval values. According to Hodge and Tasker (1995), the variance of prediction V_i at an individual location based on a GLS regression analysis is

$$V_i = \gamma^2 + x_i \left(X^t \Lambda^{-1} X \right)^{-1} x_i^t , \tag{13}$$

where

γ^2 is the model error variance (table 12),

$x_i = \left[1, \log_{10} A_i, U_{spat,i}^{1/2}, W_i^{1/2}, \log_{10} S_i \right]$ is a row vector specifying the basin characteristics of the individual location augmented with a 1,

X is a $(n \times p)$ matrix whose rows are the transformed basin characteristics for each streamgage used in the GLS model augmented by a 1 ($n = 117$ is the number of streamgages and $p = 5$ is the number of basin characteristics plus 1)

Λ^{-1} is the matrix inverse of Λ, the $(n \times n)$ covariance matrix used in the GLS regression analysis, and

X^t is the matrix transpose of X; and x_i^t is the matrix transpose of x_i.

Table 12. Measures of the average accuracy of the selected spatial regression equations in this study in northeastern Illinois.

[R^2, coefficient of determination; WLS, weighted least squares; --, no data]

Annual exceedance probability	Pseudo R^2 (percent)	Average variance of prediction (log units)	Average standard error of prediction (percent)	Model error variance γ^2 (log units)	Standard model error (percent)	Standard model error (percent), WLS fit	Standard error of estimate (percent) (from Allen and Bejcek, 1979; table 4)	Standard model error (from Soong and others, 2004; table 4, applicable to regions 2, 6, and 7)
0.5	87.5	0.0362	46.0	0.0341	44.5	45.2	36	39.1
0.2	85.6	0.0384	47.5	0.0360	45.9	46.3	38	39.3
0.1	83.9	0.0414	49.6	0.0387	47.7	48.6	40	40.6
0.04	81.0	0.0473	53.4	0.0439	51.2	52.4	43	43.1
0.02	78.6	0.0523	56.6	0.0485	54.2	55.8	45	45.2
0.01	76.5	0.0571	59.5	0.0528	56.8	59.4	48	47.3
0.005	74.2	0.0622	62.5	0.0573	59.6	63.2	--	--
0.002	71.7	0.0681	66.0	0.0624	62.6	68.5	52	52.8

The $\left(X^t \Lambda^{-1} X\right)^{-1}$ matrices for the selected AEPs are given in table 13 (available at https://doi.org/10.3133/sir20165050).

The variance of prediction V_i can be converted to a standard error of prediction in log units by taking the square root, that is, $S_i = V_i^{1/2}$ and in percent units by using the following formula:

$$S_{pi} = 100\left\{\exp\left[\left(\ln 10\right)^2 V_i\right] - 1\right\}^{1/2} \quad (14)$$

(Eng and others, 2009).

The confidence intervals of the predicted discharge quantile Q_i are computed as

$$\log_{10} Q_i \pm t_{\alpha/2,n-p} S_i \,, \quad (15)$$

where

$t_{\alpha/2,n-p}$ is the critical value of the *t* distribution at the alpha level α (for example, $\alpha = 0.05$ for 90-percent confidence intervals) and $n - p$ degrees of freedom, where $n = 117$ is the number of streamgages used in the spatial regressions and $p = 5$ is the number of basin characteristics plus 1. After inverting the logarithmic transformation, the interval is

$$\left[Q_i 10^{-t_{\alpha/2,n-p} S_i} < Q_i < Q_i 10^{t_{\alpha/2,n-p} S_i}\right]. \quad (16)$$

In equation 16, Q_i is the median prediction, and $Q_i 10^{t_{\alpha/2,n-p} S_i}$ and $Q_i 10^{-t_{\alpha/2,n-p} S_i}$ are the upper and lower $1-2\alpha$ confidence limits, respectively. For example, for $\alpha = 0.05$ (therefore, 90-percent confidence limits), according to the data and methods used in this study, the probability that the true value of the discharge quantile exceeds the upper limit $Q_i 10^{t_{\alpha/2,n-p} S_i}$ is $\alpha = 0.05$; likewise the probability that the true value of the discharge quantile is less than the lower limit $Q_i 10^{-t_{\alpha/2,n-p} S_i}$ is $\alpha = 0.05$, so that the probability that the true value lies between the limits is 90 percent.

Applications of Regression Equations

There are two sets of regression equations presented in this report, the temporal (eq. 7 and table 9) and the spatial (eq. 12 and table 11). In both sets, the values of the urbanization coefficients are positive, as expected, and the urbanization coefficients from the temporal analysis decrease substantially as the peak discharge quantiles increase, that is, with decreasing AEP. The changes in the urbanization coefficients from the spatial regression equations as a function of AEP are more modest and have a minimum at AEP = 0.1, with increases toward both smaller and larger AEP values; in fact the largest urbanization coefficient occurs at AEP = 0.002. The increase of the urbanization coefficients from the spatial analysis for decreasing AEPs beyond AEP = 0.1 does not agree with the expectation that the effect of urbanization decreases with decreasing AEP and therefore is considered anomalous. Reasons for this anomaly and implications for applications of the spatial equations are discussed below.

Because the urbanization measures to which these coefficients apply are different but approximately commensurate (fig. 13), a direct comparison of their implications regarding the effect of urbanization can be considered as meaningful. Plots of the ratios of peak discharge quantiles for the different AEPs considered here are shown in figure 14. These plots show that except for very small amounts of urbanization beginning with a completely rural basin, the larger coefficients from the temporal analysis imply larger effects of urbanization, especially for the larger AEPs (smaller floods). They also show the effect of the minimum value of the spatial coefficient occurring at AEP = 0.1; for example, the largest effect of urbanization in the spatial curves is seen for AEP = 0.002.

The urbanization coefficients in the temporal equations are estimated by a temporal analysis, that is, directly from the changes in the annual peak discharges as the basins urbanize. In the spatial equations, the urbanization coefficients are not computed from observed changes in the gaged basins, but indirectly, from the differences in flood-discharge quantiles among basins of different levels of urbanization. When applying flood-discharge regression equations, one is typically interested in the behavior at an ungaged location, and this spatial transfer of information is entirely appropriate. When it comes to urbanization, however, the primary interest is the temporal question, that is, how did or how will the flood-discharge quantiles change when the basin is urbanized. Because they are based on a direct analysis of the results of this process, the temporal urbanization coefficients are more likely to reflect the effects of urbanization on a given basin.

Two general statistical issues, at least, that affect the values of regression coefficients in a multiple regression framework also need to be considered when the value of the coefficients is of interest, as in this study with respect to the urbanization coefficients. These issues are (1) omitted variable bias (OVB) and (2) measurement errors in the explanatory variables. The issue of OVB arises when an omitted variable is correlated with both the variable of interest and the dependent variable (Greene, 1997). In this case, an omitted variable will cause a negative or positive bias in the coefficient of the variable of interest, though it does not bias the predictions of the equations. In the context of the present analysis, if there is some variable that is important in predicting the flood-discharge properties that is left out of the spatial or temporal analyses but is correlated with urbanization, the urbanization coefficient will not have its correct value. Measurement errors in an explanatory variable cause attenuation (reduction of the absolute value) of the variable, again without biasing the prediction of the equations (Fuller, 1987).

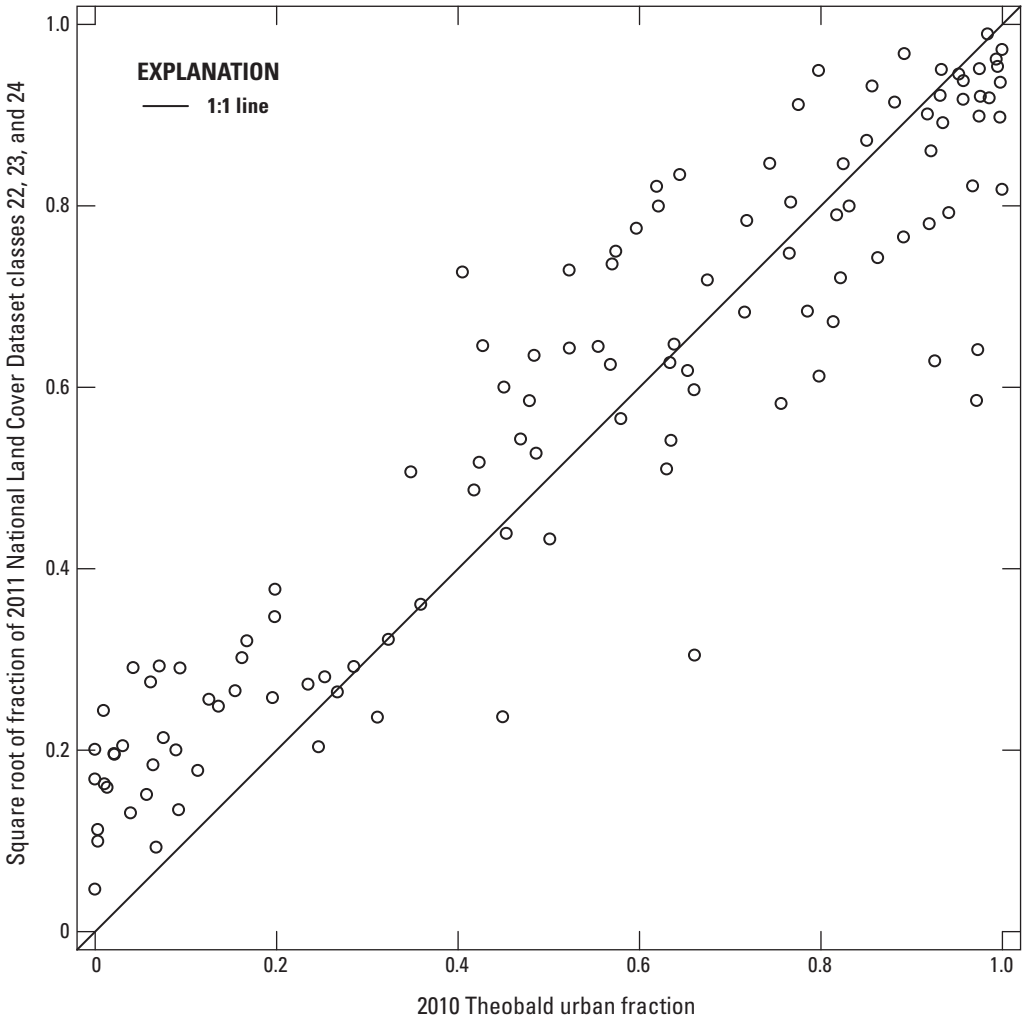

Figure 13. Comparison of square root of fraction of 2011 National Land Cover Dataset (NLCD, Jin and others, 2013) classes 22, 23, and 24 (*NLCD*_22_23_24$^{1/2}$) and 2010 Theobald urban fraction (Theobald, 2005) for 117 basins used in this study in northeastern Illinois.

It is possible that OVB is affecting either or both sets of coefficients, but because the urbanization coefficients from the spatial analysis are significantly smaller than those from the temporal analysis and measurement error always causes a reduction in positive coefficients, whereas OVB may cause an error in either direction, the first hypothesis that the results suggest is that the spatial urbanization coefficients are subject to a measurement error. In particular, if the relation between urbanization and its effects on peak discharges varies among basins because of different development practices related to stormwater and flood control, this variation would induce a measurement error relative to the hydrologically effective urbanization value. Such an error would, in addition, affect the spatial analyses more than the temporal ones, because the temporal analyses depend only on the changes in time of the peak discharges with interbasin differences captured in the segment intercepts, whereas the spatial analyses depend directly on the values of the peak discharges.

Given this concern regarding the accuracy of the urbanization coefficients from the spatial models (which nevertheless does not bias the predictions) and the previous assertion that the basic question when it comes to the effect of urbanization is a temporal one, it seems clearly preferable to use temporal equations to predict the effect of urbanization where possible. It is not possible to use the temporal equations for adjustment of rural estimates in ungaged basins in region 2 because there are not enough truly rural basins to develop rural-only equations unaffected by urbanization (fig. 4). Therefore to obtain flood-quantile estimates for ungaged basins in region 2, the spatial regression equations should be used. But for situations where peak discharge quantile estimates are being adjusted for the effects of urbanization, the temporal equations should be used. Such situations include ungaged basins outside region 2, assuming urbanization has proceeded similarly as for the gaged basins analyzed in this study. Such situations may also include the prediction of future effects of urbanization for basins in region 2, again assuming urbanization will proceed as it did for the basins analyzed in this study. These situations are discussed in more detail in the "Applications of the Temporal Urbanization Coefficients" section.

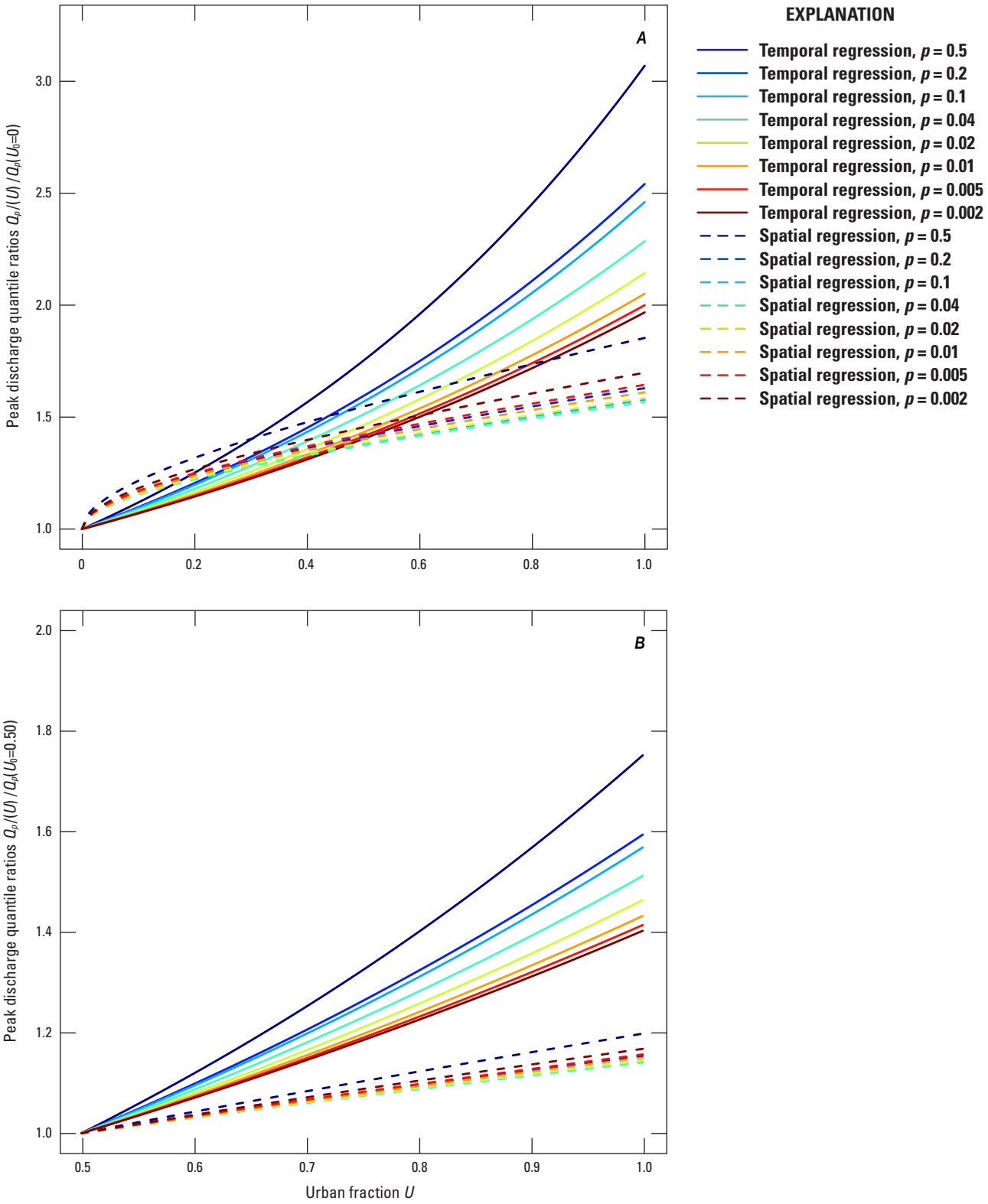

Figure 14. Ratios of peak discharge quantiles $Q_p(U)/Q_p(U_0)$ as a function of urban fraction U for selected annual exceedance probabilities (AEPs) p as implied by the two sets of urbanization coefficients obtained in this study in northeastern Illinois: *A*, basin initially having no urbanization ($U_0 = 0$); *B*, basin initially 50-percent urbanized ($U_0 = 0.5$).

Applications of the Spatial Regression Equations

The details of application of the updated Illinois region 2 spatial regression equations depend on the nearness of the location of interest to a streamgage. If the location of interest is far from a streamgage, the spatial regression equations are used. If the location is at a streamgage, a weighted average of the quantiles from regional equations and the quantiles from the streamgage record itself are used. If the location is near a streamgage, a weighted average of the quantiles from regional equations and an adjusted version of the quantiles from the streamgage record itself are used. The details of the different applications are described in this section.

Ungaged Locations Far from a Streamgage

For a general ungaged location in Illinois flood-frequency region 2, the final, real-space regression equation 12 should be used. The USGS StreamStats application (https://streamstats.usgs.gov) could be used to select the location of interest, delineate the basin, and compute the basin characteristics and the peak discharge quantiles.

It is important to realize that the regression equations represented by equation 12 only apply within the ranges of the basin characteristics used to fit the equations. These ranges are given in table 14. StreamStats will not enforce this limitation, though it does provide a warning.

At a Streamgage

Because of the finite length of streamgage records, the regional equations can improve the accuracy of the peak discharge quantile estimates at streamgages by incorporating regional information. The procedure recommended by Cohn and others (2012; see also Tasker, [1975]) is to compute this peak discharge quantile from the weighted average of the regression equation estimate and the result of the frequency analysis of the streamgage record, where the weights are the inverses of the variance of each of the discharge estimates. The weighted discharges are computed with the following equation:

$$\log_{10}\left(Q_p\right)_{g,w}=\frac{\left(V_p\right)_{g,r}\log_{10}\left(Q_p\right)_{g,s}+\left(V_p\right)_{g,s}\log_{10}\left(Q_p\right)_{g,r}}{\left(V_p\right)_{g,r}+\left(V_p\right)_{g,s}}, \quad (17)$$

where

$\left(Q_p\right)_{g,w}$ is the weighted peak discharge quantile at the streamgage for an AEP of p,

$\left(Q_p\right)_{g,s}$ is the peak discharge quantile for an AEP of p computed from the streamgage record by using EMA with weighted skew as described in the "Frequency Analysis" section,

$\left(Q_p\right)_{g,r}$ is the peak discharge quantile for the selected AEP obtained from regression equation 12 applied at the streamgage,

$\left(V_p\right)_{g,r}$ is the variance of prediction of $\left(Q_p\right)_{g,r}$ for the an AEP of p computed by using equation 13, and

$\left(V_p\right)_{g,s}$ is the variance of prediction of $\left(Q_p\right)_{g,s}$ for the selected AEP computed by PeakFQ as part of the frequency analysis.

The values of $\left(Q_p\right)_{g,s}$, $\left(Q_p\right)_{g,r}$, and $\left(Q_p\right)_{g,w}$ for both the redundant and nonredundant stations in this study are tabulated in table 2, in the third, fourth, and fifth rows, respectively, for each streamgage.

The variance of prediction for the weighted discharge $\left(Q_p\right)_{g,w}$ is given by

$$\left(V_p\right)_{g,w}=\left(V_p\right)_{g,s}\left(V_p\right)_{g,r}\Big/\left[\left(V_p\right)_{g,s}+\left(V_p\right)_{g,r}\right] \quad (18)$$

(Tasker, 1975). With this value of $\left(V_p\right)_{g,w}$, the standard error of prediction $\left(S_p\right)_{g,w}$ can be computed as $\left(S_p\right)_{g,w}=\left(V_p\right)_{g,w}^{1/2}$, and then equations 14–16 can be used to compute the standard error of prediction in percent units and confidence intervals.

Table 14. Ranges of basin characteristic values used to fit selected spatial regression equations in this study in northeastern Illinois.

[*NLCD*_22_23_24, fraction of 2011 National Land Cover Database (NLCD) classes 22, 23, and 24 (low, medium, and high intensity developed); Theobald_Urban, fraction of 2010 (Theobald, 2005) classes 7–10 (housing with no more than 10 acres per unit plus commercial/industrial/transportation land use); DrainageClass1a, Soil Survey Geographic (SSURGO) Database fraction "very poorly drained" and "unknown (likely water)"; *DEM*_1_0_*P*, basin elevation range divided by basin perimeter]

Basin characteristic name	StreamStats name	Units	Minimum	Maximum	Median
Drainage area	DRNAREA	square mile	0.078	1,351	13.6
*NLCD*_22_23_24	FLC11DVLMH	decimal fraction	0.0022	0.979	0.391
Theobald_Urban	URBTHE2010	decimal fraction	0.000	1.00	0.580
DrainageClass1a	FSSURGDC78	decimal fraction	0.000	0.256	0.0511
*DEM*_1_0_*P*	RELRELF	foot per mile	0.821	37.2	4.79

Ungaged Location Near a Streamgage

If the ungaged location of interest is near to and on the same stream as a streamgage, the accuracy of the flood-discharge quantile estimate at the ungaged location can be improved if the estimate from the regional equation is combined with the estimate at the streamgage (Ries, 2007). There are a few different methods in the literature for this adjustment; the method used here follows that of Soong and others (2004) (as corrected August 10, 2010), which is the same as the method presented in the IDOT Drainage Manual (Drainage Manual Committee, 2011). According to this method, the near-gage adjustment has an effect only if the ratio A_u/A_g of the drainage area of the ungaged basin of interest A_u to that of a gaged basin A_g is between 0.5 and 1.5 (see eq. 19); this constraint on the effect of the adjustment method defines being "near" a streamgage.

First define the adjustment weighting factor w_a, which is given by

$$w_a = \begin{cases} 2\left|\left(A_u/A_g\right)-1\right| \; if \; 0.5 < \left(A_u/A_g\right) < 1.5 \\ 1 \; otherwise \end{cases}, \quad (19)$$

where

A_u is the drainage area at the ungaged location of interest and

A_g is the drainage area at the streamgage.

The near-gage adjustment equation can then be written as follows:

$$\left(Q_p\right)_{u,w} = w_a\left(Q_p\right)_{u,r} + \left(1-w_a\right)\left(Q_p\right)_{g,w}\left(A_u/A_g\right) \quad (20)$$

where

$\left(Q_p\right)_{u,w}$ is the gage-adjusted flood-discharge quantile estimate for an AEP of p at the ungaged location of interest,

$\left(Q_p\right)_{u,r}$ is the flood-discharge quantile estimate for an AEP of p at the ungaged location of interest from the spatial regression equations (eq. 12),

$\left(Q_p\right)_{g,w}$ is the flood-discharge quantile estimate for an AEP of p at the gage, weighted with the spatial regression equations (eq. 17, table 2), and

w_a, A_u, and A_g are as defined for equation 19.

According to equations 19 and 20, the near-gage adjustment has no effect when $A_u/A_g \le 0.5$ or $A_u/A_g \ge 1.5$, because $w_a = 1$ (eq. 19) and therefore (eq. 20) the near-gage adjusted value $\left(Q_p\right)_{u,w}$ is identical to the value $\left(Q_p\right)_{u,r}$ from the regional regression equations. At a streamgage, $A_u = A_g$ and the near-gage adjusted value reduces to the weighted flood-discharge at the gage $\left(Q_p\right)_{g,w}$ because $w_a = 0$. When $0.5 < A_u/A_g < 1.5$, then both $\left(Q_p\right)_{u,r}$ and $\left(Q_p\right)_{g,w}$ contribute to the value of $\left(Q_p\right)_{u,w}$ according to the values of the weights w_a and $1-w_a$.

Applications of the Temporal Urbanization Coefficients

As discussed, there are two situations where the temporal urbanization coefficients may be appropriate for estimating the effects of urbanization, if it is the judgment of the analyst that the hydrologic effects of urbanization are or will be similar to those of the basins analyzed in this study: (1) to adjust the prediction of rural regression equations outside of Illinois flood-frequency region 2 for urbanization, and (2) to predict the future effects of urbanization for any basin in Illinois. For either situation the urbanization-adjusted flood-discharge quantile $Q_p\left(U\right)$ is given by:

$$Q_p\left(U\right) = Q_p\left(U_0\right)10^{\left(b_U\right)_p\left(U-U_0\right)}, \quad (21)$$

or, in log-transformed form,

$$\log_{10} Q_p\left(U\right) = \log_{10} Q_p\left(U_0\right) + \left(b_U\right)_p\left(U-U_0\right), \quad (22)$$

where

$Q_p\left(U\right)$ is the peak discharge quantile at the location of interest with AEP p adjusted to correspond to Theobald (2005) urbanization fraction U,

$Q_p\left(U_0\right)$ is the peak discharge quantile with AEP p at the initial urbanization fraction U_0, and

$\left(b_U\right)_p$ is the temporal urbanization coefficient for AEP p from table 9.

The urbanization-adjustment factors $10^{\left(b_U\right)_p\left(U-U_0\right)}$ in equation 21 are the same ratios $Q_p\left(U\right)/Q_p\left(U_0\right)$ as are plotted with solid lines in figure 14*A* and 14*B* for particular values of U_0 (0.0 and 0.5, respectively). Because of the functional form, the urbanization effect as indicated by this relation depends only on the coefficient $\left(b_U\right)_p$ and the urban fraction increase $U-U_0$; the effect is estimated to be the same for equivalent increases of $U-U_0$ regardless of the value of the initial urban fraction U_0.

For an application outside region 2 using StreamStats, the initial urbanization fraction U_0 would be zero, and the unadjusted flood-discharge quantile $Q_p\left(U_0\right)$ would come from the rural regional flood-frequency equation where the basin of interest is found. For an application inside region 2 using StreamStats, the initial urbanization fraction U_0 might be positive, and the unadjusted flood-discharge quantile $Q_p\left(U_0\right)$ would come from the spatial regression equations for region 2, such as the methods described in the section, "Applications of the Spatial Regression Equations." Whether inside or outside of region 2, the unadjusted flood-discharge quantile $Q_p\left(U_0\right)$ also could be a quantile estimate at or near

a gage. The Theobald (2005) data for 2010 as adjusted has been installed in StreamStats so that fractions of urbanization appropriate for use with equations 21 and 22 can be computed within StreamStats.

The variance of prediction V_U of the urbanization-adjusted flood-discharge quantile in log units, $\log_{10} Q_p(U)$, can be derived from equation 22 by computing the variances of both sides as

$$V_U = V_{U_0} + V_{b_U}\left(U - U_0\right)^2 \quad (23)$$

where

V_{U_0} is the variance of prediction of the unadjusted flood-discharge in log units, $\log_{10} Q(U_0)$, and

V_{b_U} is the variance of the urbanization coefficient $(b_U)_p$, which is the square of the standard error given in table 9.

The standard error of prediction of $\log_{10} Q_p(U)$, S_U, can be computed from V_U as $S_U = V_U^{1/2}$, and then S_U can be used in equations 14–16 to obtain a standard error in percent and confidence intervals.

Near-gage adjustment of peak discharge quantiles outside region 2 would be applicable only if the peak discharge quantiles at the streamgage arose from the same urbanization conditions as for the basin upstream from the site of interest.

Example Computations

To provide further clarification on the use of the results presented in this report, five example computations are provided in this section. Basic information about the examples is given in table 15.

Example 1: Ungaged Location in the Study Region, Far from a Streamgage

Consider a hypothetical ungaged basin with a drainage area (A) of 50 mi^2, urbanized land use fractions (U) *NLCD*_22_23_24 of 20 percent and Theobald_Urban of 40 percent, water and wetland fraction (W) DrainageClass1a of 15 percent, and slope (S) *DEM*_1_0_*P* of 3.67 feet per mile. These values usually will be obtained by StreamStats after delineation of the basin. First, it can be seen that the basin characteristic values are well within their corresponding ranges (table 14). If the basin is within region 2, the peak discharge quantiles should be computed by using the spatial regression equations, defined by equations 11 or 12, with coefficient values given in table 11. Taking the peak discharge quantile with AEP = 0.01 as an example, using equation 12, this quantile is computed as follows:

$$Q_{0.01} = 10^{(b_0)_{0.01}} A^{(b_A)_{0.01}} 10^{(b_U)_{0.01} U^{1/2}} 10^{(b_W)_{0.01} W^{1/2}} S^{(b_S)_{0.01}} \quad (24)$$

$$Q_{0.01} = 10^{1.968} 50^{0.771} 10^{0.207*0.20^{1/2}} 10^{-1.025*0.15^{1/2}} 3.67^{0.494}$$

$$Q_{0.01} = 1{,}790 \text{ ft}^3/\text{s},$$

where an *NLCD*_22_23_24 value of 20 percent is used for the urbanization measure U. Notice the values of W and U enter the equation as decimal fractions, whereas S enters in feet per mile.

The uncertainty of this estimate is computed by using equations 13–16. The variance V_i of the estimate is computed from equation 13:

$$V_i = \gamma^2 + x_i\left(X^t \Lambda^{-1} X\right)^{-1} x_i^t,$$

where

$\gamma^2 = 0.0528$ is the model error variance (table 12),

$$x_i = \left[1, \log_{10} A_i, U_i^{1/2}, W_i^{1/2}, \log_{10} S_i\right]$$

$$x_i = \left[1, \log_{10} 50, 0.20^{1/2}, 0.15^{1/2}, \log_{10} 3.67\right]$$

$$x_i = \left[1, 1.699, 0.4472, 0.3873, 0.5647\right],$$

Table 15. Example peak discharge quantile computations in this study in northeastern Illinois.

Number	Description	Equation used to compute discharge values
1	Ungaged location in study region, far from a streamgage	12
2	Ungaged location in study region, near a streamgage[1]	20
3	At a streamgage in study region	[2]17
4	Locations outside study region	21
5	Adjusting for future effects of urbanization	21

[1]In this study, an ungaged location is considered to be near a streamgage if ratio A_u/A_g of the drainage area at the ungaged location A_u to the drainage area at the gage A_g is between 0.5 and 1.5 and they are on the same stream.

[2]Values were computed with equation 17 and are tabulated in table 2.

and the matrix

$$\left(X^t\Lambda^{-1}X\right)^{-1} = 0.001\begin{bmatrix} 31.003 & -8.3921 & -7.6988 & -4.5311 & -20.598 \\ -8.3921 & 3.2522 & 1.1394 & -2.6149 & 5.9206 \\ -7.6988 & 1.1394 & 10.542 & -1.2200 & 2.4035 \\ -4.5311 & -2.6149 & -1.2200 & 40.324 & -1.2044 \\ -20.598 & 5.9206 & 2.4035 & -1.2044 & 18.346 \end{bmatrix}$$

(matrix data from table 13). With these values, the second term of V_i, $x_i\left(X^t\Lambda^{-1}X\right)^{-1}x_i^t$, is computed as $x_i\left(X^t\Lambda^{-1}X\right)^{-1}x_i^t =$

$$0.001\left[1, 1.699, 0.4472, 0.3873, 0.5647\right]\begin{bmatrix} 31.003 & -8.3921 & -7.6988 & -4.5311 & -20.598 \\ -8.3921 & 3.2522 & 1.1394 & -2.6149 & 5.9206 \\ -7.6988 & 1.1394 & 10.542 & -1.2200 & 2.4035 \\ -4.5311 & -2.6149 & -1.2200 & 40.324 & -1.2044 \\ -20.598 & 5.9206 & 2.4035 & -1.2044 & 18.346 \end{bmatrix}\begin{bmatrix} 1 \\ 1.699 \\ 0.4472 \\ 0.3873 \\ 0.5647 \end{bmatrix}$$

$$= 0.00214.$$

Therefore $V_i = 0.0528 + 0.00214 = 0.0549$.

Given the V_i value, the standard error of prediction in log units is $S_i = V_i^{1/2} = 0.234$, and from equation 14, the standard error of prediction in percent is

$$S_{pi} = 100\left\{\exp\left[\left(\ln 10\right)^2 V_i\right] - 1\right\}^{1/2} \tag{25}$$

$$S_{pi} = 100\left\{\exp\left[\left(\ln 10\right)^2 0.0549\right] - 1\right\}^{1/2}$$

$$S_{pi} = 58.1 \text{ percent.}$$

The confidence intervals are $\log_{10} Q_i \pm t_{\alpha/2,n-p}S_i$ (eq. 15), where $t_{\alpha/2,n-p}$ is the critical value of the *t* distribution at the alpha level α and $n-p$ degrees of freedom, where $n = 117$ is the number streamgages used in the spatial regressions and $p = 5$ is the number of basin characteristics plus 1. Here, for the 90-percent confidence intervals $t_{\alpha/2,n-p} = t_{0.95,112} = 1.659$, so the confidence intervals in log units are

$$\log_{10} Q_i \pm t_{\alpha/2,n-p}S_i = \log_{10}\left(1790\right) \pm 1.659 * 0.234 \tag{26}$$

$$\log_{10} Q_i \pm t_{\alpha/2,n-p}S_i = \left[2.864,\ 3.641\right].$$

After inverting the logarithmic transformation, the 90-percent confidence intervals are (eq. 16)

$$\left[Q_i 10^{-t_{\alpha/2,n-p}S_i}, Q_i 10^{t_{\alpha/2,n-p}S_i}\right] = \left[1790 * 10^{-1.659*0.234}, 1790 * 10^{1.659*0.234}\right] \tag{27}$$

$$\left[Q_i 10^{-t_{\alpha/2,n-p}S_i}, Q_i 10^{t_{\alpha/2,n-p}S_i}\right] = 10^{[2.864,3.641]}$$

$$\left[Q_i 10^{-t_{\alpha/2,n-p}S_i}, Q_i 10^{t_{\alpha/2,n-p}S_i}\right] = [730,\ 4{,}380]\ \text{ft}^3/\text{s}.$$

Summing up, the estimated 1-percent AEP peak discharge quantile $Q_{0.01}$ for this hypothetical ungaged basin on a stream in region 2 far from a streamgage is 1,790 ft^3/s with a standard error of prediction of 58.1 percent and a 90-percent confidence interval of [730, 4,380] ft^3/s.

Example 2: Ungaged Location in the Study Region, Near a Streamgage

Next assume that this hypothetical ungaged basin is located, still in region 2, upstream from USGS streamgage 05527950, Mill Creek at Old Mill Creek, Illinois, which has a drainage area of 59.87 mi^2 (table 1). In this case the value of the ratio A_u/A_g is $50/59.87 = 0.835$, and the adjustment weighting factor w_a takes the value $2|50/59.87 - 1| = 0.330$ (eq. 19), so a near-gage adjustment (eq. 20) is applicable (see discussion immediately following eq. 20). From table 2, the weighted AEP 0.01 at-gage flood-discharge quantile $(Q_{0.01})_{g,w}$ at streamgage 05527950 is 2,050 ft^3/s, and as previously computed the regional regression estimate at the ungaged site of interest $(Q_{0.01})_{u,r}$ is 1,790 ft^3/s. Therefore, the weighted estimate at the ungaged site of interest is

$$(Q_{0.01})_{u,w} = w_a (Q_{0.01})_{u,r} + (1 - w_a)(Q_{0.01})_{g,w}(A_u/A_g) \quad (28)$$

$$(Q_{0.01})_{u,w} = (0.330 * 1{,}790) + (0.670 * 2{,}050 * 0.835)$$

$$(Q_{0.01})_{u,w} = 1{,}740\ \text{ft}^3/\text{s}.$$

Summing up, the estimated 1-percent AEP peak discharge quantile $Q_{0.01}$ for this hypothetical ungaged basin on a stream in region 2 near to streamgage 05527950 ($A_u/A_g = 0.835$) is 1,740 ft^3/s, compared to 1,790 ft^3/s without the near-gage adjustment.

Example 3: At a Streamgage in the Study Region

To obtain an estimate at an applicable streamgage in the study region, no computations are needed. Although the method of computation is presented in the "At a Streamgage" section (eq. 17), the results of the computations have been tabulated (table 2). The particular value from table 2 to be used is the same weighted at-gage flood-discharge quantile $(Q_p)_{g,w}$ used in the previous near-gage adjustment computation. Following that example, for USGS streamgage 05527950, Mill Creek at Old Mill Creek, Illinois, the appropriate AEP 0.01 at-gage flood-discharge quantile $(Q_{0.01})_{g,w}$ is 2,050 ft^3/s.

Example 4: At a Location Outside the Study Region

If instead the hypothetical ungaged basin were outside region 2, then the adjustment of a rural estimate for urbanization described in the "Applications of the Temporal Urbanization Coefficients" section would be applicable (eq. 21). For example, if the AEP = 0.01 quantile estimate from the rural regional regression equations from Soong and others (2004) is 2,000 ft^3/s, then the urbanization-adjusted AEP = 0.01 quantile value at the location of interest is

$$Q_{0.01}(U) = Q_{0.01}(U_0) 10^{(b_U)_{0.01}(U - U_0)}, \quad (29)$$

where the urban fraction of interest, U, is, by assumption, 40 percent or 0.4, and the current urban fraction, U_0, is 0, because the discharge quantile value being adjusted, $Q_{0.01}(U_0)$, is being estimated by using a rural regression equation. Therefore,

$$Q_{0.01}(U) = 2{,}000 * 10^{0.312*(0.40-0.0)}$$

$$Q_{0.01}(U) = 2{,}000 * 1.333$$

$$Q_{0.01}(U) = 2{,}670\ \text{ft}^3/\text{s},$$

where

$(b_U)_{0.01} = 0.312$ is taken from table 9.

The variance of prediction of this estimate in log units can be computed from equation 23 as follows:

$$V_U = V_{U_0} + V_{b_U}(U - U_0)^2 \quad (30)$$

$$V_U = 0.0549 + 0.134^2 (0.4 - 0.0)^2$$

$$V_U = 0.05777,$$

where V_{U_0}, the variance of prediction of the unadjusted flood-discharge in log units, $\log_{10} Q(U_0)$, is assumed, just for this example, to have the same value as V_i which was computed previously for region 2 (in an actual computation it would be

necessary to compute this value by the relevant method, such as the method given in Soong and others (2004), which is currently (2016) implemented in StreamStats), and V_{b_U} is the square of the standard error of $(b_U)_{0.01}$, the value of which is given in table 9.

Given this value of V_U, the standard error is $S_U = (V_U)^{1/2} = 0.240$, and the standard error in percent units is

$$S_{pU} = 100\left\{\exp\left[(\ln 10)^2 V_U\right] - 1\right\}^{1/2} \quad (31)$$

$$S_{pU} = 100\left\{\exp\left[(\ln 10)^2\, 0.05777\right] - 1\right\}^{1/2}$$

$$S_{pU} = 59.9 \text{ percent.}$$

Confidence intervals for this estimate can be computed by using equation 16 as already shown; the resulting 90-percent confidence interval in log10 units is $[3.0269, 3.8247]$ and in cubic feet per second, $[1{,}060, 6{,}680]$.

Summing up, the estimated 1-percent AEP peak discharge quantile $Q_{0.01}$ for this hypothetical ungaged basin on a stream outside region 2 increases from 2,000 to 2,670 ft^3/s as a result of adjusting for the effects of urbanization increasing from 0 to 40 percent. The estimated adjusted quantile has a standard error of prediction of 59.9 percent and a 90-percent confidence interval of $[1{,}060, 6{,}680]$ ft^3/s.

Example 5: Adjustment for Effects of Future Urbanization

Finally, assume the hypothetical basin is as originally assumed, with the same basin characteristics, but an estimate of the peak discharge quantile at "build-out" (100 percent urbanization) is desired. If the future urbanization is expected to have similar hydrologic effects as the basins used in this study, the temporal urbanization coefficients would again be applicable, and the estimate of the AEP = 0.01 peak discharge quantile would be obtained by equation 21 as follows:

$$Q_{0.01}(U) = Q_{0.01}(U_0)\,10^{(b_U)_{0.01}(U - U_0)}, \quad (32)$$

where the future urban fraction of interest, U, is taken to be 100 percent or 1.0, and the current urban fraction, U_0, is 40 percent or 0.40, according to the original assumptions on this hypothetical basin.
Therefore

$$Q_{0.01}(U) = 1{,}790 * 10^{0.312*(1.0-0.4)}$$

$$Q_{0.01}(U) = 1{,}790 * 1.539$$

$$Q_{0.01}(U) = 2{,}750 \text{ ft}^3\text{/s},$$

where

$Q_{0.01}(U_0) = 1{,}790$ is taken from the first example calculation (eq. 24), and

$(b_U)_{0.01} = 0.312$ is taken from table 9.

The uncertainty of this estimate can be obtained from equation 23 as in the previous example; the resulting uncertainty S_{pU} is 62.0 percent, and the 90-percent confidence interval is $[3.0286, 3.8507]$ in $\log_{10}$ units and $[1{,}070, 7{,}090]$ in cubic feet per second.

Summing up, the estimated 1-percent AEP peak discharge quantile $Q_{0.01}$ for this hypothetical ungaged basin increases from 1,790 ft^3/s to 2,750 ft^3/s as a result of adjusting for the effects of urbanization increasing from 40 to 100 percent. The estimated adjusted quantile has a standard error of prediction of 62.0 percent and a 90-percent confidence interval of $[1{,}070, 7{,}090]$ ft^3/s.

A future increase in urbanization does not need to take the urban fraction to completed build-out, that is, $U = 1.0$. Any value of U greater than the current urban fraction ($U_0 = 0.40$, in the example) could be used to estimate the effects of future increases in urbanization.

Summary

This report provides two sets of equations for estimating peak discharge quantiles at annual exceedance probabilities (AEPs) of 0.50, 0.20, 0.10, 0.04, 0.02, 0.01, 0.005, and 0.002 (recurrence intervals of 2, 5, 10, 25, 50, 100, 200, and 500 years, respectively) for urbanized and urbanizing watersheds in Illinois based on analysis of 117 streamgage records in and near Illinois flood-frequency region 2. One set of equations was developed through a temporal analysis by using a two-step least squares-quantile regression technique that measures the average effect of changes in the urbanization of the gaged watersheds used in the study and were used to adjust the annual maximum peak discharge records to 2010 urbanization conditions. The other set of equations was developed through a spatial analysis using generalized least-squares (GLS) regression applied to quantiles estimated from the urbanization-adjusted records.

The effect of urbanization indicated by the two sets of equations is substantially different, with the temporal analysis indicating a larger effect, especially for larger AEPs (smaller recurrence intervals). This difference in urbanization effect was attributed to coefficient biases in the spatial analysis, and as a result, the urbanization coefficients from spatial equations are recommended for use only at ungaged locations in

the study region. Other applications discussed in the report, which are estimating the effect of urbanization in regions of Illinois outside flood-frequency region 2 in combination with rural regression equations and estimating the effect of future urbanization anywhere in Illinois, use the results of the temporal analysis.

The peak discharge quantiles for the spatial analysis were computed by using the Expected Moments Algorithm following the censoring of potentially influential low floods identified by a multiple Grubbs-Beck test. To improve the skew estimates used for the peak discharge quantile estimation, weighted skew coefficients were computed as the variance-weighted average of at-site and regional skew coefficients. The regional skew coefficients were obtained from a new regional skew model, which estimates skewness as an increasing linear function of the urbanized land use fraction, with values ranging from -0.39 to +0.58.

Several urbanization, water and wetland, and slope variables, in addition to drainage area, were considered for use as basin characteristics in the spatial equations in a preliminary weighted least-squares analysis. The combination of variables giving the best results—drainage area, the fraction of developed land, the fraction of land with poorly drained soils or likely water, and the basin slope estimated as the ratio of the basin relief to basin perimeter—were used in the GLS analysis to develop the final spatial regression equations.

In addition to this report, which details the development of the two sets of equations and provides guidance on their application, including numerical examples, the products of the study include the urbanization-adjusted annual maximum peak discharge records and peak discharge quantile estimates at 181 streamgages: the 117 streamgages used to develop the spatial regression equations and 64 additional streamgages in the region that originally were considered for use in the study but later deemed to be redundant. The equations and quantile estimates are available in the web application StreamStats, and the urbanization-adjusted peak discharge records are provided in a table as part of this report and as a collection of tables and plots by streamgage at https://doi.org/10.3133/sir20165050.

References Cited

Allen, H.E., Jr., and Bejcek, R.M., 1979, Effects of urbanization on the magnitude and frequency of floods in northeastern Illinois: U.S. Geological Survey Water-Resources Investigations Report 79–36, 48 p.

Angel, J.R., and Changnon, S.A., 2008, Record heavy rains in August 2007—Cause, magnitude, and impacts: Transactions of the Illinois State Academy of Science, v. 101, p. 187–199.

Arnold, T.L., Sullivan, D.J., Harris, M.A., Fitzpatrick, F.A, Scudder, B.C., Ruhl, P.M., Hanchar, D.W., and Stewart, J.S., 1999, Environmental setting of the Upper Illinois River Basin and implications for water quality: U.S. Geological Survey Water-Resources Investigations Report 98–4268, 67 p.

Belda, M., Holtanová, E., Halenka, T., and Kalvová, J., 2014, Climate classification revisited—From Köppen to Trewartha: Climate Research, v. 59, p. 1–13.

Canay, I.A., 2011, A simple approach to quantile regression for panel data: The Econometrics Journal, v. 14, p. 368–386.

Changnon, S.A., 1999, Record flood-producing rainstorms of 17–18 July 1996 in the Chicago metropolitan area, Part III—Impacts and responses to the flash flooding: Journal of Applied Meteorology, v. 38, p. 273–280.

Changnon, S.A., 2010, Stormwater management for a record rainstorm at Chicago: Journal of Contemporary Water Research and Education, no. 146, p. 103–109.

Changnon, S.A., 2011, Major damages in northern Illinois from a record-setting rainstorm in 2010: Transactions of the Illinois State Academy of Science, v. 104, p. 119–125.

Changnon, S.A., Angel, J.R., Kunkel, K.E., and Lehman, C.M.B, 2004, Climate atlas of Illinois: Champaign, Ill., Illinois State Water Survey, 309 p.

Changnon, S.A., and Demissie, M., 1996, Detection of changes in streamflow and floods resulting from climate fluctuations and land use-drainage changes: Climatic Change, v. 32, p. 411–421.

Changnon, D., Fox., D., and Bork, S., 1996, Differences in warm-season, rainstorm-generated stormflows for northeastern Illinois urbanized basins: Water Resources Bulletin, v. 32, no. 6, p. 1307–1317.

Changnon, S.A., and Westcott, N.E., 2002a, Heavy rainstorms in Chicago—Increasing frequency, altered impacts, and future implications: Journal of the American Water Resources Association, v. 28, no. 5, p. 1467–1475.

Changnon, S.A., and Westcott, N.E., 2002b, A record number of heavy rainstorms in Chicago in 2001: Transactions of the Illinois State Academy of Science, v. 95, no. 2, p. 73–85.

Cohn, T.A., Berenbrock, C., Kiang, J.E., and Mason, R.R., Jr., 2012, Calculating weighted estimates of peak streamflow statistics: U.S. Geological Survey Fact Sheet 2012–3038, 4 p. [Also available at https://pubs.usgs.gov/fs/2012/3038/.]

Cohn, T.A., England, J.F., Berenbrock, C.E., Mason, R.R., Stedinger, J.R., and Lamontagne, J.R., 2013, A generalized Grubbs-Beck test statistic for detecting multiple potentially influential low outliers in flood series: Water Resources Research, v. 49, p. 5047–5058. [Also available at https://doi.org/10.1002/wrcr.20392.]

Cohn, T.A., Lane, W.L., and Baier, W.G., 1997, An algorithm for computing moments-based flood quantile estimates when historical flood information is available: Water Resources Research, v. 33, no. 9, p. 2089–2096.

Cohn, T.A., Lane, W.L., and Stedinger, J.R., 2001, Confidence intervals for expected moments algorithm flood quantile estimates: Water Resources Research, v. 37, no. 6, p. 1695–1706.

Cowardin, L.M., Carter, V., Golet, F.C., and LaRoe, E.T., 1979, Classification of wetlands and deepwater habitats of the United States: Washington, D.C., U.S. Department of the Interior, Fish and Wildlife Service, FWS/OBS–79/31, 131 p. [Also available at https://www.fws.gov/wetlands/Documents/Classification-of-Wetlands-and-Deepwater-Habitats-of-the-United-States.pdf.]

Croissant, Y., and Millo, G., 2008, Panel data econometrics in R—The plm package: Journal of statistical software, v. 27, no. 2, 51 p., accessed December 29, 2010, at http://www.jstatsoft.org/v27/i02/.

Drainage Manual Committee for IDOT Division of Highways, 2011, IDOT drainage manual: Springfield, Ill., Illinois Department of Transportation [variously paged].

Eng, Ken, Chen, Yin-Yu, and Kiang, J.E., 2009, User's guide to the weighted-multiple-linear-regression program (WREG version 1.0): U.S. Geological Survey Techniques and Methods, book 4, chap. A8, 21 p.

Espey, W.H., Jr., and Winslow, D.E., 1974, Urban flood frequency characteristics: Journal of the Hydraulics Division, Proceedings of the American Society of Civil Engineers, v. 100, no. HY2, p. 279–293.

Farmer, W.H., 2017, WREG: USGS WREG v. 2.02 R package version 2.02: U.S. Geological Survey WREG software web page, accessed November 15, 2019, at https://rdrr.io/github/USGS-R/WREG/.

Fazio, D.J., and Sharpe, J.B., 2012, Flood of September 13–16, 2008, in northeastern Illinois: U.S. Geological Survey Data Series 726, 40 p. [Also available at https://pubs.usgs.gov/ds/726/.]

Fehrenbacher, J.B., Alexander, J.D., Jansen, I.J., Darmody, R.G., Pope, R.A., Flock, M.A., Voss, E.E., Scott, J.W., Andrews, W.F., and Bushue, L.J., 1984, Soils of Illinois: University of Illinois, College of Agriculture, Agricultural Experiment Station, and U.S. Department of Agriculture, Soil Conservation Service, 85 p.

Frees, E.W., 2004, Longitudinal and panel data: Analysis and applications in the social sciences: Cambridge, Cambridge University Press, 467 p.

Fuller, W.A., 1987, Measurement error models: New York, John Wiley and Sons, 440 p.

Gesch, D.B., Oimoen, M.J., Greenlee, S.K., Nelson, C.A., Steuck, M., and Tyler, D.J., 2002, The National Elevation Dataset: Photogrammetric Engineering and Remote Sensing, v. 68, no. 1, p. 5–11. [Also available at https://www.asprs.org/wp-content/uploads/pers/2002journal/january/highlight.html.]

Greene, W.H., 1997, Econometric analysis (3d ed.): Upper Saddle River, N.J., Prentice Hall, 1075 p.

Grimaldi, S., Petroselli, A., Alonso, G., and Nardi, F., 2010, Flow time estimation with spatially variable hillslope velocity in ungauged basins: Advances in Water Resources, v. 33, p. 1216–1223.

Griffis, V.W., and Stedinger, J.R., 2007, The use of GLS regression in regional hydrologic analyses: Journal of Hydrology, v. 344, p. 82–95.

Griffis, V.W., and Stedinger, J.R., 2009, Log-Pearson type 3 distribution and its application in flood frequency analysis. III—Sample skew and weighted skew estimators: Journal of Hydrologic Engineering, v. 14, no. 2, p. 121–130.

Gruber, A.M., Reis, D.S., Jr., and Stedinger, J.R., 2007, Models of regional skew based on Bayesian GLS regression, Paper 40927–3285, *in* Kabbes, K.C., ed., Restoring our natural habitat—Proceedings of the 2007 World Environmental and Water Resources Congress—May 15–19, Tampa, Florida: Reston, Va., American Society of Civil Engineers [variously paged].

Gruber, A.M., and Stedinger, J.R., 2008, Models of LP3 regional skew, data selection and Bayesian GLS regression, Paper 596, *in* Babcock, R.W., and Walton, Raymond, eds., World Environmental and Water Resources Congress 2008–Ahupua'a—Proceedings of the congress—May 12–16, 2008, Honolulu, Hawaii: Reston, Va., American Society of Civil Engineers [variously paged].

Hansel, A.K., and McKay, E.D., III, 2010, Quaternary period, *in* Kolata, D.R., and Nimz, C.K., eds., Geology of Illinois: Champaign, Ill., Illinois State Geological Survey, p. 216–247.

Hayden, B.P., 1988, Flood climates, *in* Baker, V.R., Kochel, R.C., and Patton, P.C., eds., Flood geomorphology: New York, John Wiley and Sons, p. 13–26.

Helsel, D.R., and Hirsch, R.M., 2002, Statistical methods in water resources: U.S. Geological Survey Techniques of Water-Resources Investigations, book 4, chapter A3, 522 p.

Hejazi, M.I., and Markus, M., 2009, Impacts of urbanization and climate variability on floods in northeastern Illinois: Journal of Hydrologic Engineering, v. 14, no. 6, p. 606–616. [Also available at https://doi.org/10.1061/(ASCE)HE.1943-5584.0000020.]

Hodge, S.A., and Tasker, G.D., 1995, Magnitude and frequency of floods in Arkansas: U.S. Geological Survey Water-Resources Investigations Report 95–4224 [variously paged; see p. 37–39].

Hodgkins, G.A., Hebson, Charles, Lombard, P.J., and Mann, Alexander, 2007, Comparison of peak-flow estimation methods for small drainage basins in Maine: U.S. Geological Survey Scientific Investigations Report 2007–5170, 32 p.

Illinois Department of Natural Resources, 1996, Illinois land cover, an atlas: Springfield, Ill., Illinois Department of Natural Resources, 157 p.

Ishii, A.L., Soong, D.T., and Sharpe, J.B., 2010, Implementation and evaluation of the Streamflow Statistics (StreamStats) web application for computing basin characteristics and flood peaks in Illinois: U.S. Geological Survey Scientific Investigations Report 2009–5197, 25 p.

Jin, S., Yang, L., Danielson, P., Homer, C., Fry, J., and Xian, G., 2013, A comprehensive change detection method for updating the National Land Cover Database to circa 2011: Remote Sensing of Environment, v. 132, p. 159–175.

Juhl, A.R., 2005, Flood control and drainage, *in* Reiff, J.L., Keating, A.D., and Grossman, J.R., The Electronic Encyclopedia of Chicago: Chicago, Chicago Historical Society, accessed August 4, 2015, at http://www.encyclopedia.chicagohistory.org/pages/460.html.

Karstensen, K.A., Shaver, D.K., Alexander, R.L, Over, T.M., and Soong, D., 2013, Land change in the Central Corn Belt Plains ecoregion and hydrologic consequences in developed areas—1939–2000: U.S. Geological Survey Open-File Report 2013–1157, 21 p. [Also available at https://pubs.usgs.gov/of/2013/1157/.]

Koenker, R., 2005, Quantile regression: Cambridge, England, Cambridge University Press, 349 p.

Koenker, R., 2013, quantreg—Quantile Regression: R package version 5.05, accessed November 6, 2014, at http://CRAN.R-project.org/package=quantreg.

Konrad, C.P., 2003, Effects of urban development on floods: U.S. Geological Survey Fact Sheet FS–076–03, 4 p.

Leighton, M.M., Ekblaw, G.E., and Horberg, L., 1948, Physiographic divisions of Illinois: The Journal of Geology, v. 56, no. 1, p. 16–33.

Maidment, D.R., ed., 2002, Arc Hydro—GIS for water resources: Redlands, Calif., Esri, 220 p.

Mariner, R.D., 2005, Land use, *in* Reiff, J.L., Keating, A.D., and Grossman, J.R., The Electronic Encyclopedia of Chicago: Chicago, Chicago Historical Society, accessed August 6, 2015, at http://www.encyclopedia.chicagohistory.org/pages/721.html.

Moglen, G.E., and Shivers, D.E., 2006, Methods for adjusting USGS rural regression peak discharges in an urban setting: U.S. Geological Survey Scientific Investigation Report 2006–5270, 65 p.

Over, T.M., Saito, R.J., and Soong, D.T., 2016, Adjusting annual maximum peak discharges at selected stations in northeastern Illinois for changes in land-use conditions: U.S. Geological Survey Scientific Investigations Report 2016–5049, 33 p. [Also available at https://doi.org/10.3133/sir20165049.]

Peel, M.C., Finlayson, B.L., and McMahon T.A., 2007, Updated world map of the Köppen-Geiger climate classification: Hydrology and Earth Systems Sciences, v. 11, p. 1633–1644.

Piskin, K., and Bergstrom, R.E., 1975, Glacial drift in Illinois—thickness and character: Illinois State Geological Survey, Circular 490, 35 p., 2 plates.

R Core Team, 2014, R—A language and environment for statistical computing: Vienna, Austria, R Foundation for Statistical Computing, accessed November 6, 2014, at http://www.R-project.org.

R Core Team, 2020, R—A language and environment for statistical computing: Vienna, Austria, R Foundation for Statistical Computing, accessed April 24, 2020, at https://www.R-project.org/.

Rao, A.R., 2006, Flood frequency relationships for Indiana: West Lafayette, Ind., Joint Transportation Research Program, Purdue University, Final Report FHWA/IN/JTRP-2005/18, 140 p.

Reis, D.S., Jr., Stedinger, J.R., and Martins, E.S., 2005, Bayesian generalized least squares regression with application to the log Pearson type 3 regional skew estimation: Water Resources Research, v. 41, no. 10, 14 p. [Also available at https://doi.org/10.1029/2004WR003445.]

Resource Coordination Policy Committee, 1998, Our community and flooding: A report of the status of floodwater management in the Chicago Metropolitan Area, 72 p., accessed August 6, 2015, at https://www.dnr.illinois.gov/WaterResources/Documents/OurCommunityAndFlooding_Oct1998.pdf.

Ries III, K.G., 2007, The national streamflow statistics program—A computer program for estimating streamflow statistics for ungaged sites: U.S. Geological Survey Techniques and Methods, book 4, chap. A6, 37 p.

Rosbjerg, D. and others, 2013, Prediction of floods in ungauged basins, chap. 9 *of* Günter Blöschl, G., and others, eds., Runoff prediction in ungauged basins: Cambridge, Cambridge University Press, p. 189–226, accessed August 4, 2015, at https://doi.org/10.1017/CBO9781139235761.012.

Rougé, C., and Cai, X., 2014, Crossing-scale hydrological impacts of urbanization and climate variability in the greater Chicago area: Journal of Hydrology, v. 517, p. 13–27. [Also available at https//doi.org/10.1016/j.jhydrol.2014.05.005.]

Sauer, V.B., Thomas, W.O., Jr., Stricker, V.A., and Wilson, K.V., 1983 Flood characteristics of urban watersheds in the United States: U.S. Geological Survey Water-Supply Paper 2207, 63 p.

Schneider, A.F., 1966, Physiography, *in* Lindsey, A.A., ed., Natural features of Indiana: Indianapolis, Indiana Academy of Science, p. 40–56.

Soil Survey Staff, Natural Resources Conservation Service, United States Department of Agriculture, Web Soil Survey, 2013, website accessed October 2013 at https://websoilsurvey.nrcs.usda.gov/.

Soong, D.T., Ishii, A.L., Sharpe, J.B., and Avery, C.F., 2004, Estimating flood-peak discharge magnitudes and frequencies for rural streams in Illinois: U.S. Geological Survey Scientific Investigations Report 2004–5103, 158 p.

Stedinger, J.R., and Tasker, G.D., 1985, Regional hydrologic analysis, 1, ordinary, weighted, and generalized least squares compared: Water Resources Research, v. 21, no. 9, p. 1421–1432.

Tasker, G.D., 1975, Combining estimates of low-flow characteristics of streams in Massachusetts and Rhode Island: Journal of Research of the U.S. Geological Survey, v. 3, no. 1, p. 107–112.

Tasker, G.D., and Stedinger, J.R., 1989, An operational GLS model for hydrologic regression: Journal of Hydrology, v. 111, p. 361–375.

Theobald, D., 2005, Landscape patterns of exurban growth in the USA from 1980 to 2020: Ecology and Society, v. 10, no. 1, article 32, 29 p. [Also available at https://www.ecologyandsociety.org/vol10/iss1/art32/.]

Thiessen, A.H., 1911, Precipitation averages for large areas: Monthly Weather Review, v. 39, no. 7, p. 1082–1089.

U.S. Army Corps of Engineers, 2013, National Inventory of Dams: U.S. Army Corps of Engineers, digital data, accessed August 16, 2013, at http://geo.usace.army.mil/pgis/f?p=397:12. [Updated version available at https://nid.sec.usace.army.mil/ords/f?p=105:1:.]

U.S. Geological Survey, 2013, Peak streamflow for the Nation—National Water Information System: Web Interface, accessed December 2, 2013, at https://nwis.waterdata.usgs.gov/usa/nwis/peak.

U.S. Interagency Advisory Committee on Water Data, 1982, Guidelines for determining flood flow frequency—Bulletin #17B of the Hydrology Subcommittee (revised and corrected): U.S. Geological Survey, Office of Water Data Coordination, 28 p. [plus appendixes].

Veilleux, A.G., 2009, Bayesian GLS regression for regionalization of hydrologic statistics, floods, and Bulletin 17 skew: Ithaca, N.Y., Cornell University, unpublished M.S. thesis.

Veilleux, A.G., 2011, Bayesian GLS regression, leverage and influence for regionalization of hydrologic statistics: Ithaca, N.Y., Cornell University, unpublished Ph.D. dissertation.

Veilleux, A.G., Cohn, T.A., Flynn, K.M., Mason, R.R., Jr., and Hummel, P.R., 2013, Estimating magnitude and frequency of floods using the PeakFQ 7.0 program: U.S. Geological Survey Fact Sheet 2013–3108, 2 p. [Also available at https://doi.org/10.3133/fs20133108.]

Villarini, G., Smith, J.A., Baeck, M.L., Smith, B.K., and Sturdevant-Rees, P., 2013, Hydrologic analyses of the July 17–18, 1996, flood in Chicago and the role of urbanization: Journal of Hydrologic Engineering, v. 18, p. 250–259. [Also available at https://doi.org/10.1061/(ASCE)HE.1943-5584.0000462.]

Vogel, R.M., 2006, Regional calibration of watershed models, chap. 3 *of* Singh, V.P., and Frevert, D.K., Watershed models: Boca Raton, Fla., CRC Press, p. 47–71.

Walker, J.F., and Krug, W.R., 2003, Flood-frequency characteristics of Wisconsin streams: U.S. Geological Survey Water-Resources Investigations Report 03–4250, 37 p.

Westcott, N.E., 2015, Continued operation of a 25-raingage network for collection, reduction, and analysis of precipitation data for Lake Michigan diversion accounting—Water year 2014—Contract Report 2015-01, Champaign, Illinois: Illinois State Water Survey, Prairie Research Institute, University of Illinois at Urbana-Champaign, 82 p.

Winters, B.A., Angel, J., Ballerine, C., Byard, J., Flegel, A., Gambill, D., Jenkins, E., McConkey, S., Markus, M., Bender, B.A., and O'Toole, M.J., 2015, Report for the Urban Flooding Awareness Act: Illinois Department of Natural Resources, 89 p., accessed August 9, 2015, at https://www2.illinois.gov/dnr/waterresources/documents/Final_UFAA_Report.PDF

Wisconsin Department of Natural Resources, 1992, Wisconsin wetland inventory classification guide: Publication PUBL–WZ–WZ023, 3 p. [Also available at https://www2.illinois.gov/dnr/waterresources/documents/Final_UFAA_Report.PDF.]

Xian, G., Homer, C., Dewitz, J., Fry, J., Hossain, N., and Wickham, J., 2011, The change of impervious surface area between 2001 and 2006 in the conterminous United States: Photogrammetric Engineering and Remote Sensing, v. 77, no. 8, p. 758–762.

Appendix 1

Appendix 1. Northeastern Illinois Regional Skew Analysis

For the log-transformation of annual peak discharges, Bulletin 17B (U.S. Interagency Advisory Committee on Water Data, 1982) recommends using a weighted average of the station skew coefficient and a regional skew coefficient to improve estimates of annual flood-probability discharges (AFPDs). Bulletin 17B supplies a national map but also encourages hydrologists to develop more specific local relations. From the publication of the national map based on data through 1973 through the end of this study in 2009, some 36 years of additional information has accumulated and improved spatial estimation procedures have been developed (Stedinger and Griffis, 2008). Furthermore, prior national and Illinois analyses of regional skew such as that in Soong and others (2004) did not consider urbanization. For these reasons, for this study in northeastern Illinois a regression analysis was done to develop a regional skew model.

Reis and others (2005), Gruber and others (2007), and Gruber and Stedinger (2008) developed a Bayesian generalized least-squares (GLS) regression model for regional skewness analyses. The method provides a more reasonable description of the model error variance than either the generalized least-squares method-of-moments or maximum likelihood point estimates (Veilleux, 2011). However, because of complications introduced by the use of the Expected Moments Algorithm (EMA), with multiple Grubbs-Beck censoring of potentially influential low floods (Cohn and others, 2013) and large cross-correlations between annual peak discharges at pairs of streamgages, an alternate regression procedure was developed to provide stable and defensible results for regional skew regression (Veilleux and others, 2012; Veilleux, 2011; Lamontagne and others, 2012). This alternate procedure is referred to as the Bayesian weighted least-squares/Bayesian generalized least-squares (B–WLS/B–GLS) regression framework (Veilleux and others, 2011; Veilleux, 2011; Veilleux and others, 2012).

The B–WLS/B–GLS regression analysis uses an ordinary least-squares (OLS) analysis to fit an initial regional skewness model; the OLS model is then used to generate a regional skew-coefficient estimate for each streamgage. This regional estimate is the basis for computing the variance of each station skew-coefficient estimator used in the weighted least-squares (WLS) analysis. Then, B–WLS is used to generate estimators of the regional skew-coefficient model parameters. Finally, B–GLS is used to estimate the precision of those WLS parameter estimators, to estimate the model error variance and the precision of that variance estimator, and to compute various diagnostic statistics. The methodology for the regional skewness model is described in detail in Eash and others (2013).

Application of B–WLS/B–GLS Method in Northeastern Illinois

This regional skew study is based on the temporally adjusted annual peak discharge data from the 117 nonredundant streamgages in northeastern Illinois and the surrounding states that were included in the regional regression analyses described in the main report (table 1). As stated in Bulletin 17B, the skew coefficient of the station is sensitive to extreme events, and more accurate estimates can be obtained from longer records. Thus, for regional skew studies it is preferred that each streamgage have a minimum of 30 to 35 years of record. However, because of the nature of the data available in northeastern Illinois, in particular at the urban stations, the minimum was reduced to 15 years to ensure that the entire study area was represented. Applying this minimum reduced the number of streamgages used in the regional skew study to 110 (table 1–1, available at https://doi.org/10.3133/sir20165050).

Because the dataset includes censored data and historic information, the effective record length used to compute the precision of the skewness estimators is no longer simply the number of annual peak discharges at a streamgage. Instead, a more complex calculation is used to take into account the availability of historic information and censored values. Although historic information and censored peaks provide valuable information, they often provide less information than an equal number of years with systematically recorded peaks (Stedinger and Cohn, 1986). The calculations made to compute the pseudo record length (PRL) are described in Eash and others (2013). PRL equals the systematic record length if such a complete record is all that is available for a site.

The station logarithmic skew coefficient, $\hat{\gamma}_S$ (table 1–1), and its mean square error, $MSE\left[\hat{\gamma}_S\right]$, were computed by using expected moments analysis (EMA) (Cohn and others, 1997; Griffis and others, 2004). The streamgage skewness estimates are ensured to be unbiased by using the correction factor developed by Tasker and Stedinger (1986) and used in Reis and others (2005). In addition to the skew data, selected basin characteristics for each of the streamgages were available as explanatory variables for the regional skew study.

A model for the cross-correlation of the logarithms of the annual maximum peak discharges between streamgage pairs is needed for the analysis because sample cross-correlations commonly are unavailable and are subject to large uncertainty, usually including unphysical negative values. Such a model for the northeastern Illinois study area was developed by using the 39 streamgages with at least 45 years of concurrent systematic peaks. A logit model, termed the Fisher Z transformation (Kendall and Stuart, 1961), where $Z = \ln\left[\left(1+r\right)/\left(1-r\right)\right]$, was used to transform the sample correlations r_{ij} from their $\left(-1,+1\right)$ range to a $\left(-\infty,+\infty\right)$ range that is appropriate for least-squares fitting. Various models relating the transformed cross-correlations to various basin characteristics were considered. The adopted model relates the cross-correlations to the distance D_{ij} between streamgage basin centroids according to the fitted equation $Z_{ij} = 0.32 + \exp\left[-0.40 - 0.042D_{ij}\right]$ (fig. 1–1*A*). The fitted relation between Z and the distance between basin centroids together with sample data from the 567 streamgage pairs of data is shown in figure 1–1*A*. The equivalent function relation between the cross-correlations and basin centroid distance, which is obtained by back-transforming from *Z* to *r* as $r = \left[\exp\left(2Z\right)-1\right]/\left[\exp\left(2Z\right)+1\right]$ is shown in figure 1–1*B*.

Results of Regional Skew Analysis in Northeastern Illinois

The more promising basin characteristics from a preliminary analysis of the regional spatial regressions were selected for testing as explanatory variables in the regression analysis for regional skew. These selected basin characteristics included drainage area, the urbanization measure *NLCD*_22_23_24, the DEM-based slope variable DEM_slope, and several water and wetness variables: NWI. total, NWI.emergent, DrainageClass1, DrainageClass1a, and *NLCD*_11_95 (see table 3 for definitions). Of these, only *NLCD*_22_23_24 was statistically significant in explaining the site-to-site variability in skewness, with a square-root transformation providing the better result as compared to untransformed values. Thus, the best model, as classified by having the smallest model error variance, σ^2_δ, and largest pseudo R^2_δ is the model using *NLCD*_22_23_24$^{1/2}$, denoted URBAN. Results for the URBAN model, as well as the constant regional model, denoted CONSTANT, for comparison are provided in table 1–2.

Pseudo R^2_δ, included in table 1–2, describes the estimated fraction of the variability in the true skewness from site-to-site explained by each model (Gruber and others, 2007; Parrett and others, 2011). A constant model does not explain any variability, so the pseudo R^2_δ for the CONSTANT model is equal to 0 percent. The URBAN model has a pseudo R^2_δ of 14 percent indicating that inclusion of the *NLCD*_22_23_24 basin characteristic in the model explains 14 percent of the variability in the true skews. Although the URBAN model accounts for a relatively small portion of the total variation in skews, it is important to note that the focus of the study is on the effects of urbanization. A statistically significant dependence of skewness on the *NLCD*_22_23_24 characteristic, a measure of urbanization, suggests that not including it in the skewness model could negatively affect the final spatial regression equations. Also, the posterior mean of the model error variance, σ^2_δ, for the URBAN model was 0.16, which is smaller than that of the CONSTANT model (σ^2_δ = 0.19). Thus, the URBAN model was chosen as the final regional skew model for the northeastern Illinois study area.

The average variance of prediction at a new site (AVP_{new}) describes the precision of the regional skew. In table 1–2, the URBAN model has the lower AVP_{new}, equal to 0.19. This AVP_{new} is an average value computed by averaging the variance of prediction at a new site (VP_{new}) for all of the 110 streamgages in the analysis. Just as regional skew varies from streamgage to streamgage, depending on *NLCD*_22_23_24, so too do the values of VP_{new}. Values of the variance of prediction for the regional skew, VP_{new}, and effective record length (ERL) for the URBAN model for values of *NLCD*_22_23_24 between 0 and 1 are given in table 1–3. Thus, the URBAN skew model for northeastern Illinois has VP_{new} values ranging from 0.18 to 0.22 and effective record lengths ranging from 39 to 43 years, depending on *NLCD*_22_23_24. It is important to note that for the purposes of this study, the AVP_{new} of 0.19 was used when weighting the at-site skew with the regional skew.

The URBAN model provides a reasonable fit for the northeastern Illinois regional skew data (fig. 1–2). As compared to the CONSTANT model, the URBAN model provides smaller values of regional skew for basins with less development (smaller *NCLD*_22_23_24 values) and larger values of regional skew for basins with more development (larger *NCLD*_22_23_24 values). The URBAN model indicates that skewness increases substantially with urbanization from a value of -0.39 for a basin with *NLCD*_22_23_24 equal to 0 to +0.58 for a basin where the *NLCD*_22_23_24 fraction is equal to one.

Pseudo analysis of variance (Pseudo ANOVA) statistics for the northeastern Illinois regional skew analysis were determined as additional diagnostics for the selected model (table 1–4). Explanations of how the statistics were computed can be found in Eash and others (2013).

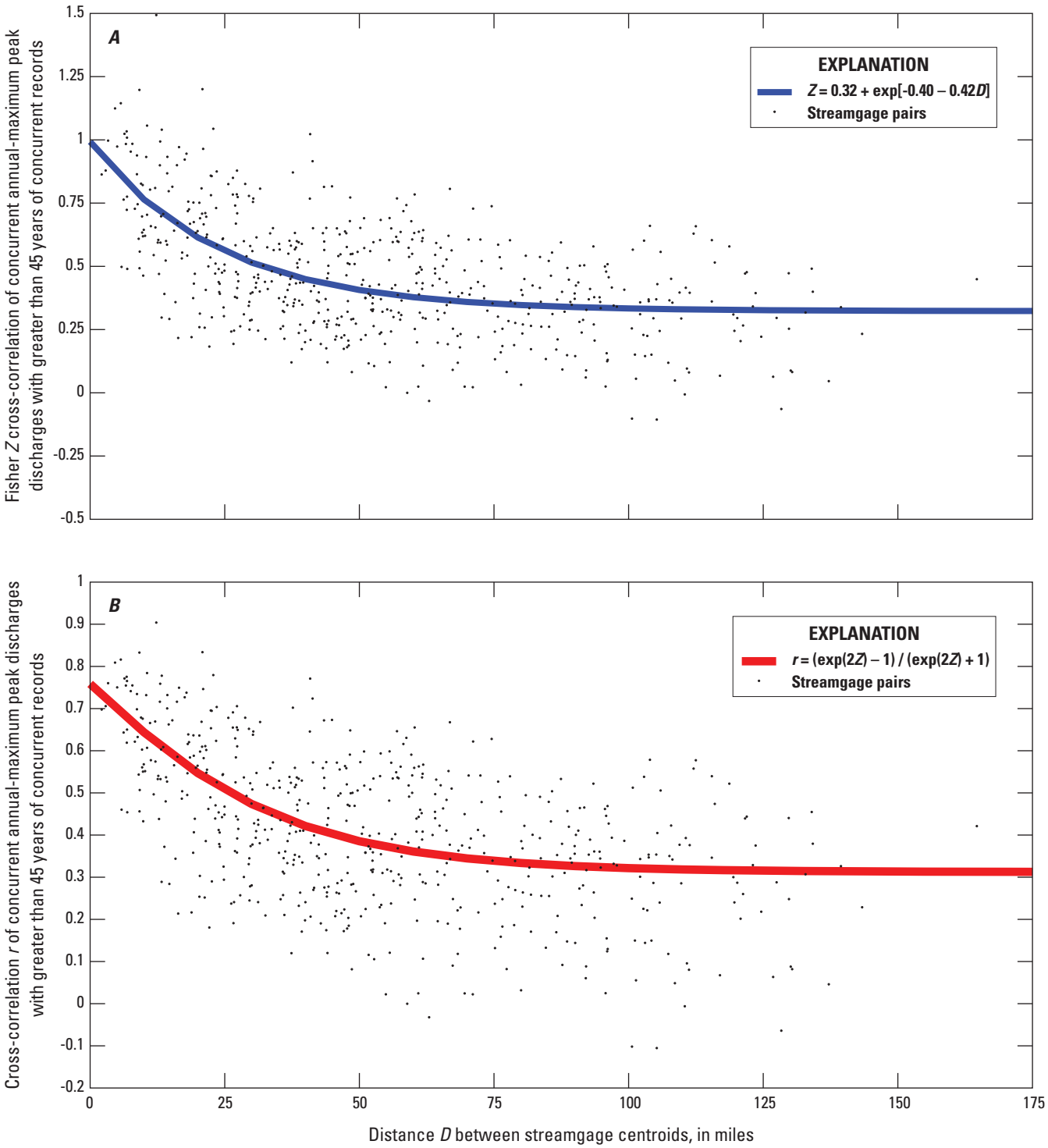

Figure 1–1. Fitting of cross-correlation model of the log-annual maximum peak discharges in this study in northeastern Illinois: *A*, relation between Fisher Z transform of cross-correlation and distance; *B*, relation between cross-correlation and distance.

Table 1–2. Regional skewness models and corresponding metrics in this study in northeastern Illinois.

[β_1, skew model intercept; SE, standard error; β_2, skew model slope; σ^2_δ, model error variance; ASEV, average sampling error variance; AVP_{new}, average variance of prediction for a new site; pseudo R^2_δ, fraction of the variability in the true skews explained by each model (Gruber and others, 2007); $\hat{\gamma}_R$, estimated regional skewness; --, not applicable; *NLCD*_22_23_24, fraction of the basin that has 2011 National Land Cover Database land cover classes 22, 23, and 24 (low, medium, and high intensity development, respectively.)]

Skew model	Intercept β_1	Intercept SE	Slope β_2	Slope SE	Bayesian plausibility, in percent	Error variance σ^2_δ	Error variance SE	ASEV	AVP_{new}	Pseudo R^2_δ, in percent
CONSTANT model										
$\hat{\gamma}_R = \beta_1$	0.16	0.15	--	--	--	0.19	0.05	0.022	0.21	0
URBAN model										
$\hat{\gamma}_R = \beta_1 + \beta_2\left[\left(NLCD\_22\_23\_24\right)^{0.5}\right]$	-0.39	0.19	0.97	0.34	0.4	0.16	0.05	0.032	0.19	14

Table 1–3. Average regional skew, variance of prediction, and equivalent record length for URBAN regional skew model for various values of *NLCD*_22_23_24, in this study in northeastern Illinois.

[VP_{new}, variance of prediction; ERL, equivalent record length; *NLCD*_22_23_24, the fraction of the basin that has 2011 National Land Cover Database land cover classes 22, 23, and 24 (low, medium, and high intensity development, respectively)]

*NLCD*_22_23_24 (fraction)	Average regional skew	VP_{new}	ERL (years)
0.0	-0.39	0.196	42
0.1	-0.29	0.180	43
0.2	-0.20	0.180	42
0.3	-0.10	0.182	41
0.4	0.00	0.186	40
0.5	0.10	0.191	39
0.6	0.19	0.196	39
0.7	0.29	0.203	39
0.8	0.39	0.208	40
0.9	0.48	0.215	40
1.0	0.58	0.222	41

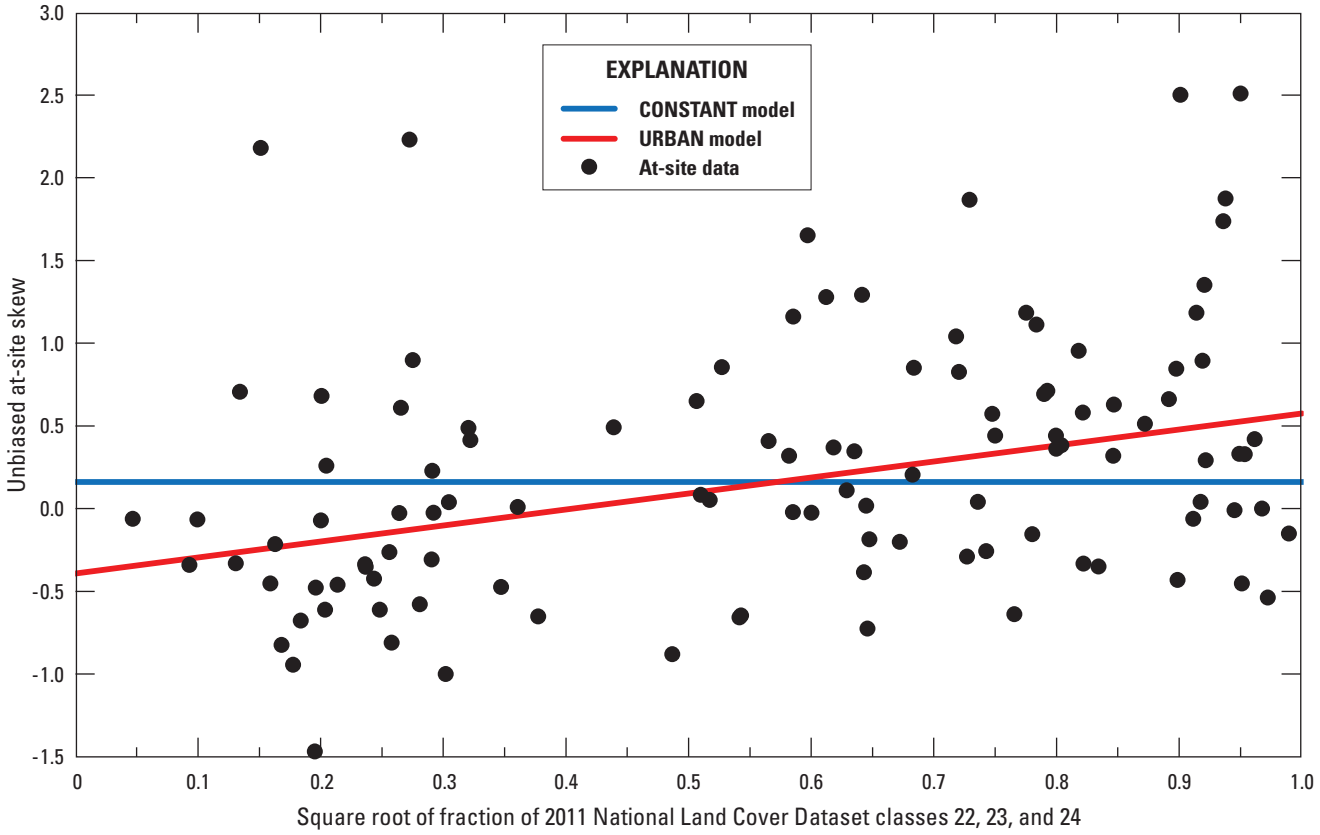

Figure 1–2. Relations between the unbiased at-site skew and urbanization measure for 110 streamgages in northeastern Illinois regional skew study area. The lines represent a model based on a constant skew (CONSTANT) and a model with a linear relation between skew and the square root of fraction of National Land Cover Dataset classes 22, 23, and 24 (*NLCD*_22_23_24$^{1/2}$) urbanization measure (URBAN). The models were developed from Bayesian weighted least-squares/Bayesian generalized least-squares analyses.

Table 1–4. Pseudo analysis of variance (ANOVA) statistics for the northeastern Illinois URBAN regional skew model.

[k, number of estimated regression parameters not including the constant; n, number of observations (streamgages) used in regression; $\sigma_\delta^2(0)$, model error variance of a constant model; $\sigma_\delta^2(k)$, model error variance of a model with k regression parameters and a constant; $Var(\hat{\gamma}_i)$, variance of the estimated sample skew at site i; EVR, error variance ratio; MBV*, misrepresentation of the beta variance; pseudo R_δ^2, fraction of variability in the true skews explained by each model (Gruber and others, 2007); --, not applicable]

Source	Degrees-of-freedom		Sum-of-squares	
	Equations	URBAN model	Equations	URBAN model
Model	k	1	$n\left[\sigma_\delta^2(0)-\sigma_\delta^2(k)\right]$	2.9
Model error	n-k-1	108	$n\left[\sigma_\delta^2(k)\right]$	18
Sampling error	n	110	$\sum_{i=1}^{n} Var(\hat{\gamma}_i)$	37
Total	2n-1	219	$n\left[\sigma_\delta^2(k)\right]+\sum_{i=1}^{n} Var(\hat{\gamma}_i)$	58
EVR	--	--	--	2.1
MBV*	--	--	--	5.7
Pseudo R_δ^2 (in percent)	--	--	--	14

References Cited

Cohn, T.A., Lane, W.L., and Baier, W.G., 1997, An algorithm for computing moments-based flood quantile estimates when historical flood information is available: Water Resources Research, v. 33, no. 9, p. 2089–2096.

Cohn, T.A., England, J.F., Berenbrock, C.E., Mason, R.R., Stedinger, J.R., and Lamontagne, J.R., 2013, A generalized Grubbs-Beck test statistic for detecting multiple potentially influential low outliers in flood series: Water Resources Research, v. 49, p. 5047–5058. [Also available at https://doi.org/10.1002/wrcr.20392.]

Eash, D.A., Barnes, K.K., and Veilleux, A.G., 2013, Methods for estimating annual exceedance-probability discharges for streams in Iowa, based on data through water year 2010: U.S. Geological Survey Scientific Investigations Report 2013–5086, 63 p. [Also available at https://pubs.usgs.gov/sir/2013/5086/.]

Griffis, V.W., 2006, Flood frequency analysis—Bulletin 17, regional information, and climate change: Ithaca, N.Y., Cornell University, unpublished Ph.D. dissertation.

Griffis, V.W., Stedinger, J.R., and Cohn, T.A., 2004, LP3 quantile estimators with regional skew information and low outlier adjustments: Water Resources Research, v. 40, no. 7, 17 p. [Also available at https://doi.org/10.1029/2003WR002697.]

Gruber, A.M., Reis, D.S., Jr., and Stedinger, J.R., 2007, Models of regional skew based on Bayesian GLS regression, Paper 40927–3285, *in* Kabbes, K.C., ed., Restoring our natural habitat—Proceedings of the 2007 World Environmental and Water Resources Congress—May 15–19, Tampa, Florida: Reston, Va., American Society of Civil Engineers [variously paged].

Gruber, A.M., and Stedinger, J.R., 2008, Models of LP3 regional skew, data selection and Bayesian GLS regression, Paper 596, *in* Babcock, R.W., and Walton, Raymond, eds., World Environmental and Water Resources Congress 2008–Ahupua'a—Proceedings of the congress—May 12–16, 2008, Honolulu, Hawaii: Reston, Va., American Society of Civil Engineers [variously paged].

Kendall, M.G., and Stuart, A., 1961, The advanced theory of statistics, v. 2: New York, Hafner Publishing Company, 676 p.

Lamontagne, J.R., Stedinger, J.R., Berenbrock, Charles, Veilleux, A.G., Ferris, J.C., and Knifong, D.L., 2012, Development of regional skews for selected flood durations for the Central Valley Region, California, based on data through water year 2008: U.S. Geological Survey Scientific Investigations Report 2012–5130, 60 p.

Parrett, Charles, Veilleux, A.G., Stedinger, J.R., Barth, N.A., Knifong, D.L., and Ferris, J.C., 2011, Regional skew for California, and flood frequency for selected sites in the Sacramento–San Joaquin River Basin, based on data through water year 2006: U.S. Geological Survey Scientific Investigations Report 2010–5260, 94 p.

Reis, D.S., Jr., Stedinger, J.R., and Martins, E.S., 2005, Bayesian generalized least squares regression with application to the log Pearson type 3 regional skew estimation: Water Resources Research, v. 41, no. 10, 14 p. [Also available at https://doi.org/10.1029/2004WR003445.]

Soong, D.T., Ishii, A.L., Sharpe, J.B., and Avery, C.F., 2004, Estimating flood-peak discharge magnitudes and frequencies for rural streams in Illinois: U.S. Geological Survey Scientific Investigations Report 2004–5103, 158 p.

Stedinger, J.R., and Cohn, T.A., 1986, Flood frequency analysis with historical and paleoflood information: Water Resources Research, v. 22, no. 5, p. 785–793.

Stedinger, J.R., and Griffis, V.W., 2008, Flood frequency analysis in the United States—Time to update [editorial]: Journal of Hydrologic Engineering, v. 13, no. 4, p. 199–204.

Tasker, G.D., and Stedinger, J.R., 1986, Regional skew with weighted LS regression: Journal of Water-Resources Planning and Management, v. 112, no. 2, p. 225–237.

U.S. Interagency Advisory Committee on Water Data, 1982, Guidelines for determining flood flow frequency—Bulletin #17B of the Hydrology Subcommittee (revised and corrected): U.S. Geological Survey, Office of Water Data Coordination, 28 p. [plus appendixes].

Veilleux, A.G., 2011, Bayesian GLS regression, leverage and influence for regionalization of hydrologic statistics: Ithaca, N.Y., Cornell University, unpublished Ph.D. dissertation.

Veilleux, A.G., Cohn, T.A., Flynn, K.M., Mason, R.R., Jr., and Hummel, P.R., 2013, Estimating magnitude and frequency of floods using the PeakFQ 7.0 program: U.S. Geological Survey Fact Sheet 2013–3108, 2 p. [Also available at https://doi.org/10.3133/fs20133108.]

Veilleux, A.G., Stedinger, J.R., and Eash, D.A., 2012, Bayesian WLS/GLS regression for regional skewness analysis for regions with large crest stage gage networks, Paper 227, *in* Loucks, E.D., ed., World Environmental and Water Resources Congress 2012—Crossing boundaries—Proceedings of the 2012 congress, May 20–24, Albuquerque, N.M.: Reston, Va., American Society of Civil Engineers, p. 2253–2263.

Veilleux, A.G., Stedinger, J.R., and Lamontagne, J.R., 2011, Bayesian WLS/GLS regression for regional skewness analysis for regions with large cross-correlations among flood flows, *in* Beighley, R.E., and Kilgore, M.W., eds., World Environmental and Water Resources Congress 2011—Bearing knowledge for sustainability—Proceedings of the 2011 World Environmental and Water Resources Congress, May 22–26, Palm Springs, Calif.: Reston, Va., American Society of Civil Engineers, p. 3103–3112.

Publishing support provided by:
Rolla and Indianapolis Publishing Service Centers

For additional information concerning this publication, contact:
Director, USGS Illinois Water Science Center
405 North Goodwin Avenue
Urbana, IL 61801
(217) 328–8747

Or visit the Illinois Water Science Center website at:
https://www.usgs.gov/centers/cm-water.

ISSN 2328-0328 (online)
https://doi.org/10.3133/sir20165050